PORE STRUCTURE AND PORE SOLUTION IN ALKALI ACTIVATED FLY ASH GEOPOLYMER CONCRETE AND ITS EFFECT ON ASR OF AGGREGATES WITH WIDE SILICATE CONTENTS

A Thesis
Submitted to the Graduate Faculty
of the
North Dakota State University
of Agriculture and Applied Science

By

Shree Raj Paudel

In Partial Fulfillment of the Requirements
for the Degree of
MASTER OF SCIENCE

Major Department:
Civil and Environmental Engineering

April 2019

Fargo, North Dakota

North Dakota State University

Graduate School

Title

PORE STRUCTURE AND PORE SOLUTION IN ALKALI ACTIVATED FLY ASH GEOPOLYMER CONCRETE AND ITS EFFECT ON ASR OF AGGREGATES WITH WIDE SILICATE CONTENTS

By

Shree Raj Paudel

The Supervisory Committee certifies that this ***disquisition*** complies with North Dakota State University's regulations and meets the accepted standards for the degree of

MASTER OF SCIENCE

SUPERVISORY COMMITTEE:

Mijia Yang, PhD, PE
Chair

Zhibin Lin, PhD, PE

Ravi Yellavajjala, PhD

Long Jiang, PhD

Approved:

04/15/2019	David R. Steward, PhD, PE
Date	Department Chair

ABSTRACT

Alkali silica reaction (ASR) is detrimental to concrete. It is a time-dependent phenomenon, which can lead to strength loss, cracking, volume expansion, and premature failure of concrete structures. In essence, it is a particular chemical reaction involving alkali hydroxides and reactive form of silica present within the concrete mix.

Geopolymer is a type of alkaline activated binder synthesized through polycondensation reaction of geopolymeric precursor and alkali polysilicates. In this thesis, three types of reactive aggregates with different chemical compositions were used. Systematic laboratory experiments and microstructural analysis were carried out for the geopolymer concrete and the OPC concrete made with the same aggregates. The result suggests that the extent of ASR reaction due to the presence of three reactive aggregates in geopolymer concrete is substantially lower than that in OPC based concrete, which is explained by the pore solution change and verified through their microstructural variations and FTIR images.

ACKNOWLEDGEMENTS

I would like to express my earnest appreciation to many individuals who provided their invaluable guidance and support throughout this study. First of all, my deep gratitude goes to my advisor, **Dr. Mijia Yang** for his continued attention, helpful guidance, and endless support during my MS study. I consider myself fortunate to have a supportive advisor like him.

Besides my advisor, I would like to thank the rest of my thesis committee: **Dr. Zhibin Lin**, **Dr. Ravi Yellavajjala**, and **Dr. Long Jiang** for their reviews and insightful advice with this research project.

I am particularly indebted to American Engineering Testing Inc. for their support and assistant in obtaining different types of aggregates for this study. I would like to convey my appreciation to **Scott Payne** and **Jayma Moore** for their help in conducting microstructural analysis at electron microscopy lab, NDSU. I would like to thank **Chunju Gu** from coating and polymeric materials department for providing help on several lab works during this study.

I would like to take a moment and thank **Jan Lofberg** and all the Civil and Environmental Engineering department for their direct and indirect help, encouragement and professional instructions throughout my research.

Finally, I would like to take this opportunity to thank my beautiful parents, my sister, my brother, all my friends, colleagues and all the faculty at North Dakota State University.

TABLE OF CONTENTS

LIST OF TABLES

LIST OF FIGURES

CHAPTER 1. INTRODUCTION

1.1. Background

Forms of concrete have been used as a durable construction material at least since Roman times, and concrete structures based on cement hydration of Roman origin can still be seen in many parts of Europe today **(Sims and Poole 2017)**. As early as the nineteenth century it was realized that, although normally a very durable material, concrete could deteriorate, with frost and sea water. In one form or another, concrete has become the most used construction material in today's world. Even though the concrete fulfills all the required specification including strength development and quality, it has been found that a few concrete starts to expand and crack after certain period of time. During late 1920s, numbers of concrete structures in North America were observed to develop sever cracking within a few years of their construction. The first comprehensive scientific investigations describing the reaction and its effects were published by Stanton in December, 1940 **(Stanton et al. 1942)**. The study showed that the problem developed only when certain types of mineral components were present in the aggregates and only when cement alkalis exceeded some minimum threshold percentage concentration. The particular problem involved gave rise to the name "Alkali-Aggregate Reaction (AAR)" which has been divided later into alkali silica reaction (ASR) and alkali carbonate reaction (ACR)**(Poole 2002)**. Since Stanton published his first findings in 1940, this problem got attention around the globe and enormous amount of studies have been started on this subject **(Buck and Mather 1987; Cox et al. 1950; De La O 1951)**. Despite this extensive amount of work, the mechanism of ASR expansion is still not thoroughly understood.

It has been found that, expansion, deterioration and perhaps even failure of concrete structural elements resulting from alkali silica reaction in the concrete are due to the swelling

pressure developed in concrete pores, which are sufficient to produce and propagate micro-fractures **(Swamy 2002)**. Alkali silica reaction is basically the reaction between alkali hydroxides which are usually (not always) derived from the cement used in concrete and reactive components in the aggregate particles used. Because ASR is a reaction that occurs throughout the concrete mass, it is very difficult or impossible to control, repair permanently, or to provide satisfactory remediation once it has been initiated. Furthermore, the cracking allows other processes of deterioration to develop.

In addition to alkali silica reaction in concrete, production of Portland cement is a very costly and energy-intensive process. Large amount of CO_2, one of the main greenhouse gases, is released into the atmosphere during manufacture **(Hardjito and Rangan 2005)**. It leads towards the study of properties of other binding materials such as fly ash, ground granulated blast furnace slag etc. that can replace the Portland cement from concrete. But ASR potential of new supplementary cementitious materials needs to be studied.

Alkali silica reaction does not only depend upon the types of cementitious materials. It has been found that the silica from aggregates used in mix takes part in reaction. Although most rocks contain reactive forms of silica, it is also incorrect to consider rock type as a criterion for an aggregate's potential of reactivity. However, the volume to produce deleterious effect needs to be studied. As little as 2% of reactive component has been reported in certain cases where severe distress in the concrete has been observed.

1.2. Objectives

This study was carried out to investigate the mechanism of ASR in fly ash geopolymer concrete, which includes;

1. To evaluate the expansion potential in several mixes of fly ash based geopolymer concrete with different types of aggregates and compare it with that of OPC concrete having similar aggregates.
2. To extract the pore solution from hardened concrete sample at different ages and investigate the alkalinity of extracted pore solution in concrete.
3. To investigate the change in chemical composition and bonding at aggregate-paste interface using SEM/EDS and FTIR spectroscopy.
4. To evaluate the change in porosity and pore size distribution of GPC and OPC concrete sample using X-ray computed micro-tomography (MicroCT)

1.3. Scope of work

The aim of this research is to examine the relationship between chemical composition of the aggregate and alkali silica reaction potential of fly ash based geopolymer concrete (GPC) and compare it with that of ordinary Portland cement based concrete (OPC). Three different types of aggregates, namely Granite, Carbonate, and Gravel, are used to prepare both OPC and GPC concrete. The gravel contains of 62% of silica, 20% of aluminum, 2% of calcium and remaining amount of other minerals. The carbonate has a composition of 30% silica, 9% aluminum, 1% of calcium, and granite has 0.2% of silica, 19% of calcium, and 0.1% of aluminum by mass respectively.

The role of chemical composition inside the aggregates on the alkali silica reaction progress was evaluated using length change measurement and pore solution alkalinity

measurement. In addition, SEM imaging and FTIR analysis were performed at aggregate-binder interface to analyze the change in chemical bonding at different ages of the samples. Finally, a 3D microstructural analysis was conducted using x-ray computed micro-tomography to evaluate the change in porosity and pore size distribution inside the concrete sample in 90 days exposed to alkaline solution.

1.4. Research methodology layout

This study was organized into four chapters.

1. Chapter 2: Literature Review
2. Chapter 3: Materials and Methodology
3. Chapter 4: Expansion measurement and pH level of pore solution in GPC and OPC concrete with different types of aggregates
4. Chapter 5: Expansion measurement and porosity analysis using micro-computed tomography (micro-CT)
5. Chapter 6: Summary, Conclusion, and Recommendations

Chapter two, literature review, reviews the history of traditional concrete and fly ash based geopolymer concrete. It discusses about the studies that have enhanced the understanding on alkali silica reaction. Chapter three, materials and methodology, gives the details of the materials and equipment used in the study. It also explains the procedure adopted for the research and experiments in detail. Chapter four, expansion measurement and pH level of pore solution in GPC and OPC concrete with different types of aggregates, presents the results obtained from expansion test of concrete prism and evaluation of pH value of pore solution extracted from hardened concrete. It also discusses the results obtained from SEM/EDS analysis and FTIR spectroscopy. Chapter five, expansion measurement and porosity analysis using micro-computed

tomography, presents the results obtained from 3D scanning of concrete prism using MicroCT. In chapter six, the summary and recommendation of the research is presented.

CHAPTER 2. LITERATURE REVIEW

2.1. Introduction

This chapter presents a review of previous researches on geopolymer concrete and ASR in concrete. Construction industries have practiced the use of fly ash and GGBS as a key binder in developing mortar and concrete for many decades. This chapter will be mainly focused on the literatures based on alkali-silica reaction occurred in microstructure level of geopolymer concrete and its effects on the durability.

2.2. Background

Concrete is the most popular material for construction on earth and has been used for thousands of years all over the world **(Provis et al. 2014)**. It is used in all types of buildings (from residential to multi-story office blocks) and in infrastructure projects (roads, bridges, etc.). The approximate amount of concrete poured worldwide per year is more than 4 billion tons. However, concrete has bad impact to environment. It is responsible for 5% - 7% of our worldwide carbon emission **(Hardjito et al. 2005)**. The CO_2 produced in the process of manufacturing of Portland cement is in the order of one ton for every ton cement **(Hardjito et al. 2008)**. It means if we can replace the Portland cement with non-harmful, effective and durable material we can reduce the human induced negative impact to the environment because of construction.

Davidovits **(Davidovits 1982)** introduced a new material named "geopolymer" which can be used as a binder material in concrete industry. The geopolymer consists of a polymeric chain of Si-Al-Si framework, similar to zeolites. The main difference is geopolymers are amorphous in nature instead of crystalline at ambient and medium temperatures. Geopolymer is an alumino-silicate polymer synthesized from predominantly silicon (Si) and aluminum (al) materials of

geological origin or industrial bi-product such as fly ash or ground granulated blast furnace slag (GGBS) **(Davidovits 1994)**. During the production of fly ash or GGBS, there is no need of burning fossil fuel. Another interesting property of geopolymer based concrete is water curing is not needed. Geopolymer mortars and concrete can be designed to have similar physical and mechanical properties as Portland cement concrete does. Recent studies have shown that geopolymer based material are very useful in fire and heat resistant coating and medicinal applications.

2.3. Geopolymer concrete

2.3.1. Introduction

Geopolymer concrete is a type of amorphous alumino-silicate cementitious material which can be synthesized by polycondensation reaction of geopolymeric precursor and alkali polysilicates. Geopolymer concrete is manufactured using source materials that are rich in silica and alumina. While the cement based concrete utilizes the formation of calcium-silica hydrates (CSHs) for matrix formation and strength, geopolymer involves the chemical reaction of alumino-silicate oxides with alkali polysilicates yielding polymeric Si-O-Al bonds **(Hardjito et al. 2004)**.

Geopolymers are the member of the family of inorganic polymers. The chemical composition of geopolymer materials is similar to the natural zeolitic materials, but the microstructure is amorphous. Geopolymer is used as the binder, instead of cement paste to produce the concrete. The manufacturing process of the geopolymer concrete is similar as that for ordinary Portland cement concrete. As in the Portland cement concrete, the aggregates occupy the largest volume **(Razak et al. 2014)**.

The formation of geopolymer material can be shown by Equations (2.1) and (2.2) **(Davidovits 1994; Van Jaarsveld et al. 1997)**.

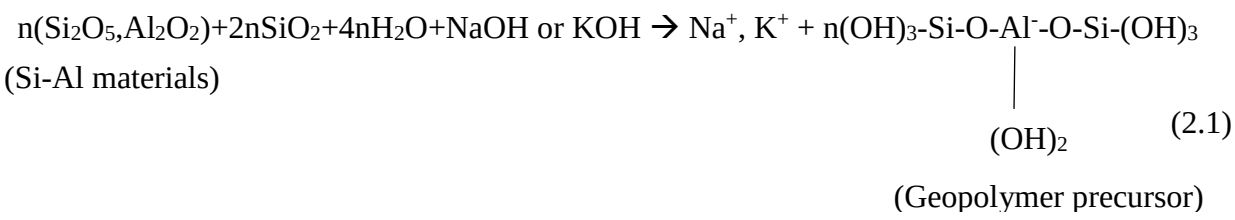

(2.1)

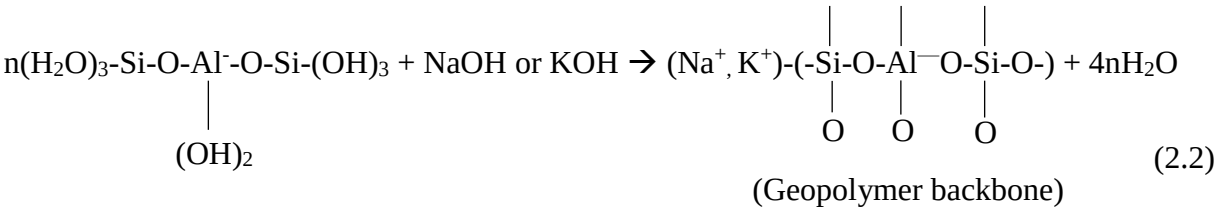

(2.2)

2.3.2. Constituents of geopolymer concrete

2.3.2.1. Source materials

2.3.2.1.1. Fly ash

Because geopolymer concrete is manufactured using source material that are rich in silica and alumina, Fly ash can be used as a major constituent for the production of geopolymer concrete. Many researchers have used other materials like GGBS and Rice husk, but fly ash has become more popular because of its physical and chemical properties. Physically, fly ash is a very fine and powdery material, in light tan to dark in color depending on its chemical composition. There are two types of fly ash i.e. class C and class F.

The primary difference between Class C and Class F fly ash is the chemical composition of the ash itself. While Class F fly ash is highly pozzolanic, meaning that it reacts with excess lime generated in the hydration of Portland cement, Class C fly ash is pozzolanic and also can be self-cementing. ASTM C618 requires that Class F fly ash contains at least 70% pozzolanic compounds (silica oxide, alumina oxide, and iron oxide), while Class C fly ash has between 50%

and 70% of these compounds. Typically, Class C fly ash also contains significant amounts of calcium oxide - over 20%. While both classes of fly ash greatly reduce concrete permeability compared to the cement only mixes, Class F tends to give proportionately greater permeability reduction. Due to the higher levels of pozzolanic compounds, Class F fly ash mitigates sulfate attack, alkali silica reaction, corrosion of reinforcement, and chemical attack. While Class C fly ash generally improves concrete durability as related to these forms of attack, higher replacement percentages may be necessary to effectively mitigate them **(Ferdous et al. 2013; Khale and Chaudhary 2007; Rangan 2008)**.

Most of fly ash available globally is low-calcium fly ash formed as a by-product of burning coal. Fly ash particles are usually finer than Portland cement and ranges in diameter from less than 1 mm to no more than 150 mm **(Farzam et al. 2005)**.

Fly ash is a byproduct of pulverized coal blown into a fire furnace of an electricity generating thermal power plant. The total fly ash production in the world is about 780 million tons per year but the utilization is only about 17-20%. Most of the fly ash is disposed off as waste material that covers several hectors of valuable land.

Ahmaruzzaman **(Ahmaruzzaman 2010)** mentioned that fly ash ranks as the planet's fifth largest raw material resource and can be used as an alternative to conventional materials in the construction. Basu et al. **(Basu et al. 2009)** illustrates that the development of production and utilization of fly ash is spreading all around the world since 2005 (Figure 2.1). China, India and the US are the three biggest contributors in the production of fly ash but the amount of utilization is very low. The relative production and utilization of fly ashes differ noticeably from one country to another (Figure 2.1). It has been believed that the disposal of fly ash will soon be too

costly if not banned. This can be seen in Netherlands, where all the fly ash must be utilized or exported since landfill is prohibited.

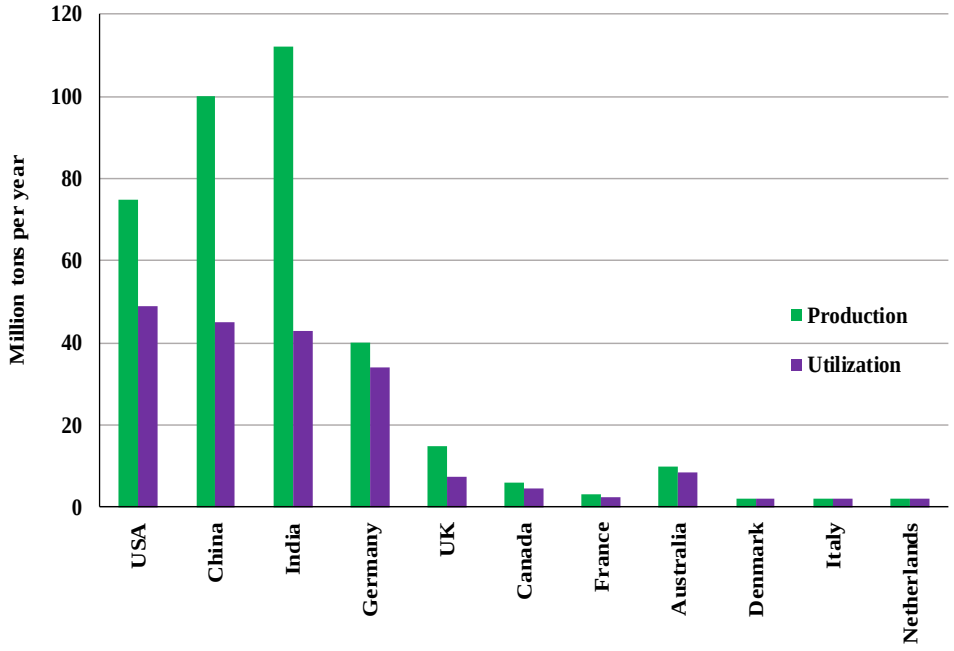

Figure 2.1. Generation and utilization of fly ash in different countries

Figure 2.2 illustrates fly ash production, utilization, and disposal rates in the USA from 1974 to 2017. It can be seen that, from 1974 to 2014, landfill rates were higher than the utilization rate, however, it has been lower than the utilization rate since 2014. In 2006, 54% of the fly ash produced was sent to landfill. This increased to 63% in 2010, while the utilization amount remained at 25 million tons. In 2017, the rate of landfill dropped to 41% **(ACAA 2014; Kalyoncu and Olson 2001)**. This shows that between 1974 and 2017, fly ash utilization in the US has an average growth rate of 3.3 percent.

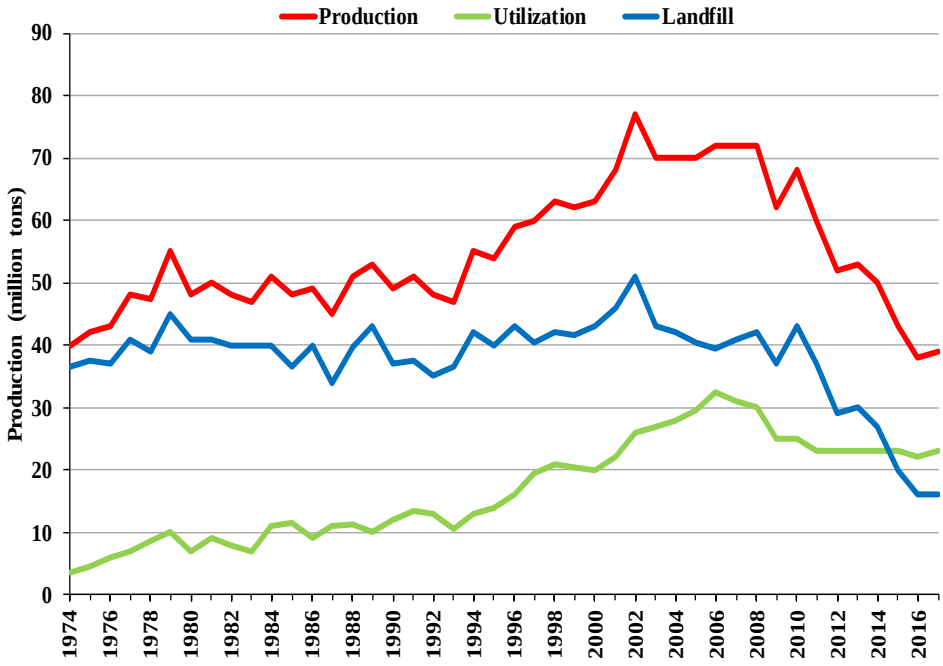

Figure 2.2. Fly ash production, utilization and disposal rates in USA from 1974 to 2017

Because of the cementitious properties of fly ash, it has a broad range of applications within the construction industry. The utilization of fly ash as a replacement for Portland cement in concrete is widespread and considerable volume are used. Looking at the US fly ash utilization in Figure 2.3 (American coal ash association), 2014, nearly 57% of the fly ash produced was unutilized in 2013. About 53% of the total utilization was on concrete and cement, 13% was in structural fills, 10% was in clinker feed, 9% was in waste stabilization, 8% was in mining application and the remaining 8% was used in other purposes **(ACAA 2014)**.

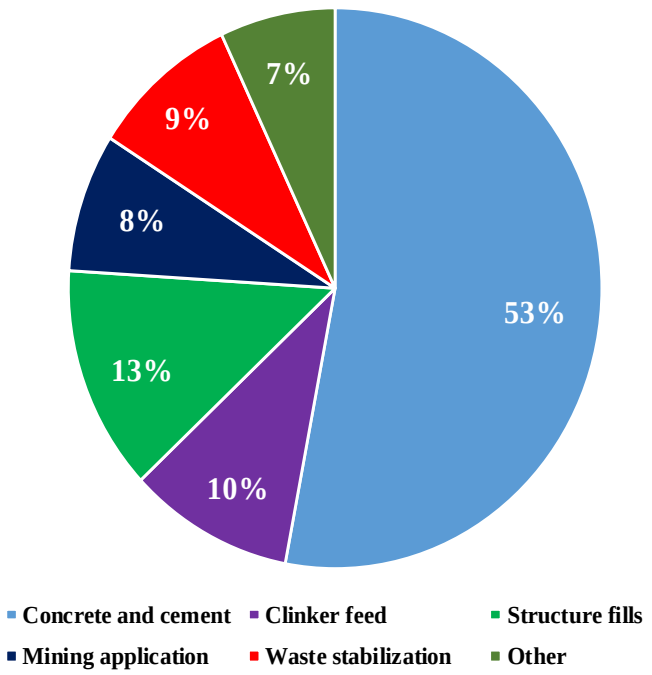

Figure 2.3. Utilization of fly ash in different areas in the USA

2.3.2.1.2. Alkaline activator

Alkaline activation in fly ash based geopolymer concrete is a chemical process in which fly ash is mixed with an alkaline activator to produce a paste capable of setting and hardening within a reasonably short period of time. The mechanical properties of the resulting material depend on the nature of fly ash and type of alkaline activator used and the other activation process variables **(Joshi and Kadu 2012)**.

The most common alkaline activator used in geopolymerisation is a combination of sodium hydroxide (NaOH) or potassium hydroxide (KOH) and sodium silicate or potassium silicate. Many researchers concluded that the types of activator play an important role in polymerization process. The reactions occur at higher rate when the alkaline activator contains

soluble silicate, either sodium or potassium silicate compared to the use of only alkaline hydroxides.

Xu and Deventer **(Xu and Van Deventer 2000)** showed that the addition of sodium silicate solution to the sodium hydroxide solution as the alkaline activator enhanced the reaction between the source material and the solution. Motorwala et al **(Motorwala et al. 2013)** reported that mostly the NaOH solution results in higher extent of dissolution of mineral than KOH solution during geopolymerisation.

But, Khale and Chaudhary **(Khale and Chaudhary 2007)** mentioned that since Potassium (K^+) is more basic, it allows a higher rate of solubilized polymeric ionization and dissolution which leads to a dense polycondensation and that provides greater overall network formation and an increase in the compressive strength.

2.3.3. Geopolymerization

The chemical reaction during the geopolymerization usually contains the following three steps **(Davidovits 1999; Xu and Van Deventer 2000)**:

- Dissolution of Si and Al atoms from the source material through the action of hydroxide ions.
- Condensation or conversation of precursor ions into monomers
- Polycondensation/polymerization of monomers into polymeric structures.

These three steps can occur almost simultaneously and may also overlap, thus making it difficult to isolate and examine each of them separately **(Palomo et al. 1999)**. According to Davidovits, the hardening mechanism for geopolymerization essentially involves the polycondensation reaction of geopolymeric precursors, usually alumino-silicate oxides, with alkali polysilicates yielding polymeric Si-O-Al bonds as shown in following equations:

$$(Si_2O_5, Al_2O_2)_n + 3nH_2O \rightarrow \underset{\text{(Orthosialate)}}{n(OH)_3 - Si - O - Al^- - (OH)_3} \quad (2.4)$$

$$n(OH)_3 - Si - O - Al^- - (OH)_3 \rightarrow (Na,K) - (- \underset{|}{\overset{|}{Si}} - O - \underset{|}{\overset{|}{Al^-}} - O -)_n + 3nH_2O \quad (2.5)$$

(Na,K)-poly(sialate)

$$(Si_2O_5, Al_2O_2)_n + n2SiO_2 + 4nH_2O \rightarrow n(OH)_3 - Si - O - \underset{|}{\overset{|}{Al^-}} - O - Si - (OH)_3 \quad (2.6)$$

$(OH)_2$

(Ortho(sialate-siloxo))

$$n(OH)_3 - Si - O - \underset{|}{\overset{|}{Al^-}} - O - Si - (OH)_3 \rightarrow (Na,K) - (- \underset{|}{\overset{|}{Si}} - O - \underset{|}{\overset{|}{Al^-}} - O - \underset{|}{\overset{|}{Si}} - O)_n + 4nH_2O \quad (2.7)$$

$(OH)_2$ O O O

(Na,K)-poly(sialate-siloxo)

Rangan **(Rangan 2008)** illustrates the reaction mechanism in Figure 2.4, which outlines the key processes occurred in the transformation of a solid aluminosilicate source into a synthetic alkali aluminosilicate. The process of geopolymerization contains several complex phenomena concurrently but in a simple way we can describe in few sentences. It has been assumed that it started with dissolution of the solid particle by alkaline hydrolysis at the surface which is responsible for the liberation of aluminate and silicate. In the second stage the complex mixture of silicate, aluminate and aluminosilicate quickly, creates a supersaturated aluminosilicate solution because of dissolution at high pH. The third stage contains the gelation of the concentration solution and release of water **(Swaddle et al. 1994)**. In this process the water plays a role of a reaction mechanism, but stays inside the gel pores. In third stage, the formation of gel and water releasing process keep continue with reorganization of the structure. As the connectivity of the gel network increases, resulting in the three dimensional aluminosilicate network commonly attributed to geopolymers. The fourth and final stage contains

polymerization of the networks already formed and hardening process **(Fernández-Jiménez et al. 2006)**.

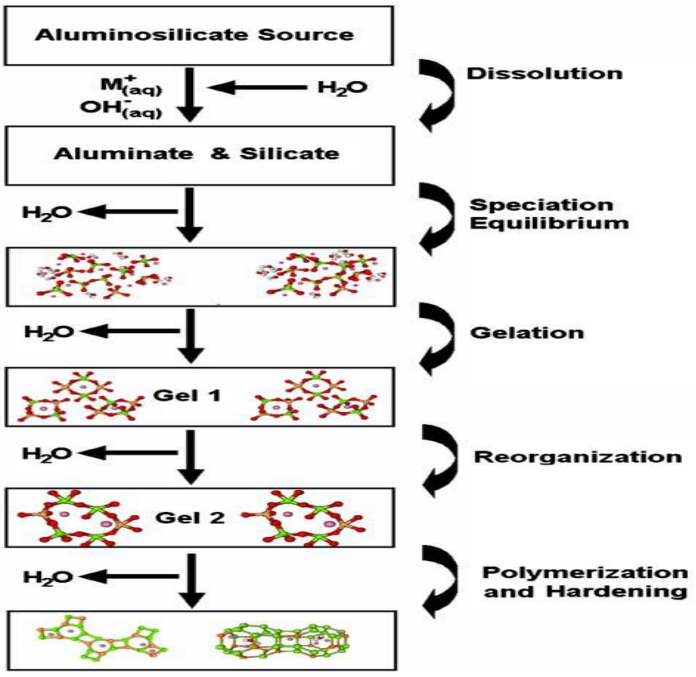

Figure 2.4. Conceptual model of geopolymerization

Some of the important factors affect the process of geopolymerization and hardening properties of geopolymeric materials can be given as **(Singh 2018).**

1. Properties and composition of raw materials containing alunimosilicate
2. Surface area and glassy phase content in the raw material
3. Amount of aluminum, iron, calcium and reactive silicon
4. Temperature, pressure and time used for curing
5. Chemical composition and concentration of alkalis used in alkaline activator
6. Water to solid ratio
7. Na_2O to SiO_2 ratio
8. SiO_2 to Al_2O_2 ratio

In general, the geopolymerization reaction increases with increase in curing temperature (upto 90°C) and the concentration of the alkalis. Whereas, increase in water content reduces the geopolymerization and decreases the strength.

2.4. Alkali aggregate reaction

Alkali aggregate reaction (AAR) is a chemical reaction between certain types of reactive aggregates and hydroxyl ions (OH^-) associated with alkalis (Sodium Oxide and Potassium Oxide) in the source materials. AAR in concrete is considered as a great menace to the durability of concrete structure. The effect of AAR becomes visible generally when the concrete is 5 to 10 years old. The damages caused by AAR in concrete takes a variety of forms. The most common damages are expansion of the concrete and surface cracking.

AAR related problems were first identified in early 1940s in Parker Dam, California (U.S.A). Since then, AAR has been recognized in more than 50 countries **(Thomas et al. 2011)**.

Two forms of alkali aggregate reactions are recognized **(Bleszynski and Thomas 1998; Fernández-Jiménez et al. 2006; Thomas et al. 2011)**:

a) Alkali carbonate reaction (ACR)
b) Alkali silica reaction (ASR)

2.4.1. Alkali carbonate reaction (ACR)

Alkali carbonate reaction was first introduced by Swenson in 1957 **(Swenson 1957)**, which occurs between some agrilliceous dolimic limestone aggregates and the hydroxyl ions in the cement and causes swelling. ACR is typically a more aggressive reaction and occurs earlier in the life of structure. ACR reaction takes place in a humid condition and is generally characterized by the formation of reaction rims up to 2mm around reactive aggregate particles.

Swenson and Gillott **(Swenson and Gillott 1964)** mentioned that ACR reaction appears to be limited in certain fine-grained, argillaceous, dolomitic limestones when they are used as coarse aggregate. The rate and extent of the expansion of the concrete increase with increase in alkali content and the presence of moisture.

Grattan-Bellew et al. (Grattan-Bellew et al. 2010) reported that the alkali carbonate reaction and alkali silica reaction are similar. Difference between them is the composition of the gel produced. In contrast to the gel produced in typical ASR affected concretes that consists of sodium/potassium calcium silicate hydrate, the gel found in ACR affected concrete consists of calcium magnesium aluminum silicate hydrate.

The deterioration caused by alkali carbonate reactions is similar to that caused by ASR; however, ACR is relatively rare because aggregates susceptible to this phenomenon are relatively less common and usually unsuitable for use in concrete for other reasons. The aggregate which are sensitive to ACR has a distinct mineralogy of dolomite crystals embedded in a clay matrix. A qualified photographer can identify this. There are no recommended methods of preventing deleterious expansion when the available aggregate source has been verified to be ACR reactive.

2.4.2 Alkali silica reaction

Alkali silica reaction was first reported in 1940 by Stanton, **(Stanton, 1940)** as ASR is a deleterious chemical reaction between alkalis in cement paste and certain amorphous silica in variety of natural aggregates. Since then, the issues related to this problem have continuously received much attention and a large volume of literature addressing various aspects of ASR is currently available.

Bleszynski and Thomas **(Bleszynski and Thomas 1998)** reported that alkali silica reaction (ASR) is the most common form of alkali aggregate reaction (AAR). It is essentially the reaction between the hydroxyl ions (OH^-), associated with alkalis (sodium and potassium) presented in the pore solution of the concrete and mortars, and the certain form of active silica constituents present in some reactive aggregates. The ASR reactive constituents include many stable silica forms including opal, chalcedony, cristobalite, tridymite, and acidic volcanic glasses **(Fernandes et al. 2013)**. There are three widely accepted and sufficient requirements for ASR to occur (Figure 2.5): 1) the presence of reactive forms of silicate in aggregates; 2) a source of alkalis; and 3) sufficient moisture. The moisture content is very important to the development of the alkali silica reaction because the ASR gel requires moisture for the expansion. A lack of moisture has a limiting effect on the growth of the gel, even though if a certain limiting moisture content is passed, further increase will not lead to an increase in gel growth **(Stokes 2011)**. Similar as the moisture, the temperature also affects the speed of the development of the alkali silica reaction. The expansion of alkali silica gel increases with increase in temperature. It is important to note that the final expansion is not going to increase. Raising the temperature just accelerates the process **(Saouma and Perotti 2006)**. Generally, the combination of conditions 1 and 2 mentioned above is necessary to initiate the alkali silica reaction whereas condition 3 is essential to cause the swelling of the gel produced form ASR **(Mukhopadhyay et al. 2009)**.

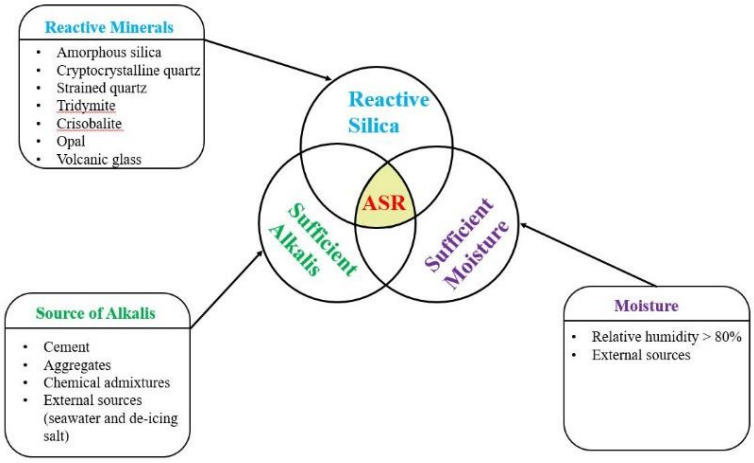

Figure 2.5. Primary factors influencing alkali silica reaction in concrete (adopted from Mukhopadhyay et al., 2009)

ASR plays a vital role for the durability of concrete structures because the reaction product in the form of gel leads to internal stresses and causes expansion and cracking of the concrete. It typically takes years to appear in the field but can be seen in a few days in laboratory setup **(Bleszynski and Thomas 1998)**. Swaddle et al. **(Swaddle et al. 1994)** stated that it is very important to differentiate the alkali silica reaction and the damage caused by alkali silica reaction. Alkali silica reaction is indicated by the presence of alkali silica gel, whereas damage due to alkali silica reaction can be identified by investigation of the presence of micro cracks in the aggregates because of the swelling of alkali silica gel. Generally, the visual sign of distress are random cracking in unrestrained concrete whereas in reinforced concrete, cracks tends to be aligned in a direction parallel to that of reinforcement. At a microscopic level, petrographic analysis and scanning electron microscopy provide the presence of ASR gel and cracks initialized and propagated in concrete **(Pan et al. 2012)**.

2.4.2.1. Mechanism of alkali silica reaction

a) Chemistry of alkali silica reaction

Alkali silica reaction (ASR) process is complicated, and typically consists of several stages. The major three steps are as follows **(Glasser and Kataoka 1981)**.

The first stage involves the rupture of the aggregate siloxane networks caused by the attack of hydroxyl ions to produce alkali silicate and silicic acid,

$$\equiv Si - O - Si \equiv + R^+ + OH^- \rightarrow \equiv Si - O - R + H - O - Si \equiv, \quad (2.8)$$

Where R^+ denotes an alkali ion such as sodium and potassium ions (Na^+ and K^+).

In the second step, this silicic acid immediately reacts with the further hydroxyl ions,

$$\equiv Si - O - H + R^+ + OH^- \rightarrow \equiv Si - O - R + H_2O, \quad (2.9)$$

The alkali silica gel (alkali silicate) resulting from Equation (2.8) and (2.9) are amorphous and hygroscopic.

In the third and last step, the alkali silicate combines with water and will result in expansion of the alkali silica gel,

$$\equiv Si - O - R + nH_2O \rightarrow \equiv Si - O^- - (H_2O)_n + R^+ ; \quad (2.10)$$

Where, n is the hydration number.

As a matter of fact, the reaction mechanism of producing alkali silica reaction gel is quite complex and not completely understood. However Hou et al. **(Hou et al. 2004)** stated that the alkali silica gel formation in alkali silica reaction involves the similar reaction sequence of the normal cement hydration. Due to the attack of hydroxyl ions, the dissolved silica reacts with CH to produce depolymerized Ca-rich C-S-H until the CH is locally consumed. When CH is not available in reaction and when silica is continuously supplied, the C-S-H will become more polymerized and rich in silica. Only then a hydrous alkali silica gel could start to form. It has

been also mentioned that K^+ and Na^+ behave very similarly in ASR reactions, except the gel with K may be somewhat more disordered than gels with Na **(Hou et al. 2005)**.

There are many researches have been done to investigate about the chemical composition of the alkali silica gel. Thaulow et al. **(Thaulow et al. 1996)** mentioned that the gel chemical composition fell within 53 to 63% silica, 20 to 30% of calcium and about relative 15% of the sodium and potassium. However, it has been also mentioned that the chemical composition of ASR varies strongly with the position of the gel. The gel within pores and cracks in cement paste has higher calcium contents compared with the gel close to and in the reactive aggregates **(Fernandes 2009; Regourd et al. 1981)**.

Powers and Willis **(Powers and Willis 1950)** stated that the composition of ASR gel has two components. Those two components are non-swelling alkali calcium silicate hydrate gel and swelling alkali silicate hydrate gel. The reaction with highly reactive aggregates could be safe or unsafe depending upon the content of gel. Pan et al. **(Pan et al. 2012)** mentioned that the high calcium content gel i.e. alkali calcium silicate hydrate gel, does not swell and will not cause the cracking problem in concrete. However, if calcium ion concentrations are quite low, both swollen and non-swollen gels are forms resulting in huge expansion and severe damage.

b) Mechanism of swelling and cracking

It is widely accepted that deterioration of ASR-affected concrete is due to gel expansion through water imbibition.

The first known theory to explain the expansion of concrete due to ASR is known as "osmotic pressure theory" **(Hanson 1944)**. This theory mentioned that the cracking that occurred in the concrete was due to the formation of an osmotic pressure cell surrounding the aggregates. It has been also stated that the reactive aggregate behaves as a semipermeable membrane which

allows water molecules to pass through the pore solution into the surrounding cement paste but prevents the alkali silicate ions. The alkali silicate that formed on the surface of an aggregate would draw the solution from the cement paste to form a liquid filled pocket. Thus, an osmotic pressure cell forms and the alkali silica gel swells with increasing in hydrostatic pressure, leading to cracks on cement paste. Glasser (**Glasser 1979)** also applied the same theory to explain the mechanism of swelling of gels and agrees on the Hansen's osmotic pressure theory.

McGowan **(McGowan 1952)** proposed a new expansion mechanism theory called "swelling theory" to challenge Hansen's theory. The theory suggests that the alkali silica gel, the product of reactive aggregates, absorbs water from the pore solution which leads to swelling in the gel and causes the expansive pressure and eventually cracking of aggregate.

Bazant and Steffens (Bažant and Steffens 2000) reported that expansion due to ASR in concrete is caused by the swelling pressure accumulated in the interfacial transition zone between the aggregate and the surrounding cement paste. The imbibition of water from adjacent capillary pores causes the swelling of the gel. The pressure build up is considered to cause part of gel to diffuse into the adjacent capillary pores and result in propagation of the cracks in the concrete matrix.

Ichikawa and Miura **(Ichikawa and Miura 2007)** completed a recent study on mechanism of ASR in concrete. They stated that ASR starts with depolymerization of silica rich aggregate by OH^- and R^+ ions present in pore solution. The consumption of OH^- ion helps the dissolution of Ca^{2+} ions into the solution because the surface region of the aggregate is homogenously covered with the rigid reaction rim. This reaction rim will not permit the dissolution of alkali silicate gel but allows penetration of R^+, Ca^{2+}, and OH^- ions. Therefore the resultant expensive pressure accumulated in the aggregate cracks the aggregate and the

surrounding cement paste when the strength of material is exceeded. The schematic mechanism of ASR induced deterioration proposed by Ichikawa and Miura is shown in Figure 2.6.

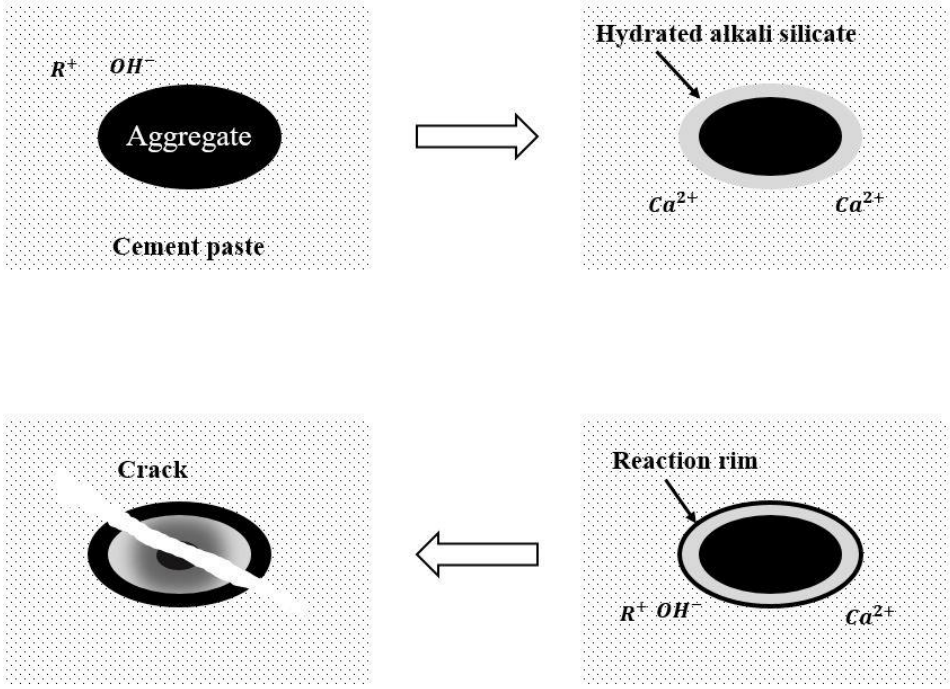

Figure 2.6. Schematic representation of the mechanism of ASR-induced cracking of concrete

2.5. ASR in Fly ash based concrete

Pouhet and Cyr (**Pouhet and Cyr 2015**) reported that although the metakolin based geopolymer mortar contained high concentrations of alkalis, were more able to resist ASR than OPC was, and no characteristic swelling or any significant loss of rigidity was observed for the geopolymer specimen. They also added that formation of a reaction product covering the entire surface of the glass grains in sand, and resulting in a significance decrease in adhesion between the sand and geopolymer was observed.

Tanzer et al. (**Tänzer et al. 2017**) mentioned that high inherent alkali content can undoubtedly increase the risk of ASR. However, it is valid only when the aggregate is alkali

reactive. They also mentioned that ASR itself does not necessarily lead to the deterioration in both Portland cement based concrete and slag based concrete. But, their study was not being able to provide a guideline on the mix design of alkali activated concrete, which can be adopted to avoid the distress due to ASR if reactive aggregates are used.

Williamson and Juenger, (**Williamson and Juenger 2016**) 2016 studied the role of activating solution concentration on ASR in fly ash based geopolymer concrete and found that increasing in concentration of alkali activator solution not only reduces that strength of the concrete, it also helps to increase the ASR potential in the concrete. They also mentioned that the ASR potential in alkali activated geopolymer concrete can be different with change in chemical composition and reactivity of aggregates used. However, Shi et al., 2017 reported that the ASR expansion decreases with increasing the alkali doses in the mix.

Shi et al. (**Shi et al. 2018**) concluded that there is an optimum doses of fly ash i.e. 30% to reduce the ASR expansion of studied mortars, whereas ASR expansion decreases with increasing the amount of metakolin. It has been also mentioned that the expansion can be completely suppressed when the slag is replaced by 70% metakolin. However, the supply of external alkalis need to be take care in order to reduce to the effects of ASR.

2.6. Microstructure analysis of ASR affected geopolymer concrete

2.6.1. Scanning electron microscopy (SEM)

Among variety of techniques, SEM is the most widely used instrument for taking microstructural images for the study of cementitious materials. There are two modes for obtaining the images from SEM. One is Secondary electrons (SE) and another is backscattered electrons (BSE). The SE mode is generally used to study the surface topography whereas the BSE mode is used to study the chemical composition and phase distribution **(Shin 2009)**.

Both optical and electron microscopic have been extensively used to study the occurrence of gel and cracking in aggregate and surrounding cement paste because of ASR. Owsiak **(Owsiak 2003)** used SEM equipped with high energy dispersive x-ray analyzer (EDX) to investigate the microcracks cement mortar bars and stated that SEM could be very useful in microstructure analysis when it is equipped with EDX. There are many current researches which used SEM images as background to model the effect of ASR and to find out a way to mitigate the ASR **(Haha et al. 2007; Jóźwiak-Niedźwiedzka et al. 2018; Kupwade-Patil and Allouche 2012; Pan et al. 2012)**.

2.6.2. Fourier transform infrared spectroscopy (FTIR)

Puertas and Jimenez **(Puertas and Fernández-Jiménez 2003)** studied about the microstructural and mineralogical characterization of cement paste obtained by alkaline activation of fly ash mixtures and cured at different temperature. FTIR results indicate the formation of reaction products as a consequence of alkaline activation of slag and fly ash. It has been mentioned that there are substantial changes in the spectra of region 1100-900 cm^{-1}, which shifted towards the higher frequencies as the reaction time increases. This result is also in agreement with the studies conducted by Palomo et al. 1999**.**

Puertas et al. (**Puertas et al. 2004**) investigated the relationship among the compositions of the pore solution in alkali activated slag cement (AAS). The pore solution was extracted from hardened AAS pastes and solid phases and analyzed using XRD, FTIR, NMR and BSE/EDX. The result obtained from FTIR and XRD confirms the formation of C-S-H and the significant change in the ionic composition of the pore solution between 3 and 24 hours of reaction. Shift in the v_3(Si-O) bonds to higher numbers (at 964 cm^{-1}) and v_4 (O-Si-O) bonds to lower wave numbers (at 450cm^{-1}) were noticed when AAS paste were activated with NaOH. It has been also

reported that, the FTIR spectra confirmed the presence, in activated paste, of crystalline calcium silicate hydrate with the largest displacement at v_3(Si-O) band.

Bakharev **(Bakharev 2005)** presented about the influence of elevated temperature curing on the phase composition, microstructure and strength development in geopolymer materials prepared using class F fly ash and sodium silicate and sodium hydroxide solutions. The result showed that, despite the presence of zeolite in some of the samples, there were no drastic modification of the bands in the 1600 cm^{-1} range corresponding to bending vibration (H-O-H), which were also observed by Palomo et al., 1999 in one of the sample cured at 85 °C. However, in this study the band was modified for all studied geopolymer materials. During the reaction, the band at 800 cm^{-1} disappears and a new band appears at around 700 cm^{-1} , while the band at 1200 cm^{-1} shifts to 960-1000 cm^{-1}. The bands below 960 cm^{-1} are enhanced in case of sodium hydroxide activated fly ash. With this findings, the researcher concluded that curing at room temperature is beneficial for the strength development of geopolymer concrete.

2.6.3. Micro computed tomography (Micro-CT)

For the first time, Provis et al. **(Provis et al. 2012)** performed micro CT on a set of sodium metasilicate-activated fly ash blends using a synchrotron beamline instruments. 3D pore connectivity data were obtained thorough cluster labelling and a contiguous set of 2D image slices were generated to represent the volume of interest by using segmentation algorithm. The volume of interest were than subjected to random-walker simulation to determine the physical properties of the pore network. The results showed increment in pore network tortuosity is directly proportional to the slag content and curing time, which indicated that the formation of space filling C-S-H gels begin to dominate the alkali activated binder system between 25% and 50% fly ash content, while samples with less than 25% fly ash content are dominated by N-A-S-

H gels which do not chemically bind water and do not provide the same extent of pore network obstruction. It has been mentioned that the accurate identification of pore and solid regions in alkali activated binder system was very difficult using CT scanning because of low elemental number and low X-ray absorption contrast. However, the researcher claimed that the use of micro CT scanning can provide a valuable information regarding porosity, pore geometry and tortuosity within a large systematic set of samples.

2.7. Summary

In this chapter several previous researches focused on geopolymer concrete and alkali silica reaction were reviewed. Since Stanton reported about alkali silica reaction on Portland cement concrete in 1940, this problem have continuously received much attention and large volume of researches are being performed in recent decade all around the world. Several methods have been implemented to investigate the mechanism of ASR but it is not fully understood yet. Some major methods utilized are expansion test and pore solution alkalinity measurement. However, the alkali silica reaction has not been much discussed in geopolymer concrete that will be discussed in upcoming chapters.

CHAPTER 3. MATERIALS AND METHODOLOGY

3.1. Introduction

This chapter provides the methods and details of the experimental process employed in the research. The present study used 100% high calcium (ASTM Class C) fly ash with the technology that is in use for Portland cement mix design and testing (ASTM C192, ASTM C143, ASTM C109), and type I Portland cement was used for the comparison purpose.

This study is divided into three major phases. In phase I, the material selection and the calculation for the mix design were carried out. The second phase contained the lab experiments including sample preparation, expansion test of concrete prism having different types of aggregates with different percentage of silica content on it, pore solution extraction from the hardened fly ash based geopolymer concrete and ordinary Portland cement concrete at different ages within a year and measurement of alkalinity of the pore solution. The third and final phase of this research includes microstructural analysis of the fly ash based geopolymer concrete using SEM/EDX imaging, FTIR, and microtomography technologies. The microstructural studies were carried out to investigate the formation of ASR gel, expansion of gel, crack formation on the aggregate, change in chemical composition and change in porosity of the samples at different ages, with the purpose to verify the result obtained from the experimental investigation. Type I ordinary Portland cement concrete was also used in every testing to compare with the properties of fly ash based geopolymer concrete.

3.2. Material used

3.2.1. Fly ash

For all the experiments containing fly ash, 100% class C fly ash (according to ASTM C618) was used. The fly ash (Figure 3.1) was produced by Minnkota Power Cooperative. The physical properties of fly ash is given in Table 3.1. The specific gravity of the fly ash is 2-2.8 g/cc. The fly ash contains significant amount of sodium, magnesium, silica and calcium as shown in Figure 3.2. The XRD analysis of fly ash is shown in Figure 3.3. Specific weight of fly ash varies much. In order to have an accurate mix design, the specific gravity of the fly ash adopted is calibrated through weighting and volume measuring (Figure 3.1). The volume measuring is conducted through measuring cup.

Table 3.1. Description of the properties of the Fly Ash

Physical State	Solid (Powder)
Odor	None
Color	Creamy yellow
Vapor Pressure	NA
Specific gravity	2000-2800 kg/m^3
Evaporation rate	NA
Viscosity	None (Solid)
Boiling point	>1000 °C
Freezing point	NA

Figure 3.1. Weighing of fly ash

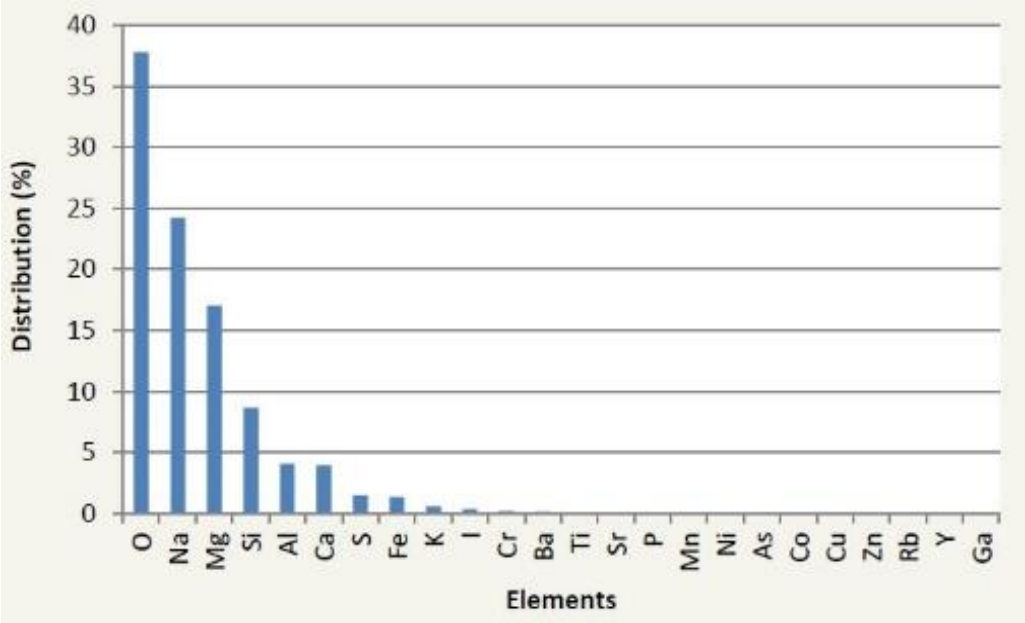

Figure 3.2. XRF chemical-component analysis of fly ash

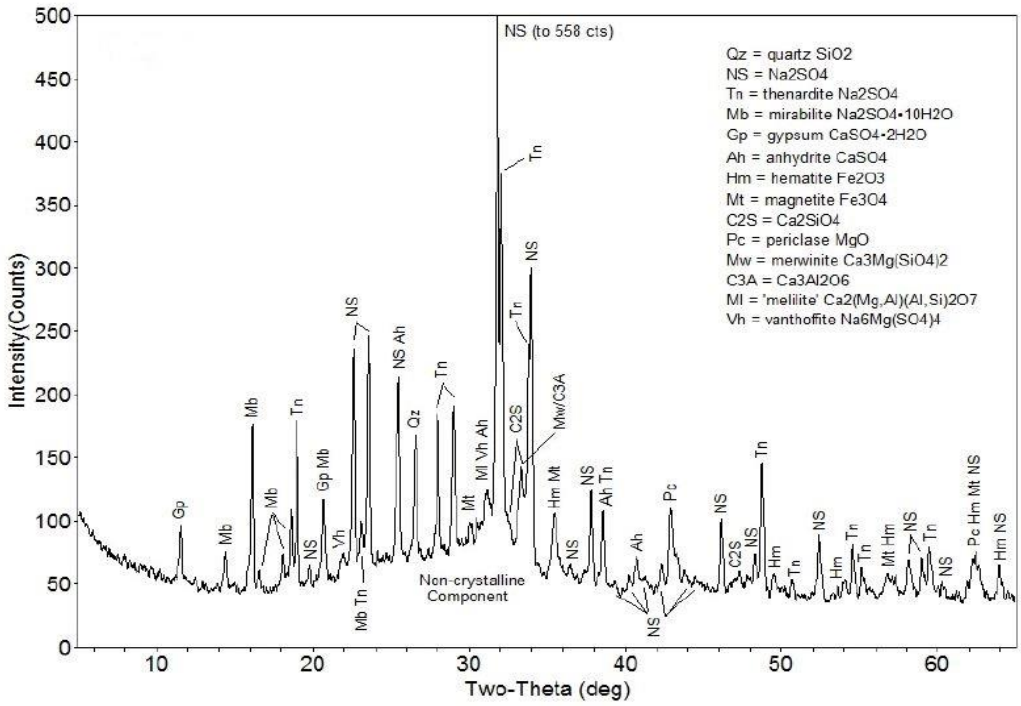

Figure 3.3. X-ray diffraction (XRD) analysis of fly ash

3.2.2. Ordinary Portland cement

To prepare all the concrete specimens containing ordinary Portland cement, type I cement is used because type I cement is the most common cement adopted for general constructions such as buildings, bridges, pavements etc. Table 3-2 provides a description of the properties of the cement used in this research.

Table 3.2. Description of the properties of cement used

Physical State	Solid (Powder)
Odor	None
Color	Grey (Greenish grey)
Vapor Pressure	NA
Specific gravity	3150 kg/m^3
Evaporation rate	NA
Viscosity	None (Solid)
Boiling point	>1000 °C
Freezing point	NA

3.2.3. Aggregates

a) Fine aggregate

Play sand (Figure 3.4) available in local market (Fargo, ND) was used. The specific gravity of the sand was 2650 kg/m^3. The detail of gradation of the sand is given in Table 3.3, through sieve analysis based on ASTM C33 **(ASTM 2018)**.

Figure 3.4. Weighing fine aggregate (sand)

Table 3.3. Gradation of fine aggregates

Sieve Sizes	**% Passing**
4.75 mm	99.21
2.36 mm	89.36
1.18 mm	74.58
600 μm	51.39
300 μm	21.12
150 μm	4.52
75 μm	2.08
Pan	0.67

b) Coarse aggregates

This research was mainly focused on the types of aggregates and effect of their sizes and chemical composition on the alkali silica reaction in fly ash based geopolymer concrete. The same aggregates were used for the similar tests of ordinary Portland cement concrete for comparison purpose. Three different types of aggregates, Granite, Carbonate, and Gravel, were collected from different locations in the United States and used for this study. The granite was collected from Minnesota; carbonate was from Texas; and gravel was from California. The gravel consists of about 63 percentage of silica whereas carbonate and granite consist of only about 30% and 1% of silica respectively. The calcium was maximum in granite at about 20% whereas carbonate and gravel contains about 3% and 2% of calcium respectively. XRF chemical component analysis of all three types of aggregates is given in Figure 3.5, 3.6, and 3.7.

Removing detrimental dust and clay is important since it may affect the water demand of the concrete mix. Therefore, the aggregate were cleaned using clean water and dried before used. Table 3.4 provides the gradation Table for all three types of coarse aggregates used.

Table 3.4. Gradation of all three coarse aggregates

Sieve Sizes	**% Passing**
25 mm	100
19 mm	95
12.5 mm	60
9.5 mm	15
4.75 mm	10
Pan	5

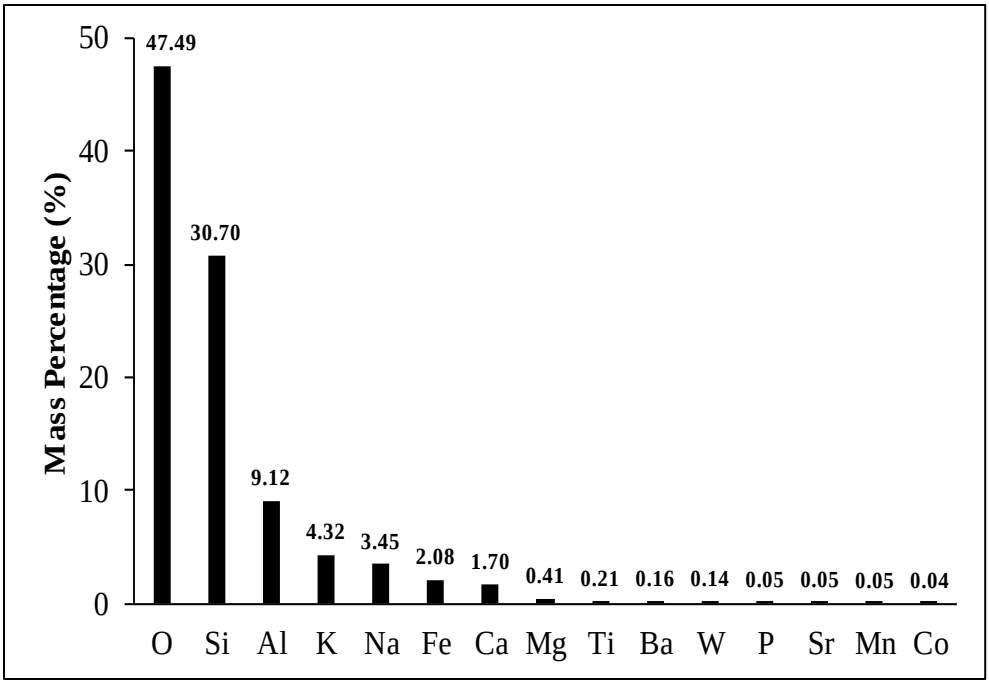

Figure 3.5. XRF chemical component analysis of Carbonate aggregate

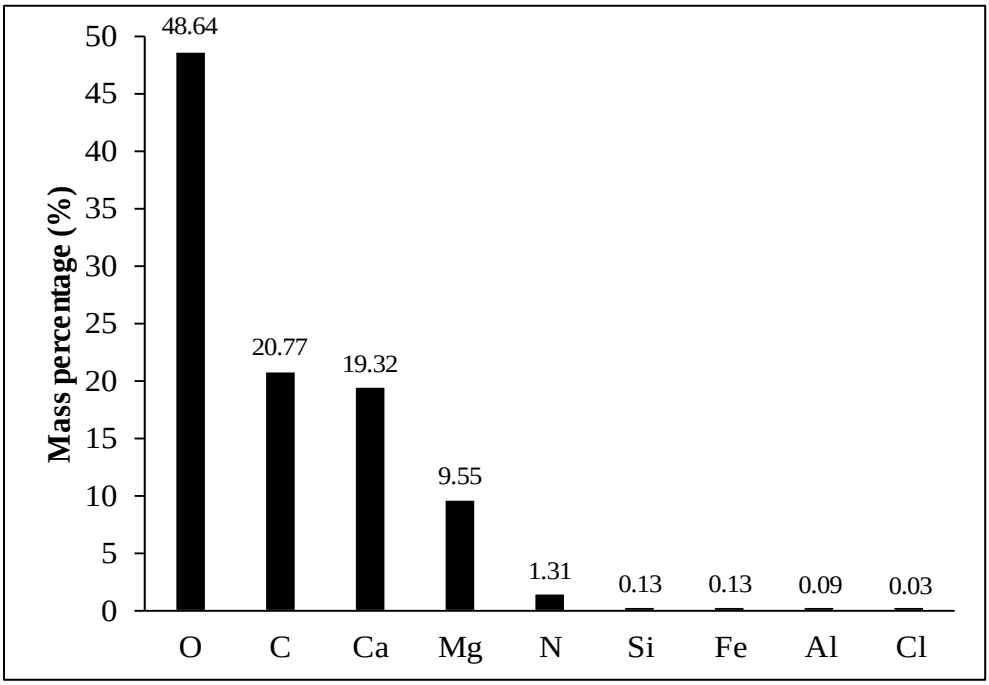

Figure 3.6. XRF chemical component analysis of Granite aggregate

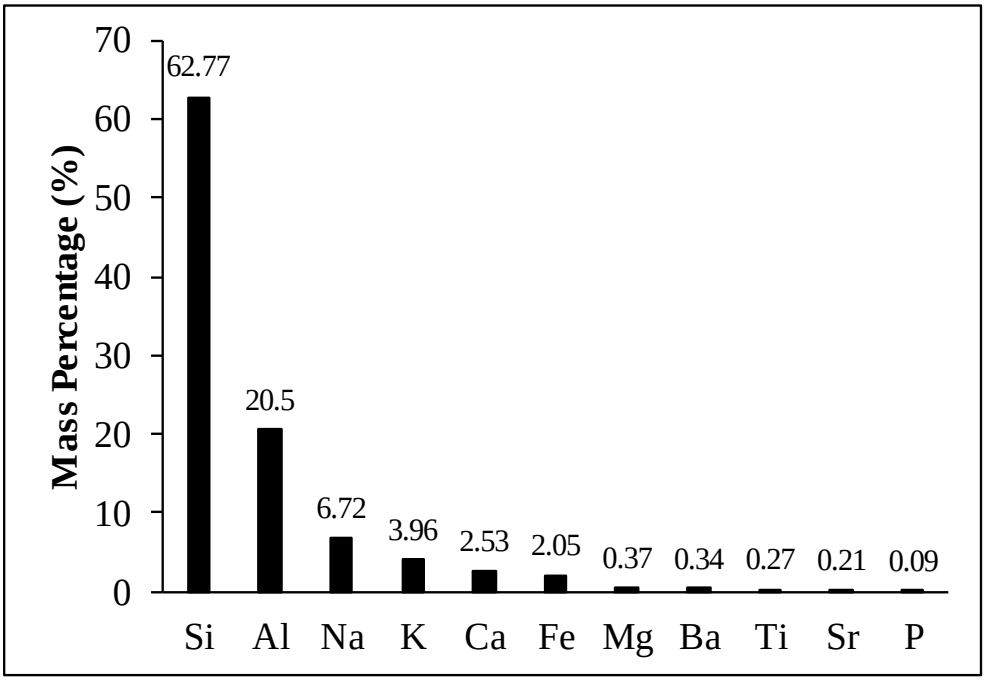

Figure 3.7. XRF chemical component analysis of Gravel aggregate

3.2.4. Alkaline activator solution

The most common alkaline activator are solution of sodium or potassium hydroxide with sodium or potassium silicate. This solution is used to enhance the polymerization of the geopolymer concrete. There are still several controversies in between the performance of sodium and potassium. Khale and Chaudhary **(Khale and Chaudhary 2007)** mentioned that since K^+ is more basic, it allows a higher rate of solubilized polymeric ionization and dissolution and leads to a denser polycondensation reaction on its overall network formation and an increase in strength of the matrix. However, Arjunan et al. **(Arjunan et al. 2001)** reported that sodium hydroxide in a low concentration was the most effective activator. Regardless of type selected, however, higher concentration of alkali activator enhances the ionization reaction and forms a stronger matrix **(Petermann et al. 2010)**.

In this study, a sodium based alkaline solution was used as the alkaline activator, which is a mixture of sodium hydroxide flakes and sodium silicate solution. The sodium silicate solution was supplied by the science company which consists of 9% Na_2O, 28% SiO_2, and 63% water, by mass. The sodium hydroxide flakes has a purity of 98%. The alkaline solution was prepared by dissolving NaOH flakes into Na_2SiO_3 solution that was proportioned to desired SiO_2/Na_2O molar ratios. This molar ratio between SiO_2 and Na_2O is defined as activator modulus. The Na_2O content in the alkaline solution includes both the Na_2O content in the Na_2SiO_3 solution and the Na_2O content equivalent in the NaOH. The Dosage of Na_2O ($\%Na_2O$), which is the mass ratio of the Na_2O content for the alkaline solution to the fly ash's mass. Three different activator modulus (1.0, 1.2, and 1.4) were used with each of 10% and 12% of Na_2O doses as shown in Table 3.5.

3.2.5. Water

Ordinary Fargo city tape water was used for mixing in the experiments.

3.3. Mix design

This section describes the basic mix design procedure used to prepare the mixes of the research. ASTM C109 and ASTM C192 were followed during the preparation of the mixes **(ASTM 2016; ASTM 2018)**.

3.3.1. Cementitious material, sand, and coarse aggregate ratio

The ratio of the cementitious material (ordinary Portland cement or fly ash), sand and coarse aggregate is the major factor that affects properties of the mix. Since the whole research is about the effect of aggregates with different chemical composition (silica content) on alkali silica reaction, the major emphasis was provided on aggregate content in the mix. For this research

experiments, cementitious material, sand and coarse aggregates were used in a ratio of 1:2:3 (Table 3.5) for both beam and cube sample preparation following ASTM C192.

Table 3.5. Geopolymer concrete mix ratios

Mix	**Activator modulus**	**Na_2O doses (%)**	**W/B ratio**	**Mix ratio**
FA-1	1.0	10%	0.3	1:2:3
FA-2	1.0	12%	0.3	1:2:3
FA-3	1.2	10%	0.3	1:2:3
FA-4	1.2	12%	0.3	1:2:3
FA-5	1.4	10%	0.3	1:2:3
FA-6	1.4	12%	0.3	1:2:3

Table 3.6. Ordinary Portland cement concrete mix ratios

Mix	**W/C ratio**	**Mix ratio**
OPC	0.3	1:2:3

3.3.2. Water-binder ratio

The primary difference between geopolymer concrete and ordinary Portland cement (OPC) concrete is the binder system. The water-binder (w/b) ratio is the controlling factor for most of the desirable properties of the concrete such as strength, durability, shrinkage potential, and permeability. In this research, experiments include the expansion measurement, analysis of pore solution, and microstructure analysis of the concrete specimen. In case of ordinary Portland cement based concrete, cement was taken as the binder where in case of fly ash based geopolymer concrete, mix of fly ash, sand and solid particles in the alkaline activator was considered as the binder. For this research experiments, the w/b of 0.3 was used (Table 3.5, 3.6).

3.3.3. Preparation of alkaline solution

Alkaline solution is used not only to increase the polymerization speed and strength of the geopolymer concrete, it also plays a vital role in the alkali silica reaction**(**In this research, the mixture of sodium hydroxide (NaOH) flakes (Figure 3.8) and sodium silicate (Na_2SiO_3) solution (Figure 3.8) were used as an alkaline activator). The solution (Figure 3.9) was prepared 24 hours prior to mixing due to heat generation while dissolving NaOH.

Figure 3.8. Sodium hydroxide flakes

Figure 3.9. Sodium silicate solution

Figure 3.10. Alkaline activator solution

3.4. Effect of different types of aggregates on expansion of geopolymer/OPC concrete

The intent of this study is to determine if the chemical composition of different type aggregates has any effect on the alkali silica reaction in fly ash geopolymer concrete and ordinary Portland concrete.

3.4.1. Sample preparation

Before mixing the materials, the interior of the mixer, pan, and all tools used for the mixing and placing concrete were coated with water to minimize the moisture loss during the mixing procedure. The mixing was performed as ASTM C192 using the mix design mentioned in Table 3.5 and 3.6. The concrete beam sample preparation for the expansion (length change) measurement were carried out as ASTM C1260 and ASTM C1293-08b **(ASTM 2008; ASTM 2014)**.

In case of manufacturing geopolymer concrete beam, the specific type of coarse aggregate was added to the drum mixture with about half of the alkaline activator solution and

then mixed for about 30 seconds. The fly ash, fine aggregate and the rest of the liquid were added to the mixture slowly while the mixing was in process. The mixture was stirred for another 2 minutes after all the ingredients were added. After that, the mixture was stopped and rested for 1 minutes and then again stirred for 2 minutes to complete the mixing process. One snapshot in the mixing process of geopolymer concrete is provided in Figure 3.11.

Figure 3.11. Mixing of geopolymer concrete

In case of Ordinary Portland Cement (OPC) concrete beam, the calculated amount of designated coarse aggregate, fine aggregate and cement was added to the drum and mixed for about 1 minute. Then, calculated amount of water was added to the mixture while the drum was running. The mix was stirred for 1 minute and then stopped and rested for 15 second. After that, the mixture was again stirred for another 1 minute to complete the mixing process. One snapshot in the mixing OPC of concrete is given in Figure 3.12.

Figure 3.12. Mixing of OPC concrete

For both fly ash and OPC concrete, after the preparation of mixture, concrete prism (Figure 3.13) of 2 x 2in cross-section and 10 in length were casted in two layers, according to ASTM C157. Each layer was manually rodded 25 times, evenly over the surface, and followed by 10 to 15 light taps with a rubber mallet on the outside of the molds. After the top layer has been compacted, the concrete was cut off with the top of the mold and smooth the surface with a few strokes of the trowel. For each mix (Table 3.5), three samples were prepared using all three different types of aggregates so there were a total of 21 beam samples.

In 24 hours after the molding, both fly ash and OPC concrete specimens were removed from the mold. The geopolymer concrete were allowed for ambient air curing whereas the OPC concrete specimens were placed in water for water curing to the required amount of curing time for testing.

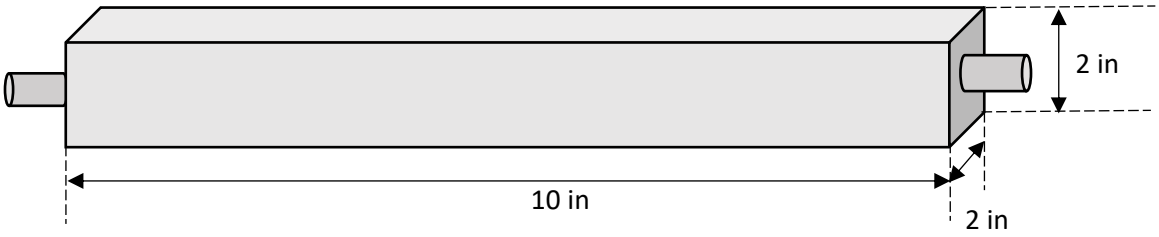

Figure 3.13. Specimen configuration used for expansion testing

3.4.2. Expansion measurement

Expansion of all the concrete specimens was measured using a digital length comparator device as shown in Figure 3.14 per ASTM C1293-08b. The accuracy of the measurement was 0.0001mm. Expansion of each concrete beam was measured up to 365 days after the sample preparation. The percentage length change on a specific day was calculated using the following expression.

Figure 3.14. Length change measurement setup

$$\Delta L = \frac{L_f - L_i}{G} \text{ X } 100\% \tag{3.1}$$

Where, ΔL = Change in length at an age of 'f' days

L_f = Length of specimen at 'f' days in inch (Considering reference bar)

L_i = Length of specimen at zero days in inch (Considering reference bar)

G = Nominal gauge length (10 inch)

3.5. Effect of different types of aggregates on pore solution chemistry of geopolymer/OPC concrete

Alkali silica reaction and its reaction product highly depend upon the chemical composition of the concrete solution. This section describes the methods used to prepare the sample using all three different types of aggregates, extract the pore solution from the concrete specimen, and examine the alkalinity of the extracted pore solution. Since there is no exact standard test to extract and examine the concrete pore solution, an unstandardized method was developed for this experiment.

3.5.1. Sample preparation

Sample preparation for the pore solution alkalinity test took several steps. It started with the preparation of concrete cylinders as shown in Figure 3.15. All the equipment including mixing drum, pan, and molds were cleaned and coated with water to minimize the moisture loss during the mixing procedure. The mixing of the materials were conducted per ASTM C109 for all the mixes mentioned in Table 3.5 and 3.6. The concrete cylinder specimens were prepared per ASTM C39 and ASTM C192 **(ASTM 2018)**.

Figure 3.15. Geopolymer concrete cylinder specimens

As mentioned in Section 3.4.1, in case of fly ash based geopolymer concrete, the concrete cylinder preparation started with mixing the coarse aggregate and half of the alkaline activator solution in mixing drum. Then all other remaining materials were added in following 30 second while the mixer is running, and the mixing continuously run for another 2 minutes. The mixing drum was stopped for 1 minutes and again and stirred for another 2 minutes to complete the mixing process. Whereas in case of the OPC concrete, all the solid particles were first mixed for about 1 minutes and water was added. The mixture was run for another 1 minute followed by 15 second rest and another 1 minute mixing. To make sure that the mixing process is consistent, the similar mixing procedure for both expansion test specimen preparation and pore solution test experiment was followed.

In case of both OPC and geopolymer concrete, the cylinder with 4 in diameter and 8 in height were casted in three layers per ASTM C192. Each layer was manually rodded 25 times

using 5/8 in diameter tamping rod evenly over the surface. The rubber mallet was used to make sure the even compaction by tapping on the outside of the mold. Three cylinders were prepared for each mix. Since there were three different types of aggregate and the testing was carried out in specific days for 1 year, total of 168 cylinder samples were prepared.

3.5.2. Pore solution extraction

Selection of proper pore solution extraction mechanism is very important because there is no exact standard method and the amount of solution obtained and the properties of extracted solution may depend upon the method used. However, there are some literatures that used different methods to extract the concrete pore solution for different purpose.

Barneyback and Diamond **(Barneyback Jr and Diamond 1981)** introduced a high pressure device to extract the pore solution from the hardened Portland cement paste. This is a highly complicated process from which only a very small amount of solution could be obtained. Li et al. **(Li et al. 2005)** reported that, this process is very complicated to be executed and it is difficult to separate the different constituents form the pore solution as well. The limitation associated with this method also includes prior saturation of the sample and lower solution yield in concrete. Cyr et al. **(Cyr et al. 2008)** mentioned that the leaching method is an efficient way to study the pore solution but it also have some limitations, such as moisture saturation is required, the affected volume needs to be assumed, and the method is time consuming. Even though, there are several researches has been carried out to build a standard test to extract the pore solution from hardened OPC concrete there are only few studies have been carried out on geopolymer concrete pore solution. Kapat et al. and Pradhan and Bhattacharjee **(Kapat et al. 2006; Pradhan and Bhattacharjee 2007)** extracted concrete pore solution by forming concrete power to perform the potentiostatic study of reinforcing steel in chlorine contaminated concrete.

This study follows the similar procedure to extract the pore solution and to investigate the alkalinity.

The extraction of pore solution of concrete cylinder was carried out on specific ages. To extract the pore solution from the concrete specimen, the specimen were first broken using compressive strength testing machine and then further crushed by using grinding machine. The crushed material was than sieved through a square sieve of 150 μm and the collected powder was stored in an air tight condition. This power includes the mixture of all the constituents that were used in the preparation of the specimen.

The powder in air tight condition was mixed with distilled water in 1:1 proportion by mass and then stirred for half an hour. The solution was then boiled for 15 minutes at 130 degree Celsius temperature and allowed to cool for 10 hours in room temperature. The solution was then filtered through Whatman No. 1 filter paper. The final solution obtained from the filtration process was considered as the pore solution. The two step flow diagram in Figure 3.16 illustrates the process used for extraction of concrete pore solution and measurement of pH value of the solution.

3.5.3. pH measurement

The pH of the pore solution has direct relation with the alkalinity of the solution. The progress of the alkali silica reaction can be explained using change in the pH of the pore solution. When the pore solution was extracted, a digital pH meter was used to measure the alkalinity of the pore solution. The pH measurement of pore solution of all the geopolymer and OPC concrete specimens prepared by using different aggregate and mix proportions were carried out in different days up to 1 year. A digital pH meter as shown in Figure 3.17 with accuracy level of 0.1 was used to measure the pH level of pore solutions.

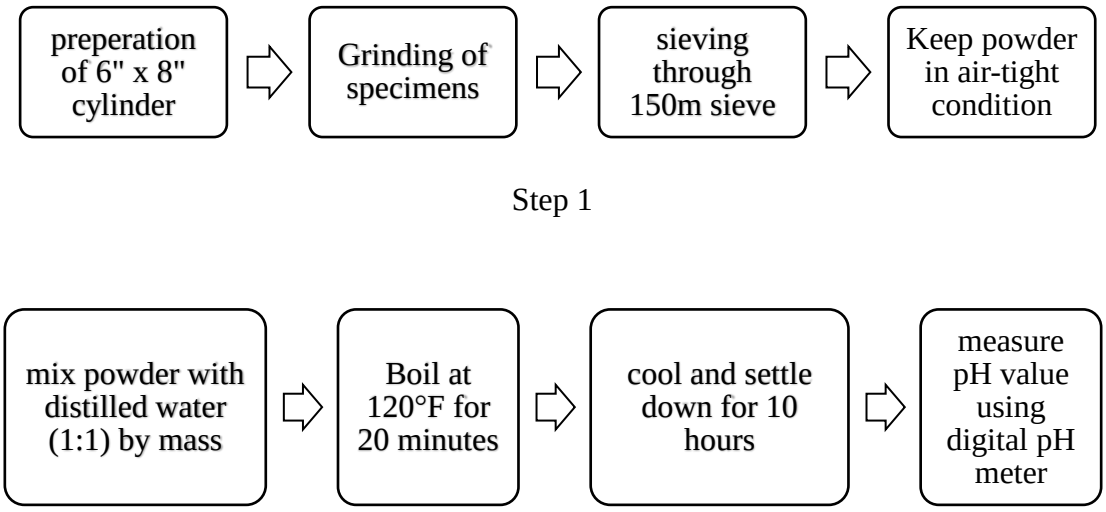

Figure 3.16. Flow diagram for extraction and pH measurement of pore solution in concrete cylinder specimens

Figure 3.17. Measurement of pH value of pore solution

3.6. Effects of different types of aggregate on ASR of GPC and OPC at microstructure

This section will describe about the microstructural analysis of alkali silica reaction mechanism on geopolymer concrete and OPC concrete. The alkali silica reaction (ASR) is characterized by the breakdown of silanol bonds in poorly crystallized silica found in aggregates

in the presence of alkaline ions. The product of this reaction is an amorphous alkali silica gel which expands in the presence of moisture, and induces stress in the microstructure. It usually takes long time (several years) to see the effect of alkali silica reaction in concrete structure in real life.

In this research, the microstructure of the geopolymer concrete and OPC based concrete specimen were studied using scanning electron microscopy (SEM), Fourier transform infrared spectroscopy (FTIR), and computer tomography (CT).

3.6.1. SEM/EDS

Scanning electron microscopy involves identifying ASR gel by its characteristic morphology. The purpose of this study was to investigate the effect of aggregates with different chemical composition in ASR gel production at microstructural level using SEM imaging. The study also included change in chemical composition of the aggregate binder interface because of the chemical composition of different aggregate types.

3.6.1.1. Sample preparation

All three types of aggregates were used to prepare the specimen. Since the laboratory experiments about expansion measurement and pore solution alkalinity test have been already done for all mix design of fly ash based geopolymer concrete and OPC concrete mentioned in Table 3.5 and 3.6, as such, only the most vulnerable cases were selected for the further microstructural analysis. Mix 6 was selected to perform the SEM analysis and make comparison with that of OPC concrete. The SEM test will investigate the mechanism of ASR in fly ash based geopolymer concrete with respect to aggregate chemical composition.

3.6.1.2. Image acquisition and analysis

The SEM test was carried out on 1 year old specimens. The specimens prepared were attached to cylindrical aluminum mounts (Figure 3.18) with high-purity conductive silver paint (Structure Probe Inc., West Chester, Pennsylvania, USA), and then sputter coated (Cressington 108 auto, Ted Pella, Redding, California USA) with a conductive layer of gold. Images were obtained with a JEOL JSM-6490LV scanning electron microscope (JEOL USA, Inc., Peabody, Massachusetts USA, shown in Figure 3.19) at an accelerated voltage of 15 kV.

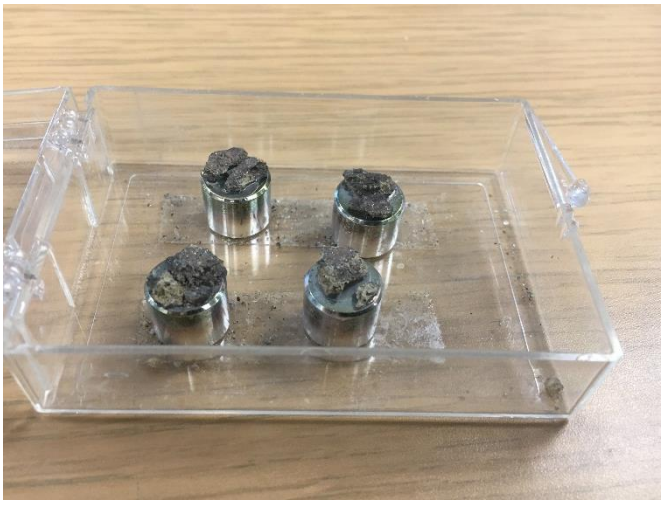

Figure 3.18. SEM/EDS Specimens

Figure 3.19. Scanning electron microscope

After acquiring the images, the attached EDS (Energy dispersive spectrum) was used to analyze the chemical composition of different locations at aggregate binder interfaces. For all different types of geopolymer concrete with different types of aggregates, different locations were selected in such a way that we could Figure out the difference between the chemical composition of those specific locations.

3.6.2. FTIR

The FTIR spectroscopy was used to determine the different chemical bonds including Si-O-Si, Si-O-Al, and Si-OH in the reactive aggregates that have been gone through alkali silica reaction.

3.6.2.1. Sample preparation

The preparation of specimen for the FTIR started from preparation of the concrete cubes (Figure 3.20). The 2in x 2in concrete cubes were prepared for all the mix design mentioned in Table 3.5 and 3.6 for both geopolymer concrete and OPC concrete.

Figure 3.20. Cube specimen used to make slices for FTIR analysis

After the preparation of the concrete cubes, in case of geopolymer concrete, the specimens were placed in ambient temperature for the air curing while OPC concrete were placed in water curing for 28 days. After 28 days, both OPC and geopolymer concrete were placed in ambient temperature until the test was carried out. Since the FTIR equipment available required a thin sample. The specimen were cut and sliced to 2/5 inch (1cm) in thickness (Figure 3.21) using diamond saw. The sliced specimens were dried and smoothed using sand paper before performing the FTIR experiment.

Figure 3.21. FTIR Specimens

3.6.2.2. FTIR spectroscopy

The FTIR spectroscopy of all the concrete specimen were carried out using Thermo Scientific Nicolet 8700 FT-IT spectrometer (Figure 3.22). This equipment is able to perform advanced FTIR spectroscopy experiments including step scan. The one year old specimen were

used for the FTIR analysis since ASR takes longer time to take place. The FTIR spectrum were observed for all the concrete specimen and compared to analyze the effect of different types of aggregates on alkali silica reaction in fly ash based geopolymer concrete and OPC.

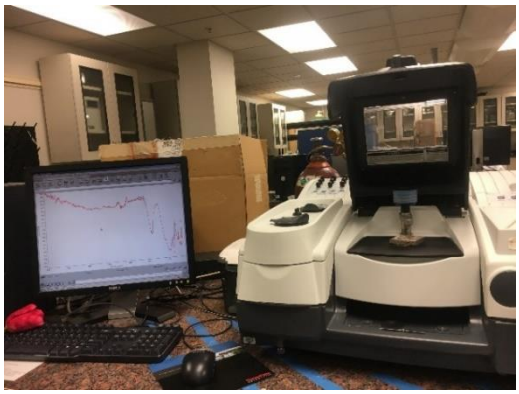

Figure 3.22. FTIR testing setup

3.6.3. Micro-CT scanning

Micro computed tomography (micro-CT) has attracted much attention as a new method for the characterization of heterogeneous materials at the microscale. This technique, by which a 3D volume of sample reconstructed from 3D projections taken at different angular steps, has proven to be very valuable for non-invasive investigation, at micron scale, of small samples. There are generally three types of CT scanning: mini-CT, micro-CT, and nano-CT based on the scale. In this researchmicro CT was used to scan the concrete specimens.

Since this technology does not require breaking the specimen, same specimen was used. Even though micro-CT scanning could be a very reliable method, it is time consuming, quite expensive, and highly sensitive.

3.6.3.1. Sample preparation

The geopolymer and OPC concrete with different types of aggregates were prepared per ASTM C109. Same as before, only mix 6 from Table 3.5 for geopolymer concrete and mixes from Table 3.6 for OPC concrete were selected.

Since the resolution of the scanned file and the time taken to scan not only depend upon the capacity of the equipment, it also depends upon the specimen size. Here the specimen were prepared in 2 x 2 in cubes.

All the tools required including mixer, pan, and trowels were cleaned and coated with water in the interior side to minimize the moisture loss during the mixture procedure. As mentioned in Section 3.4.1, in case of geopolymer concrete, the specific type of aggregate and alkaline solution was mixed first and other materials were added later with several stops and runs of mixing. The mixing procedure of OPC based concrete was slightly easier which starts with mixing of all the dry components and addition of water followed by mixing for some more time.

Figure 3.23. Molding of 2 x 2in concrete cubes

After the preparation of concrete mix, the concrete cubes of size 2 x 2 in were casted in 2 layers (Figure 3.23) per ASTM C 109. Each layer was manually rodded using rubber rectangular bar 25 times evenly over the surface and followed 5 to 8 light taps with a rubber mallet on the outside of the molds. After finishing the second layer rodding, the lop layer was smoothened using trowel. The specimens were then demolded after 24 hours of casting and placed for air curing in room temperature.

3.6.3.2. Three-dimensional scanning

All the specimens with different types of aggregates were scanned on 1 day after the demolding for the investigation of early age properties and scanned again after 90 days for the comparison purpose. During this 90 days interval all the specimens were placed in ambient temperature. The specimens were scanned using GE v|tome|x s microCT available at electron microscopy center, North Dakota State University (Figure 3.24).

Figure 3.24. GE v|tome|x s microCT scanning device

3.6.3.3. Parameters set up

Quality of MicroCT scanner depends upon several parameters. These parameters include thresholding, noise reduction, and selection of deviation factor. Thresholding is basically a method of image segmentation. Thresholding can be used to create binary images from a greyscale image. Noise reduction is very important while doing the microstructural analysis of the concrete specimens because the concrete specimens are highly complex in microstructural level and a small change in noise can have a big effect on its result. The ratio of gray value over its standard deviation provides a signal to noise ratio for the material.

It is important to realize that any image processing will affect noise on the material over background, which enhances an overall image quality- for example applying a de-noising filter during reconstruction will reduce the variation of gray value thereby increasing the signal to noise ratio. Therefore this criteria is recommended on unprocessed data.

Threshold value has a very big role while quantifying the porosity and void ratio of the sample. In this research auto threshold was used because the contrast between foreground and background was good enough. Auto threshold was chosen also to confirm that all the specimens were analyzed under similar condition.

In this research, all the specimens mentioned in Section 3.6.3.1 were scanned using GE v|tome|x s microCT scanner and software called myVGL was used for the analysis. At first, scanned files were inserted into myVGL than the region of interest was extracted based on different parameters set up such as threshold, noise, and boundary of sample. The porosity and expansion percentage on x, y, and z direction of each specimen were carried out individually and compared.

3.6.3.4. Expansion of the specimen along different directions

Expansion of both ordinary Portland cement concrete and geopolymer concrete with different types of aggregates were carried out and mentioned earlier in this chapter, using ASTM C1293. Since this method provides the expansion of the specimen only on the longitudinal directions, the 3D scanned image from microCT was used in this chapter to measure the expansion coefficient of the specimen in all three directions. The similar method as mentioned in ASTM C1293 was used for the sample preparation but the size of the sample was chosen different. Since scanning of a large sample (2" x 2" x 10") and analyzing that is quite tedious using microCT and measurement of expansion in three dimensions will be less meaningful, here specimens of 2" cube size were used.

After the application of several parameters using myVGL as mentioned earlier, each side of the cube was divided into four equal parts (Figure 3.25). The reason behind dividing each plane into four equal parts is the edge of the specimen is not perfectly straight (Figure 3.26) and measuring a single value can not give the exact amount of the expansion of specimen in that direction.

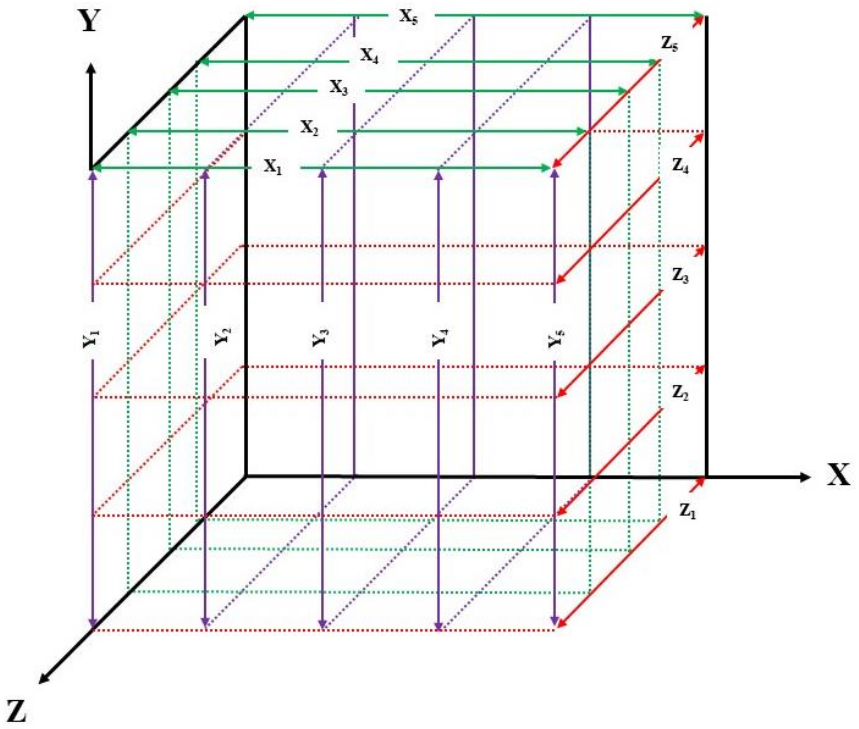

Figure 3.25. Schematic diagram of measurement of expansion in 3D specimen

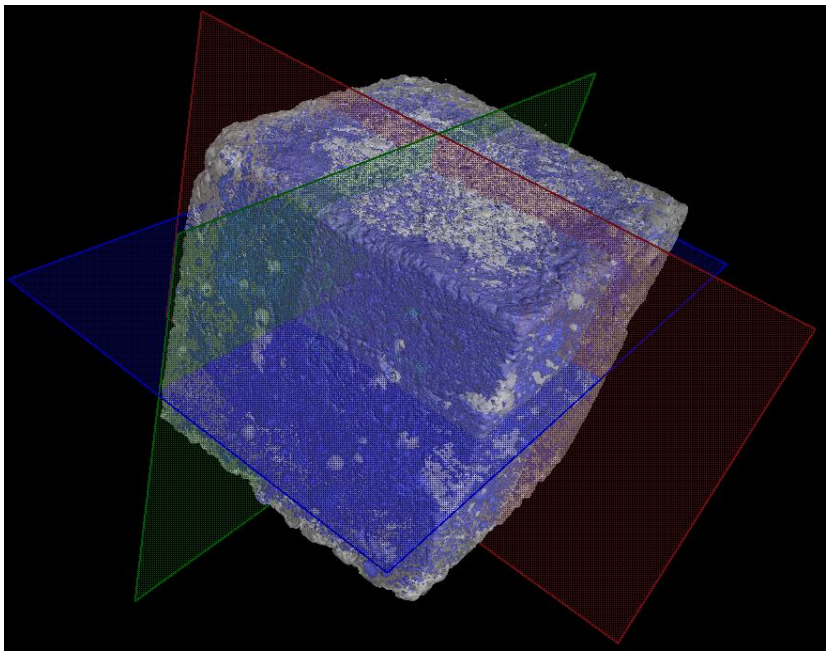

Figure 3.26. Slicing of whole block to find out the exact location for length measurement

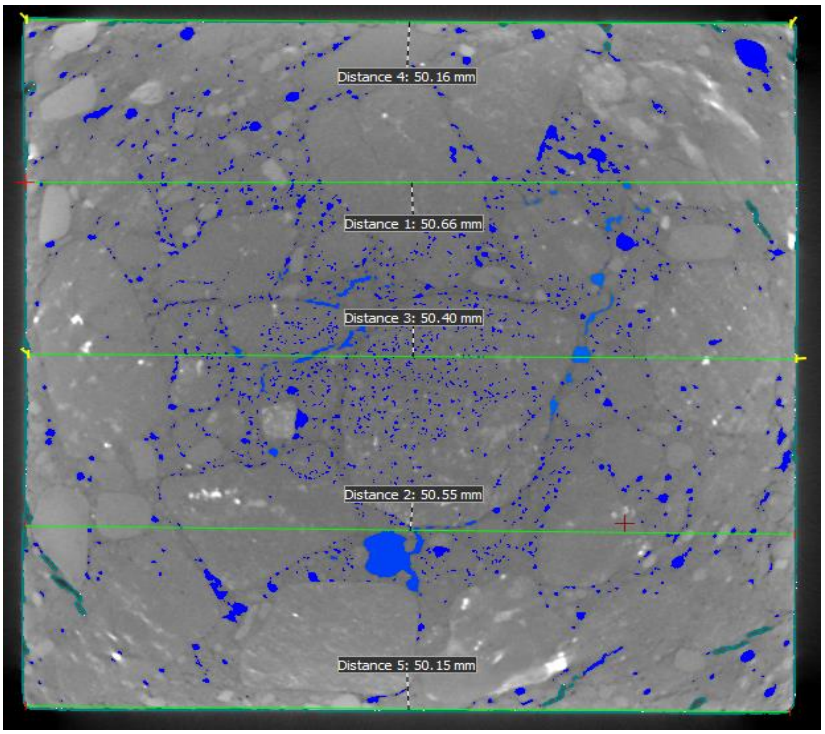

Figure 3.27. Example showing the measurement of length

Equations 3.1, 3.2, and 3.3 were used to calculate the average expansion of the each specimen in X, Y, and Z direction. Where X_1, X_2, X_3……, Z_4, and Z_5 are distances in different direction as shown in figure 3.25.

$$\text{Expansion in X} = \left(\frac{X_1+X_2+X_3+X_4+X_5}{5}\right)_{\text{final}} - \left(\frac{X_1+X_2+X_3+X_4+X_5}{5}\right)_{\text{initial}} \quad (3.2)$$

$$\text{Expansion in Y} = \left(\frac{Y_1+Y+Y_3+Y_4+Y_5}{5}\right)_{\text{final}} - \left(\frac{Y_1+Y_2+Y_3+Y_4+Y_5}{5}\right)_{\text{initial}} \quad (3.3)$$

$$\text{Expansion in Z} = \left(\frac{Z_1+Z_2+Z_3+Z_4+Z_5}{5}\right)_{\text{final}} - \left(\frac{Z_1+Z_2+Z_3+Z_4+Z_5}{5}\right)_{\text{initial}} \quad (3.4)$$

3.6.3.5. Porosity measurement

Voids in the concrete can be filled with air and water. Air voids are obvious and easily visible examples of pores in concrete. Broadly speaking, the more porous the concrete is, the weaker it will be. The most important contributor of the porosity in the concrete is the ratio of water to binder (cement or any other cementitious material). Basically, porosity or void fraction

is a measure of the empty space in a material. Sometimes there can be a confusion between void ratio and porosity. The difference between void ratio and porosity is that void ratio is defined as the ratio of volume of void to the volume of the solid whereas porosity is defined as the ratio of volume of void to the total volume of the testing sample.

Since alkali silica reaction has several steps which basically includes dissolution of silica, formation of gel, expansion of gel, and ultimately cracking of aggregates and the failure of the structure. Here in this part of the study, we are trying to measure the porosity of the geopolymer concrete and ordinary Portland cement concrete with different types of reactive aggregates at different ages to see the changes in the porosity of the concrete and also to find out the change in shape and size of the pores inside it.

The same specimen used for measuring the expansion in three directions was used for the porosity measurement. Each specimen were scanned through the microCT scanner after 1 day of demolding and porosity was calculated. The same specimen were stored per ASTM C1293 for next 90 days and scanned again to measure the porosity for comparison purpose.

Porosity of each specimen were calculated using Equation (4.4)

$$\text{Porosity } (\Phi) = \frac{V_V}{V_T} \tag{3.5}$$

Where,

V_v = Volume of the void space (volume of air plus fluid inside specimen)

V_T = Total volume of the specimen

It is very difficult to import the complete volume of the specimen into myVGL from the microCT scanned files and loss of small particles from specimen during storage (for 90 days) can have a big change in the porosity calculations. By considering the concrete was mixed uniformly

and aggregate distribution is homogenous, a volume of 1.75” x1.75” x 1.75” was extracted from the center of the specimen for porosity measurement.

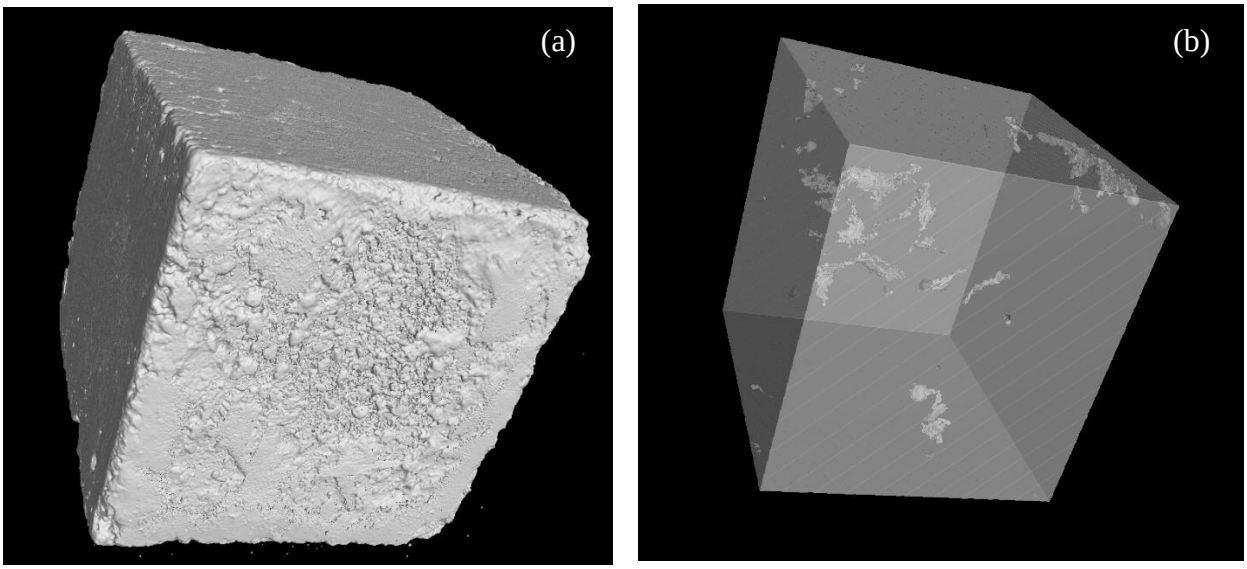

Figure 3.28. Original scanned image (a) and extracted 1.75” x 1.75” x 1.75” cube for porosity measurement (b)

3.7. Summary

In this chapter the details of materials used and experimental methods employed in this research were discussed. The chemical composition of three different types of aggregates and X-ray diffraction of fly ash used were also provided. It also described the geopolymer concrete mixes and the OPC concrete mix used in several experiments performed. The length change measurement of both OPC and geopolymer concrete were performed up to 365 days. The pore solution extraction from the hardened concrete was conducted on the same days. SEM imaging and FTIR spectroscopy of aggregate-binder interface were carried out to investigate the change in chemical composition and bonding because of alkali silica reactions. Finally, this chapter also

described the complete procedure used during microCT scanning of concrete specimens and measurement of porosity and pore size distribution at different ages.

CHAPTER 4. EXPANSION MEASUREMENT AND PH LEVEL OF PORE SOLUTION IN GPC AND OPC CONCRETE WITH DIFFERENT TYPES OF AGGREGATES

4.1. Introduction

The primary goal of this study was to investigate the ASR effect of different types of reactive aggregates in the fly ash based geopolymer concrete and compare it with ordinary Portland based concrete using lab experiments. Potential resistivity of the aggregates was performed via length change, per ASTM C1293 standard. The pore solution of hardened concrete was extracted and pH value of pore solution was determined. The SEM imaging analysis and FTIR spectroscopy were performed to analyze the change in chemical composition and bonding in the concrete mix.

4.2. Effect of type and composition of aggregates on expansion of GPC/OPC concrete prism

4.2.1. Expansion monitoring

Expansion measurements of concrete prisms were taken simultaneously with pore solution extraction at 1, 3, 28, 60, 90, 120, 240 and 365 days, as well as some other intermediate intervals. Figure 4.1 to 4.3 shows the average expansion of three prisms for each of the six mixes with different types of aggregates. Expansion of OPC concrete with different aggregates were also plotted in the same graph for the comparison purpose.

Each of these Figures indicates the reactiveness of the same aggregate in different mixes. The fly ash based geopolymer concrete has six different mixes to investigate the relationship between activator modulus and reactivity of the aggregates where OPC has only one because we didn’t use any other chemicals in OPC concrete except water. Even though the chemical composition of three types of aggregates are heavily different, the fly ash based concrete shows moderate expansion with all of these.

The OPC concrete prism made from the three aggregates (Granite, Carbonate, and Gravel) exhibit an expansion of 0.024%, 0.03%, and 0.041% after 3 days, respectively. However, the expansions in the GPC prism with the same aggregates are less than 0.025% for all six mixes. The OPC specimens made with the three aggregates all exceed the ASTM threshold (0.04%) before 28 days. To be precise, the OPC prism containing carbonate exceeds the ASTM threshold within 3 days while the OPC prisms containing granite and gravel exceed the ASTM threshold between 14 to 28 days.

The expansion rate of the OPC prisms was seen decreasing after 60 days in all three aggregates but the total expansion was keep increasing. The GPC shows a very small expansion and shrinkage rate throughout the testing period. The minimum expansion at the end of 365 days was observed in geopolymer concrete prism containing gravel with alkaline activator modulus of 1.0 and Na_2O dose of 10%.

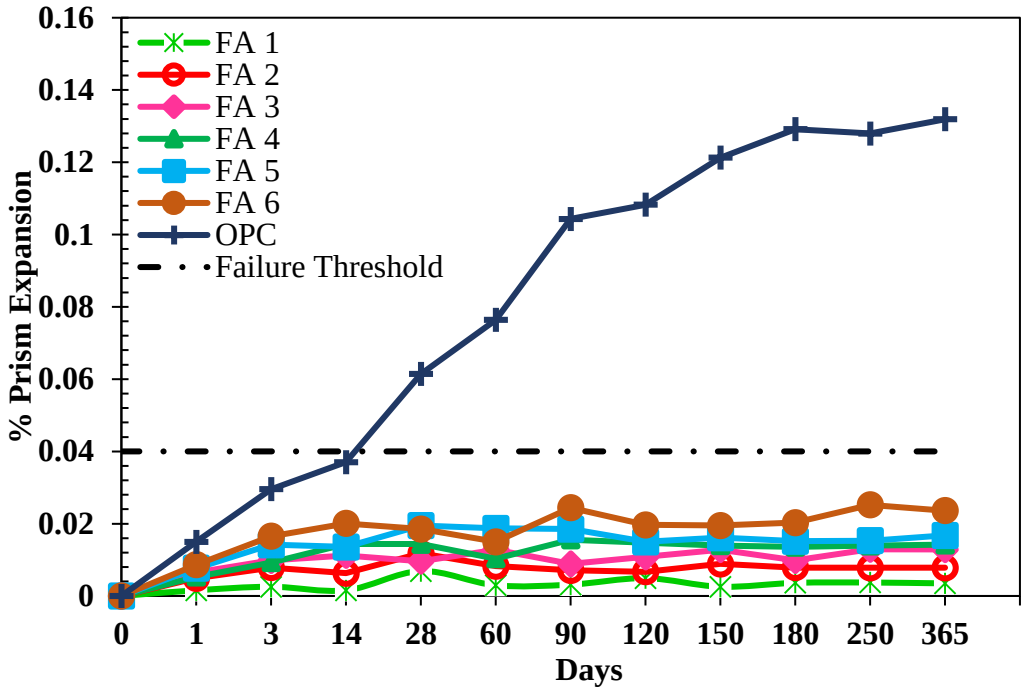

Figure 4.1. Expansion on GPC and OPC concrete specimen with Granite aggregate

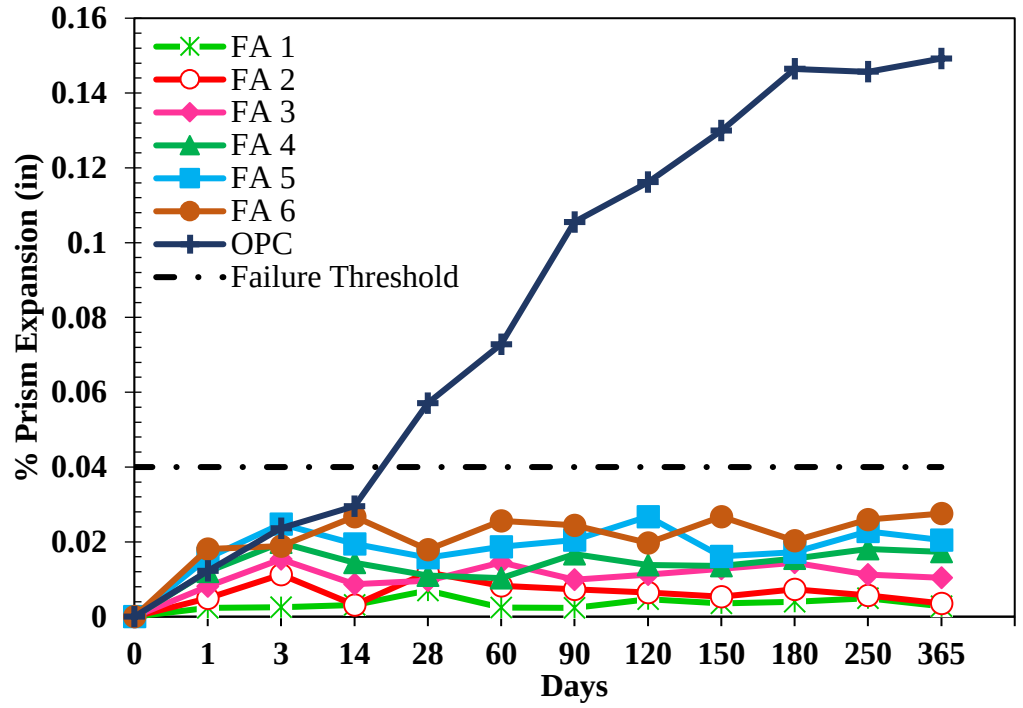

Figure 4.2. Expansion on GPC and OPC concrete specimen with Carbonate aggregate

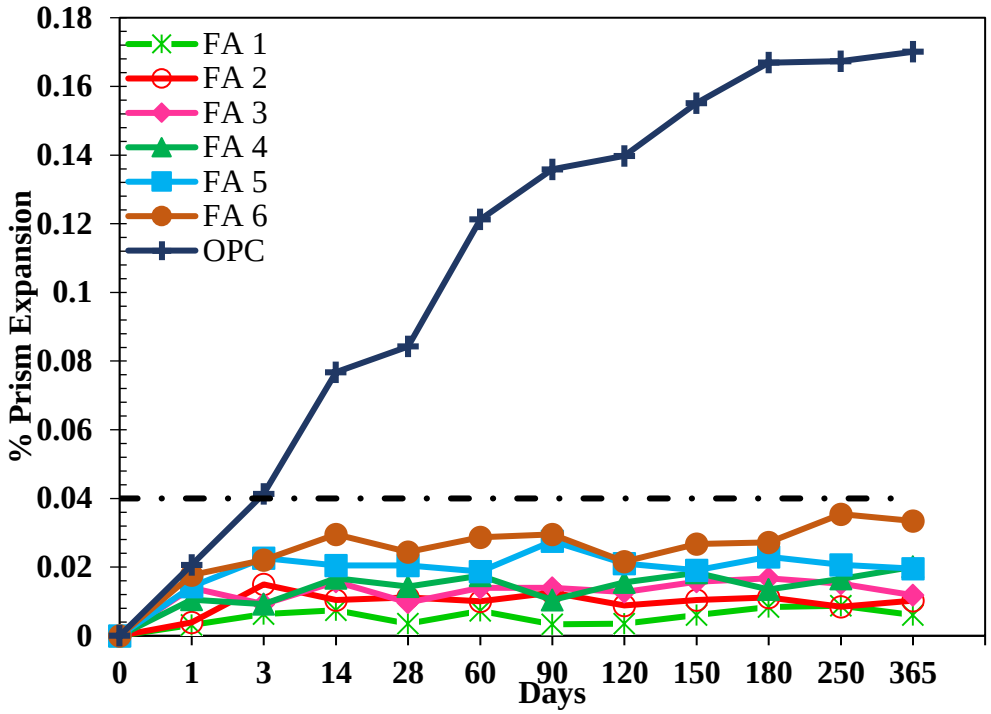

Figure 4.3. Expansion on GPC and OPC concrete specimen with Gravel aggregate

4.2.2. Effect of activator modulus

We have seen the overall expansions of the GPC prisms are very less compared to those of OPC prisms during the testing period. Figure 4.4 to 4.6 shows the expansion of the geopolymer concrete prism containing different alkaline activator modulus (1.0, 1.2, and 1.4) at 365 days. The alkaline activator modulus was defined as the molar ratio between SiO_2 and Na_2O. The Na_2O here includes both Na_2O content in Na_2SiO_3 solution and in NaOH. The expansion in prism containing carbonate shows almost the same expansion in alkaline activator of 1.0 at 365 days with different Na_2O dose, but the difference becomes wider when activator modulus changes to 1.2 and 1.4. The geopolymer concrete prism with Gravel shows more variation in expansion with different Na_2O dose, which might be because of more silica content in the aggregate.

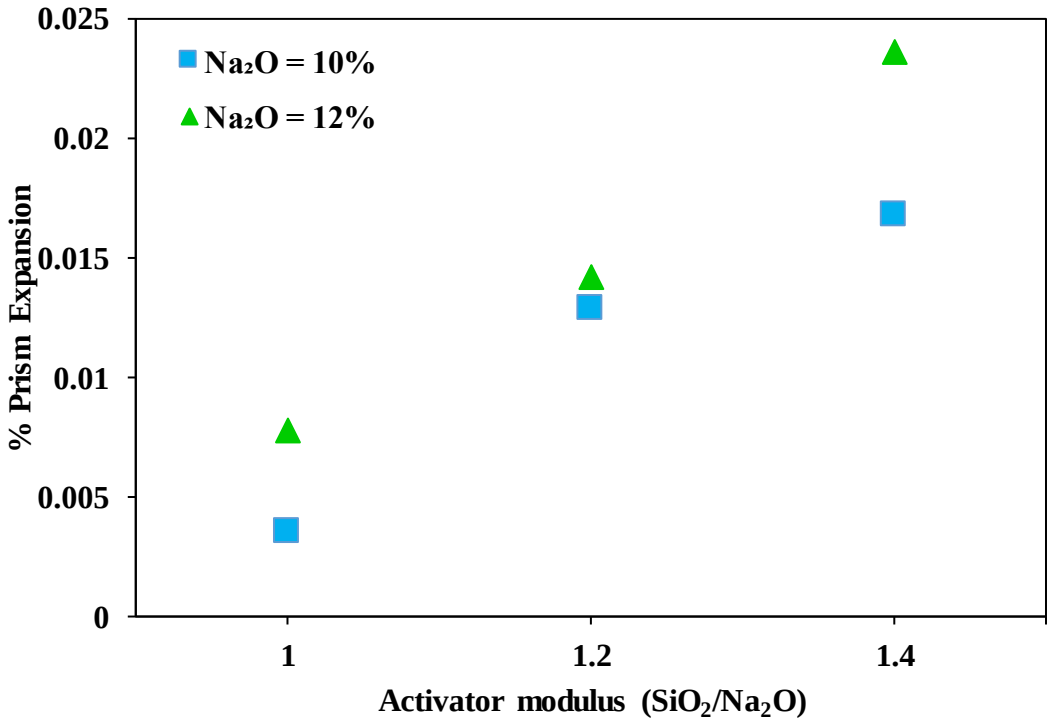

Figure 4.4. Effects of activator modulus in expansion of GPC concrete sample with Granite

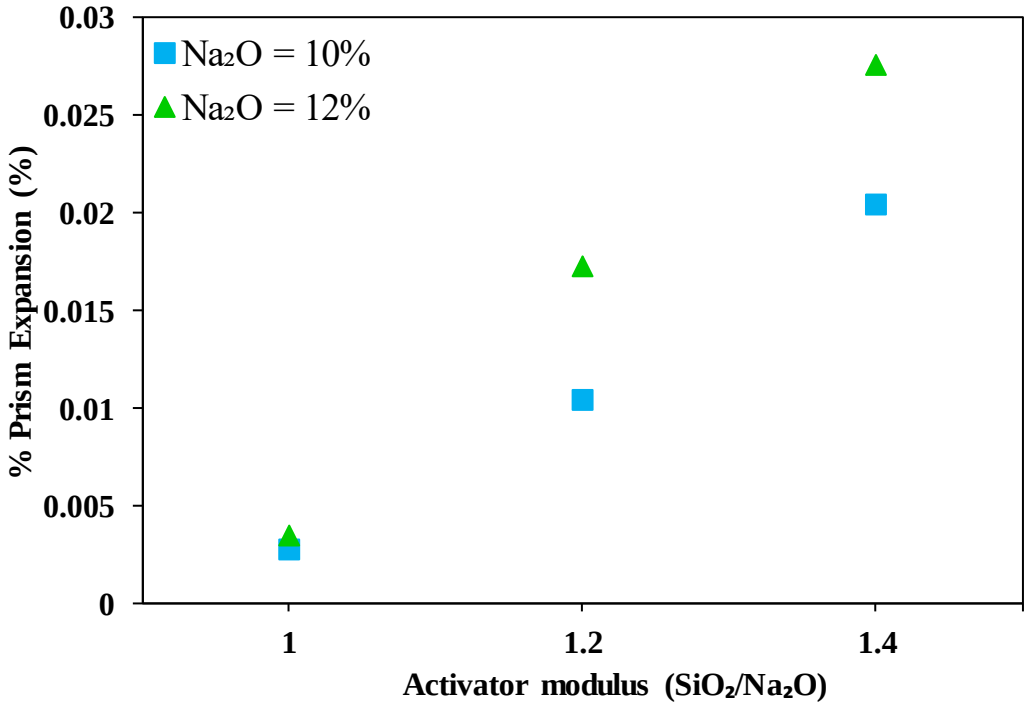

Figure 4.5. Effects of activator modulus in expansion of GPC concrete sample with Carbonate

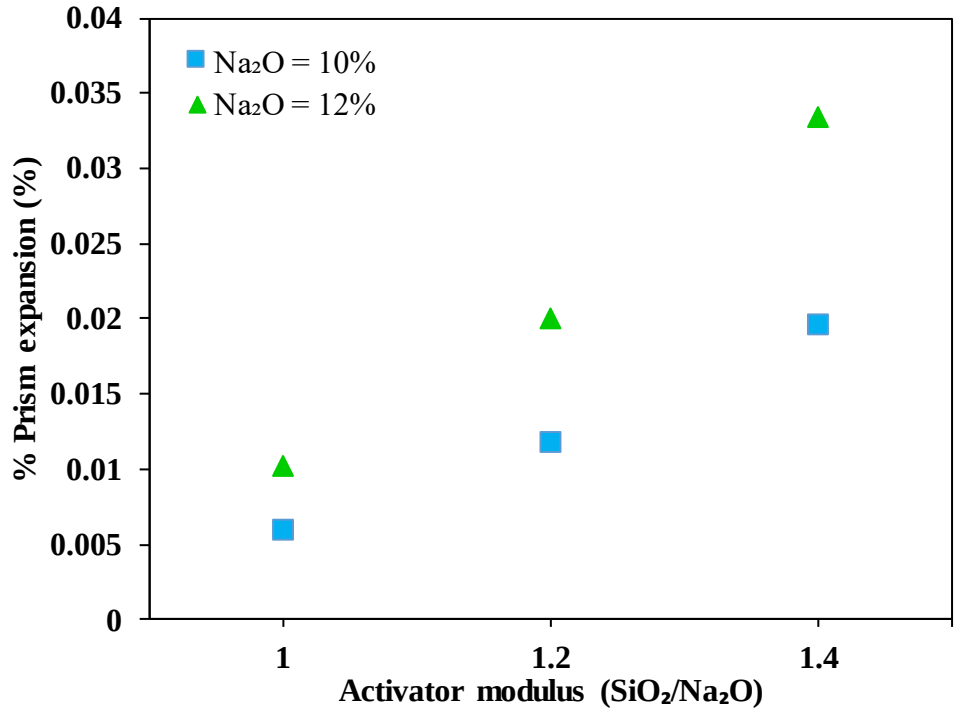

Figure 4.6. Effects of activator modulus in expansion of GPC concrete sample with Gravel

4.2.3. Effect of sodium oxide (Na_2O) dose

Since the alkali silica reaction not only depends upon the reactivity of the aggregates, it also depends upon the alkalinity of the chemicals being used in the mixes. We studied the effect of sodium oxide content in alkaline solution to enhance the alkali silica reaction. Figure 4.7 to 4.9 shows the expansion of the geopolymer concrete prism containing different Na_2O doses (10% and 12%). The expansion of the geopolymer concrete containing granite as an aggregate changes from 0.017% to 0.024% while alkaline activator modulus was kept constant at 1.4 and Na_2O dose was changed from 10% to 12%. Similarly in prisms containing gravel and carbonate, expansion increases from 0.02% to 0.0285 and 0.019% to 0.034%. It confirms the expansion of the geopolymer concrete prism increases with the increase of sodium oxide content in the alkaline solution while other variables remain constant.

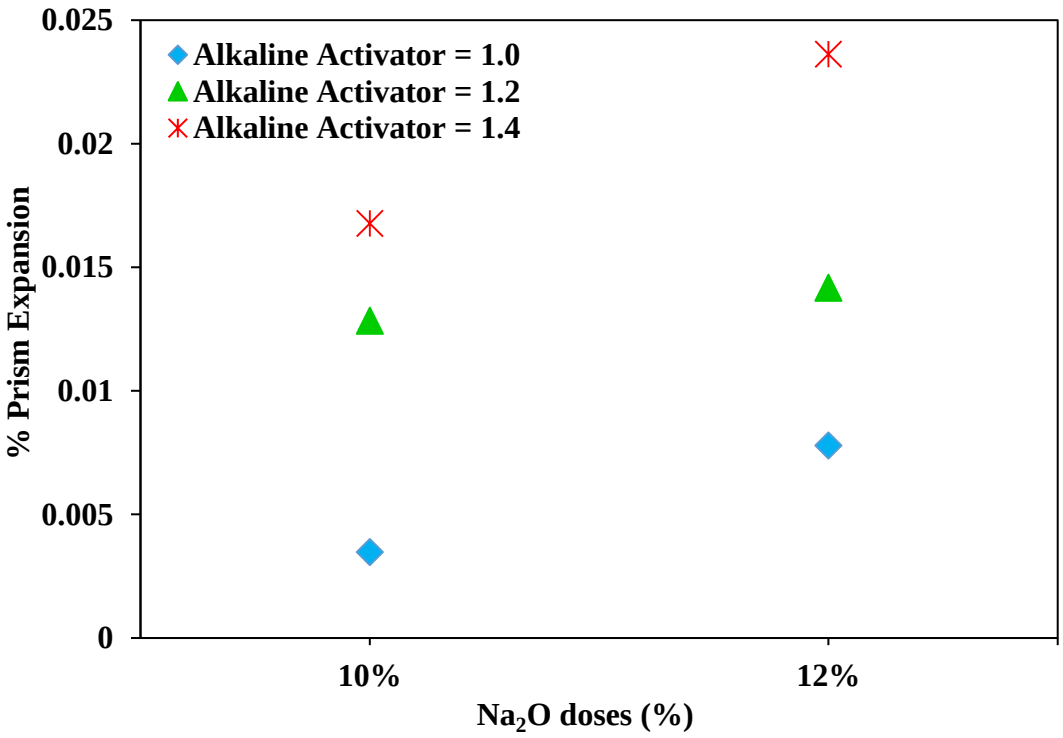

Figure 4.7. Effects of Na2O doses in expansion of GPC concrete sample with Granite

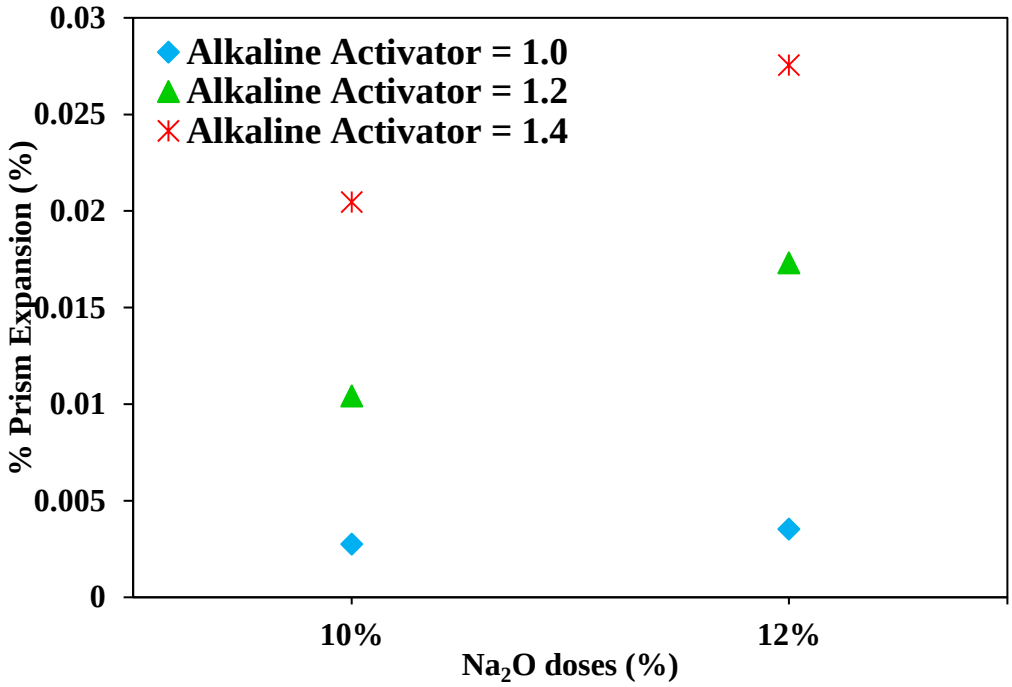

Figure 4.8. Effects of Na2O doses in expansion of GPC concrete sample with Carbonate

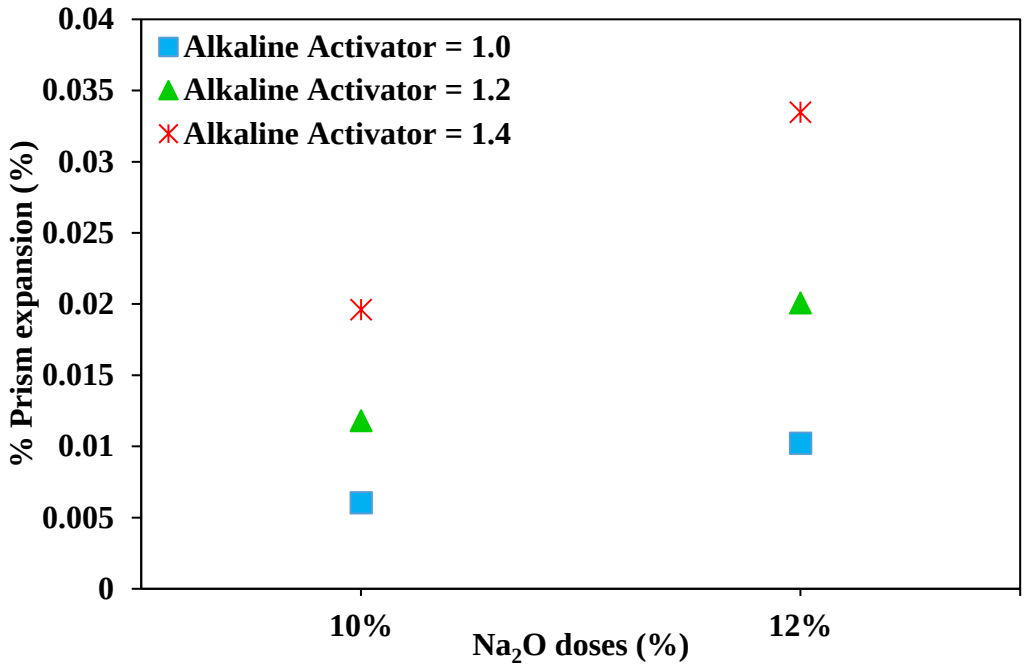

Figure 4.9. Effects of Na2O doses in expansion of GPC concrete sample with Gravel

4.2.4. Effect of calcium, silica, and aluminum content in aggregates

Different aggregates have different chemical composition. The aggregates used in this research have a wide range of silica and calcium content. The silica content is 62.77% in case of gravel whereas it is 30.7% and 0.13% in case of carbonate and granite by mass respectively. The calcium content is 19.13%, 2.53%, and 1.7% by mass in granite, gravel and carbonate respectively.

The three reactive aggregates used have shown different expansions when used in the similar mix design. The maximum expansion was found in GPC prism with granite at alkaline activator modulus of 1.4 and 12% Na_2O doses, which is 0.024% at 365 days. The expansion of GPC with gravel reaches maximum of 0.033% at 365 days and the GPC with carbonate aggregates has a maximum of 0.034% expansion at 365 days. Correspondingly, the total

expansion of OPC prism with carbonate, gravel, and granite was found to be 0.132%, 0.15%, and 0.17% respectively.

Addition of silica lowers the Ca/Si ratio of C-S-H in the system, which increases the absorption of the alkalis and formation of the ASR gel that leads to the expansion. The percentage of silica is less in case of carbonate aggregate than that in gravel but the expansion percentage was found more in both OPC and GPC prisms with carbonate than that in prisms having gravel. This might be because the calcium content is more and the aluminum content is less in case of carbonate as compared to that of gravel aggregates (Figure 4.1 to 4.3). The calcium does not have a huge impact on the alkali silica reaction but it helps to enhance the alkali carbonate reaction which can also lead towards the expansion of concrete specimen **(Brykov et al. 2014)**. This also agrees on the result found by (Chappex and Scrivener (2012). The aluminum presented in the pore solution is observed on the silica surface and limits the dissolution of the amorphous silica of the aggregates, which restricts ASR on leads to less expansion. The maximum expansion of geopolymer concrete with granite, gravel and carbonate is 5.5, 5.8, and 5.2 times smaller than the expansion of OPC and 1.75, 1.33, and 1.22 times smaller than the standard threshold. All six mixes of geopolymer concrete did not also show large variation along the test for all types of aggregates.

4.3. Effect of the type and content of aggregates on pore solution chemistry of OPC/GPC

4.3.1. pH of pore solution

The pH of the pore solution extracted from the concrete cylinders were measured at 1, 3, 28, 60, 90, 120, 240, and 365 days. Figure 4.10 to 4.12 shows the pH of the cylinders made using all six different mixes of fly ash based geopolymer concrete with different types of aggregates. The pH values of the OPC cylinders made with corresponding types of the aggregates are also

plotted for the comparison purpose. For each day testing, pore solution from three specimen were extracted and the average value was plotted. The total number of the cylinders used in this experiment is 96.

Figure 4.10 shows that pH value of the pore solution extracted from the cylinders made with granite. The Figure shows that at the beginning (1day test) the pH value of the pore solution of geopolymer concrete is highly basic (nearly equal to 14) for all the mix design whereas the pH value of the OPC concrete pore solution is just 12.85. The initial pH of pore solution extracted from geopolymer concrete made with gravel and carbonate were also close to 14 whereas the pH of OPC concrete are 12.94 and 13.15. With the increase in age of the specimen the pH value of the geopolymer concrete kept reducing whereas the pH of OPC concrete pore solution kept increasing up to 365 days.

The slope of the increment in pH of OPC concrete pore solution up to 90 days is more compared to that of pH decrement of geopolymer concrete. However, after 90 days the pH of geopolymer concrete reduced with higher slope compared to the slope of pH value increment in OPC concrete. In case of granite aggregate, the rate of pH decreasing was seen less up to 28 days and the rate was found higher in between 28 to 120 days and remained almost constant for all geopolymer mixes after 120 days whereas it kept reducing in case of gravel and carbonate. In case of OPC concrete the alkalinity of cylinder with gravel remained almost constant after 90 days whereas the alkalinity kept increasing in other two aggregates. The slopes of decreasing and increasing of pH value in case of both geopolymer and OPC concrete are not equal at the same time duration which might be because of variation in degree of reaction. In both cases the slope is higher at the initial period because there will be presence of large amount of alkalis and reactive aggregates.

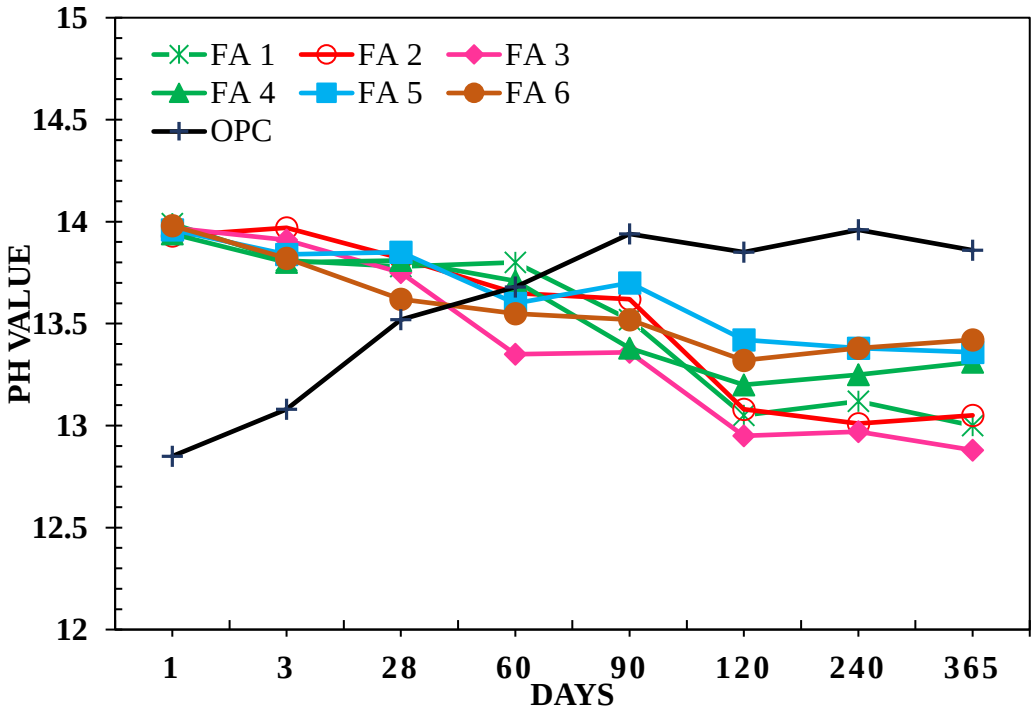

Figure 4.10. pH value of pore solution extracted form GPC and OPC concrete with Granite

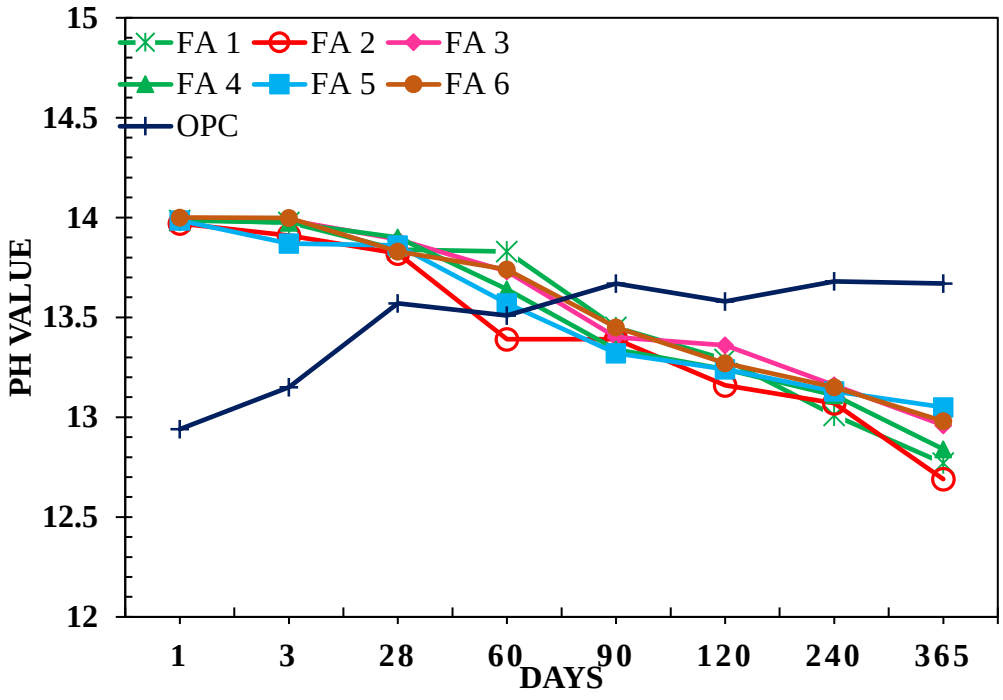

Figure 4.11. pH value of pore solution extracted form GPC and OPC concrete with Carbonate

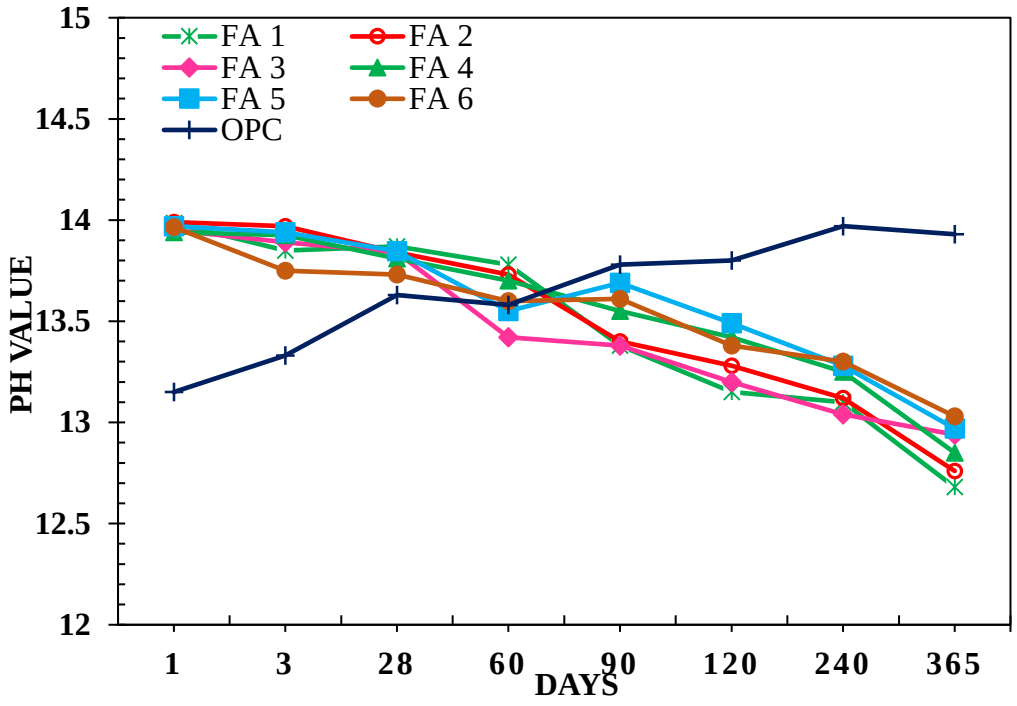

Figure 4.12. pH value of pore solution extracted form GPC and OPC concrete with Gravel

4.3.2. Effect of activator modulus

Figure 4.13 to 4.15 shows the relationship between the alkalinity of the pore solution extracted from geopolymer concrete specimens and alkaline activator modulus (1.0, 1.2, and 14) at 365 days. It has been found that the pH value of the pore solution increased with the increase of SiO_2 to Na_2O modulus. In other words, the possibility of the alkali silica reaction also increases with the increase of the activator modulus. However, in case of geopolymer concrete with granite, the pH value of the pore solution with activator modulus 1.2 was found less than that of pore solution with activator modulus of 1.4.

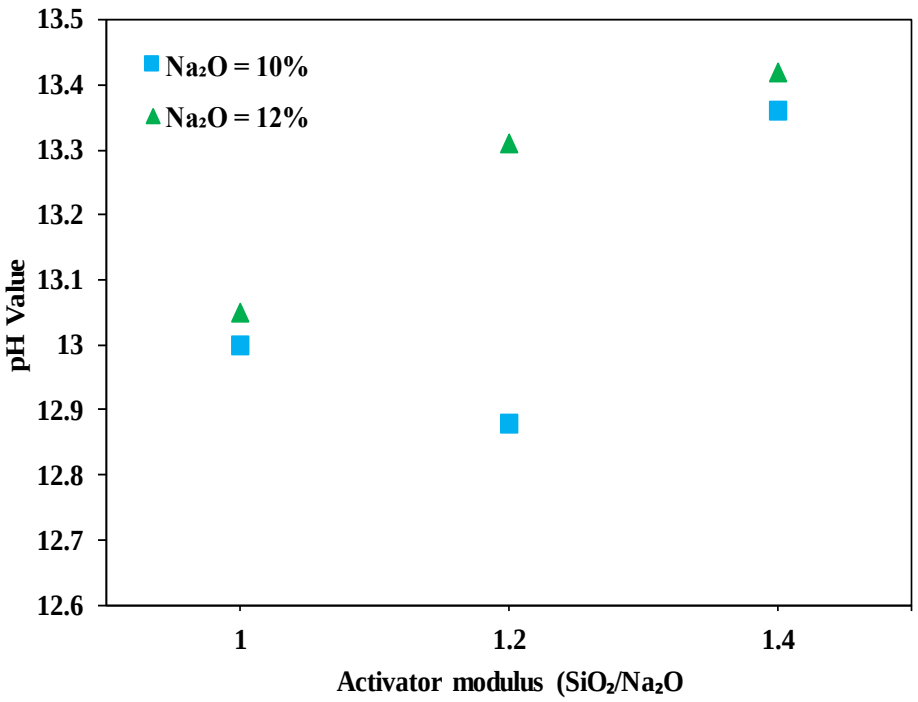

Figure 4.13. Effects of activator modulus on the pH of pore solution in GPC with Granite

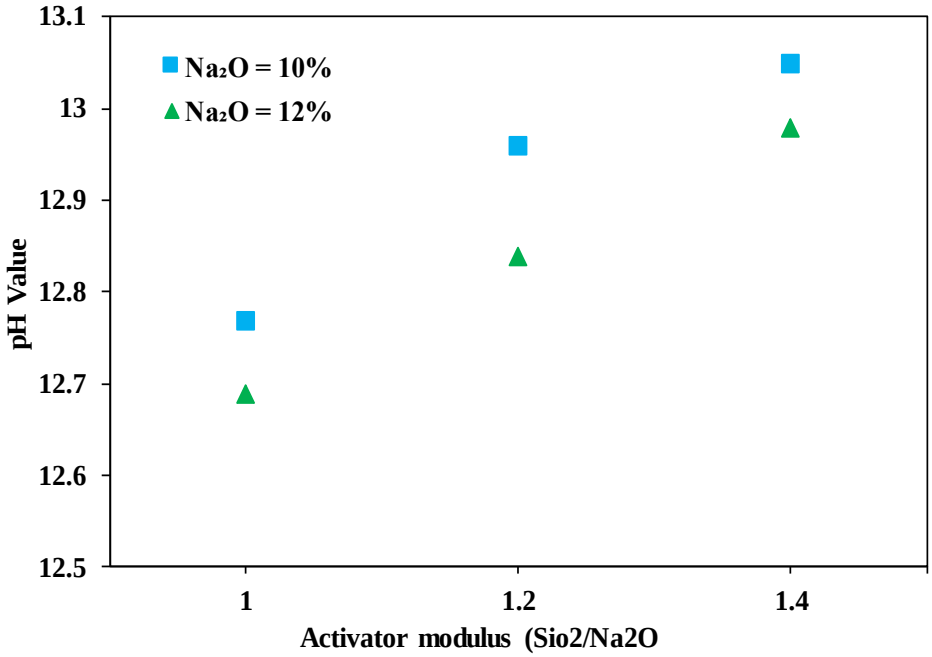

Figure 4.14. Effects of activator modulus on the pH of pore solution in GPC with Carbonate

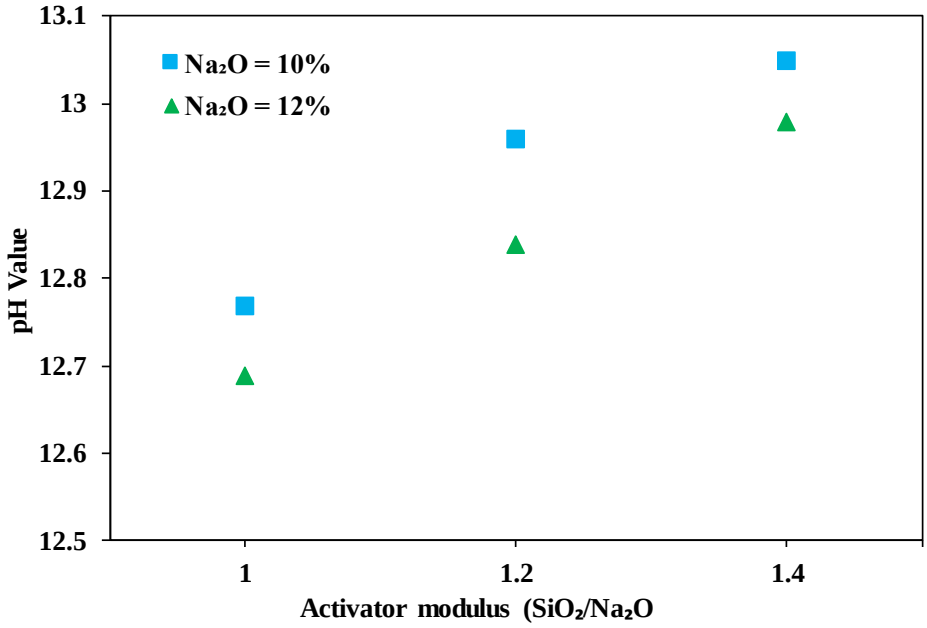

Figure 4.15. Effects of activator modulus on the pH of pore solution in GPC with Gravel

4.3.3. Effect of sodium oxide (Na_2O) dose

The relationship between the alkalinity of the pore solution of geopolymer concrete at 365 days and the sodium oxide content in the mix are given in Figure 4.16 to 4.18. The Figure shows that, in case of geopolymer concrete with gravel aggregate, the pH of the pore solution decreases with increase in Na_2O dose by keeping activator modulus constant. In case of carbonate, the pH of the pore solution increases from 12.97 to 13.03 and 12.68 to 12.76 for alkaline activator modulus 1.0 and 1.4 where it gets decreased from 12.94 to 12.85 for activator modulus of 1.2 when Na_2O concentration was changed from 10% to 12%. The geopolymer concrete with gravel aggregates shows overall decreasing in pH of pore solution when increasing Na_2O concentration from 10% to 12%. However, the mix with granite shows exactly opposite result i.e. the pH of the pore solution increases with decrease in sodium oxide concentration.

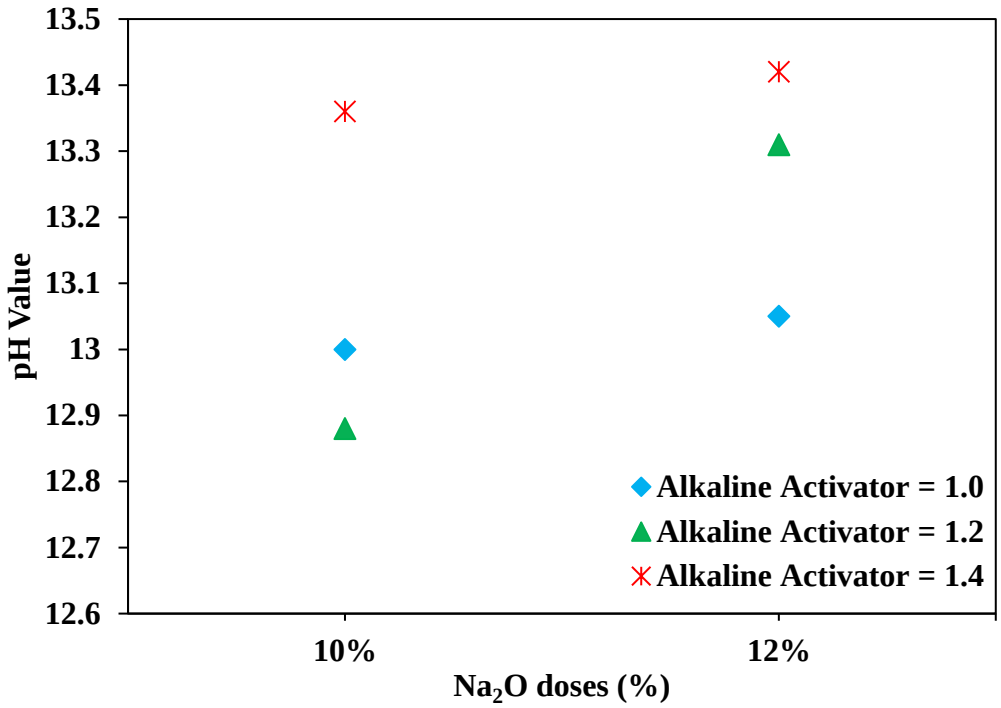

Figure 4.16. Effects of Na_2O doses on the pH of pore solution in GPC with Granite

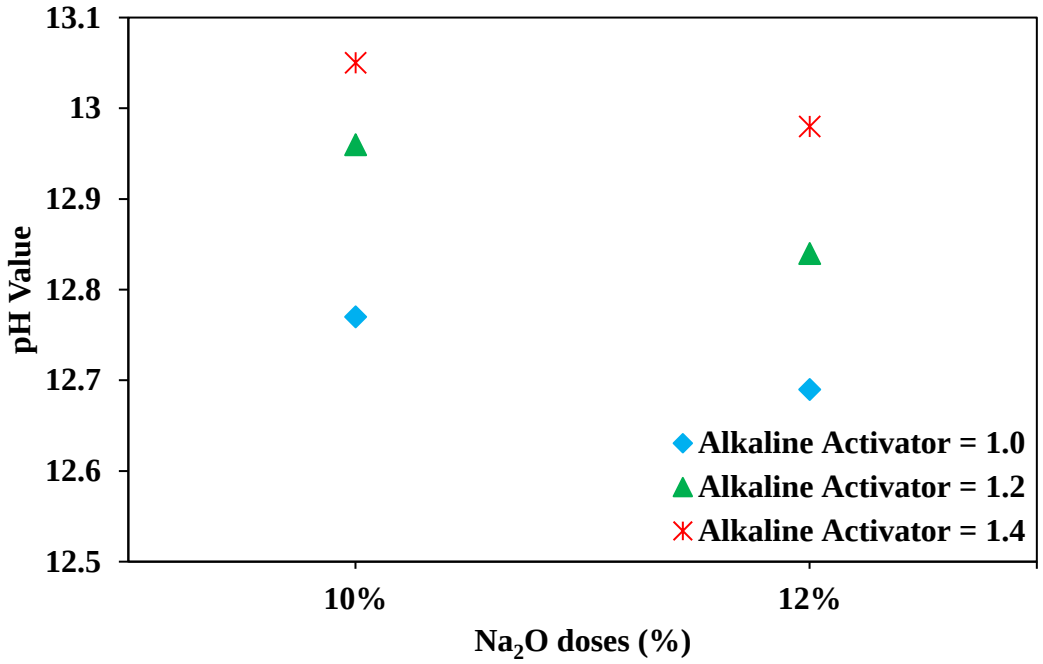

Figure 4.17. Effects of Na_2O doses on the pH of pore solution in GPC with Carbonate

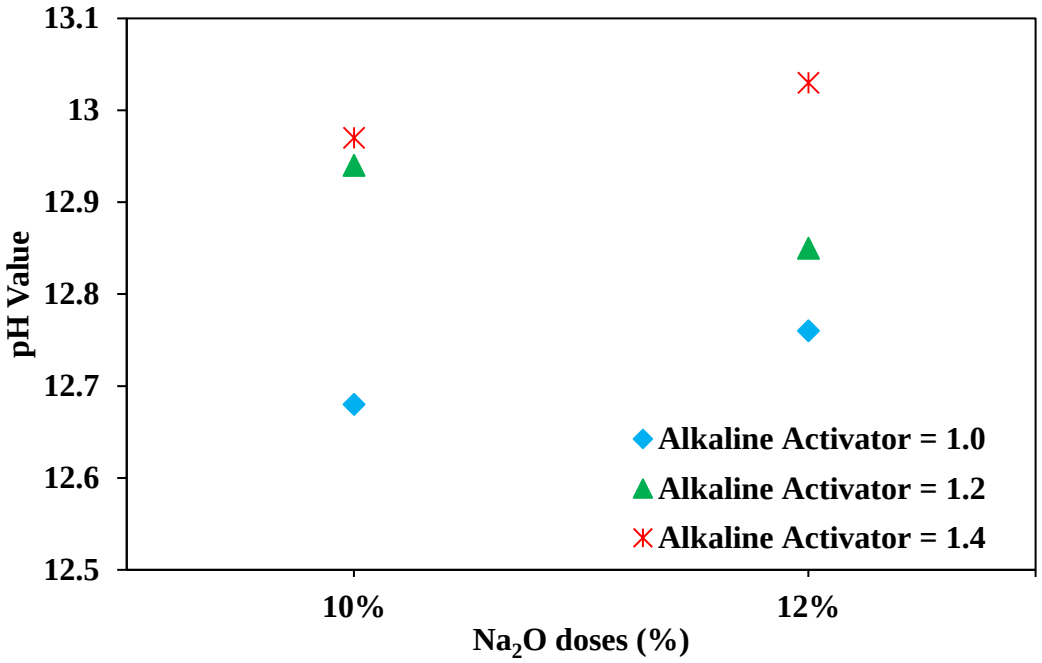

Figure 4.18. Effects of Na_2O doses on the pH of pore solution in GPC with Gravel

4.3.4. Effect of calcium, silica, and aluminum contents in aggregates

The effect of the chemical composition of aggregates on the alkalinity of concrete pore solution has been analyzed in both geopolymer and OPC concrete. The pH value of all the geopolymer concrete mixes with all three aggregates were found less than threshold level of pH = 13.4 proposed by Diamond (1983), that is necessary to sustain ASR reaction, at 365 days. However, the pH values of the OPC concrete were found less than 13.4 before 28 days for all kinds of aggregates and increased to exceed the threshold limit at 365 days.

The variation in the pH of pore solution of concrete specimen with different types of aggregatess is affected by different factors. The pH value not only depends upon the chemicals used during the mixing of the concrete, it also depends upon the chemical composition of the aggregates being used because the alkali silica reaction depends upon the reactivity of the aggregate and the concentration of different elements in it. In this experiment the OPC prisms

with granite show the lowest pH and the OPC prisms with carbonate show the highest pH of pore solution at 1 day testing. At the end of the testing on 365 days, the pH of OPC concrete with carbonate became maximum compared to the other two aggregates. This is because of the high silica content in the carbonate aggregates. The pH value of the OPC concrete with granite was found higher than that of concrete with gravel which is because of the higher presence of carbonate in granite and higher presence of aluminum in gravel. The silica content helps to increase the alkali silica reaction if the sufficient amount of alkali is present in pore solution and pH will be also increased. However, the amount of aluminum in the aggregate was found to be beneficial to reduce the alkali silica reaction. The carbonate does not actively participate into the alkali silica reaction but it also helps to increase the alkalinity of the pore solution through alkali carbonate reaction: another deleterious reaction between alkali and reactive aggregate.

4.4. Scanning electron microscopy of fly ash based geopolymer concrete

Section 4.2 and 4.3 shows that the expansion of geopolymer concrete prism is less compared to that of OPC concrete prism and alkalinity of the pore solution of geopolymer concrete reduces with time whereas it increases in case of OPC. For further explanation of effect of alkali silica reaction in geopolymer concrete at microstructural scale, SEM images of geopolymer concrete with all three types of reactive aggregates were prepared. Since mix 6 of geopolymer concrete shows the highest effect in expansion, SEM imaging was conducted on this mix only.

Figure 4.19 to 4.21 shows the SEM images of geopolymer concrete with alkaline activator 1.4 and sodium oxide dose 12% with granite, gravel and carbonate aggregates respectively at 365 days. Table 4.1 to 4.3 explains the weight percentage of different chemical elements present on the points specified in corresponding images. These SEM images were

focused on the aggregate binder interface deliberately to investigate if there is formation of ASR gel.

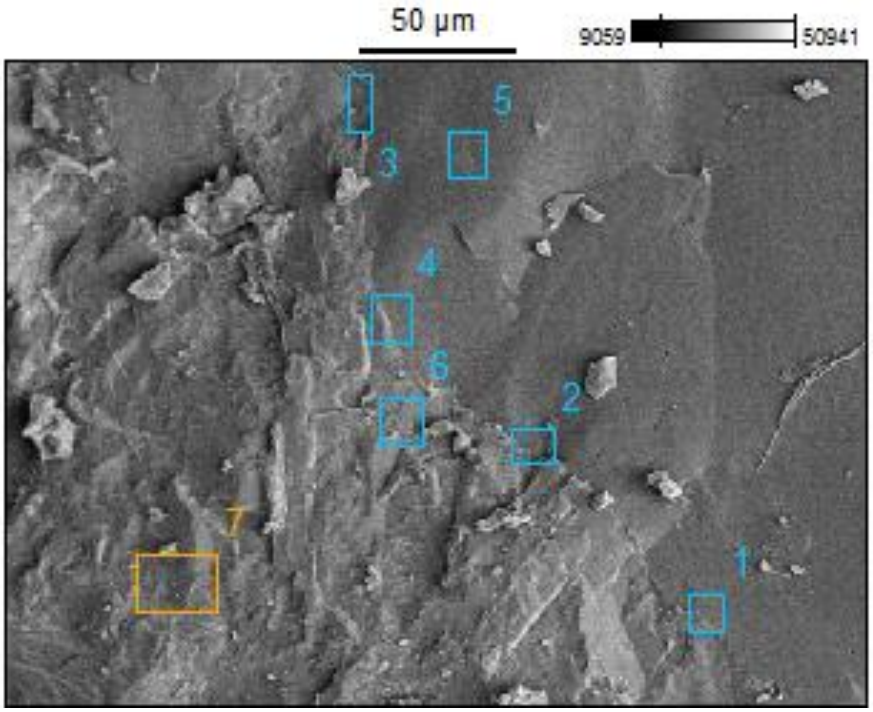

Figure 4.19. SEM image of aggregate-binder interface on GPC concrete with Granite

Table 4.1. Chemical composition of area selected from SEM on GPC with Granite using EDS

Area in image	C	O	Na	Mg	Al	Si	K	Ca	Fe
Area 1	1.57	51.42	1.33	0.51	1.29	42.70	0.51		0.66
Area 2	2.71	51.35	3.17		2.00	37.77	2.40	0.61	
Area 3	2.56	52.73	4.63	0.27	3.91	33.61	1.75	0.55	
Area 4	1.36	48.72	2.28		3.36	43.11		1.17	
Area 5	1.13	54.49				44.38			
Area 6	1.68	44.56	8.04		11.43	31.46	0.84	1.99	
Area 7	1.87	47.75	6.60		10.57	28.47	2.16	1.65	0.92

The SEM images in combination with EDS study were performed to investigate the chemical composition at the aggregate binder interface. Several points on the images were selected along the interface and at aggregate side and binder side. The Figure shows that there is

not any visible ASR gel formation. However, the chemical composition of the aggregate binder interface for different aggregates shows different reaction potential of the aggregates. In case of gravel (Figure 4.21), points 1,2,3,4 and 6 are on the interface, point 5 is at the aggregate side, and point 7 at the binder side. The weight percentage of silica is about 45% at the surface of aggregate and about 28% at the binder surface where on the interface it ranges from 30% to 40%. The calcium concentration is negligible whereas aluminum ranges from 1% to 4% at interface, 6% at binder and 8% at aggregate side. This high concentration of aluminum in the mix protects the dissolution of aluminosilicate and helps to mitigate the gel formation. Similarly in case of granite aggregate (Figure 4.18), points 1, 2, and 3 are on the interface between aggregates and binder which has silica percentage of about 25% and aluminum percentage of about 7% whereas point 4 at binder side and point 5 on aggregate side have silica percentage of 28 % and 30% and alumina percentage of about 8% and 10% by weight respectively. The SEM image of concrete with carbonate aggregate shows high percentage of silica and calcium and less percentage of alumina compared to other aggregates which leads to higher reactivity potential because of the easier dissolution of alumiosilicate presented in the mix.

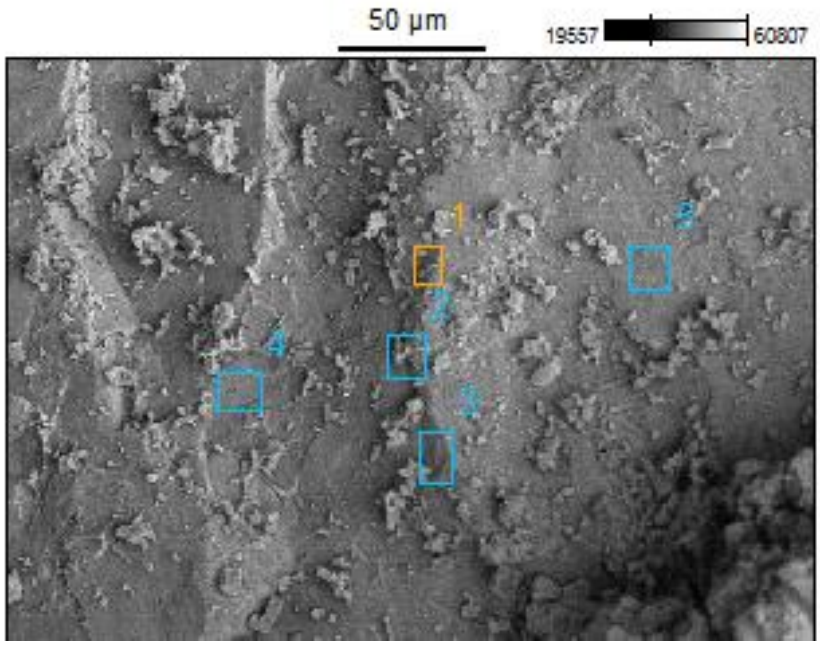

Figure 4.20. SEM image of aggregate-binder interface on GPC concrete with Carbonate

Table 4.2. Chemical composition of area selected from SEM on GPC with Carbonate using EDS

Area in image	**C**	**O**	**Na**	**Mg**	**Al**	**Si**	**K**	**Ca**	**Fe**
Area 1	4.28	48.87	5.10		7.66	25.48	8.62		
Area 2	3.04	47.68	6.75	0.29	7.43	24.44	7.20	1.62	1.54
Area 3	3.08	48.65	6.11	0.14	7.40	25.24	7.85	1.12	
Area 4	2.25	47.07	3.40		9.35	29.98	8.94		
Area 5	2.77	47.01	1.62	0.87	1.51	28.01	9.71		1.51

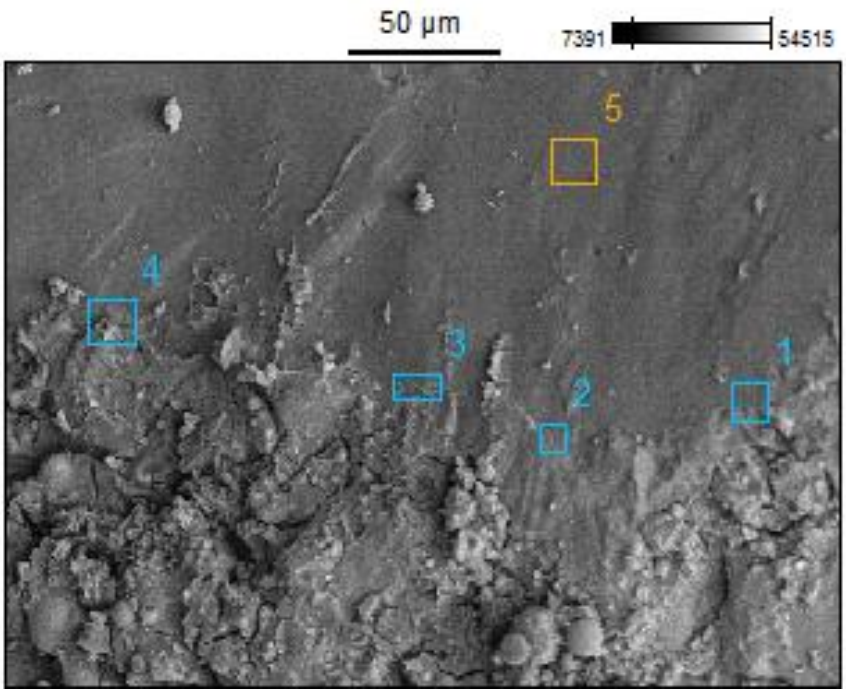

Figure 4.21. SEM image of aggregate-binder interface on GPC concrete with Gravel

Table 4.3. Chemical composition of area selected from SEM on GPC with Gravel using EDS

Area in image	**C**	**O**	**Na**	**Mg**	**Al**	**Si**	**K**	**Ca**	**Fe**
Area 1	3.08	49.68	3.68	0.32	2.01	37.13	1.15	2.00	0.97
Area 2	2.50	50.16	1.59		5.33	34.35	6.07		
Area 3	3.39	50.78	7.55	0.67	2.71	29.68	1.40	2.06	1.76
Area 4	2.74	48.59	4.24	1.89	3.77	30.11	2.52	1.43	4.72
Area 5	1.93	55.05				43.02			

From the SEM imaging of geopolymer concrete with different types of aggregates we can conclude that there is no presence of the ASR gel along the interface even though the reaction potential of different aggregates can be described based on the chemical composition of the interfacial zone. This supports the results that we obtained from prism expansion measurement and pore solution alkalinity test which is the possibility of alkali silica reaction in fly ash based geopolymer concrete with reactive aggregates is very low compared to that of the OPC concrete.

4.5. Fourier transform infrared spectroscopy (FTIR)

The Fourier transform infrared spectroscopy (FTIR) was performed on all of the 1 year old Ordinary Portland Cement concrete and geopolymer concrete specimen. Since the FTIR spectroscopy uses interference of light rather than dispersion to measure the spectrum of a substance, the specimen of 0.5 inch thickness was used for this experiment.

Figure 4.22 to 4.24 shows the FTIR spectrum obtained for the different concrete mixes with granite, gravel and carbonate respectively. The geopolymer specimen exhibited strong peaks close to 860 cm^{-1}, which can be related to Si-O-H bending. In case of OPC concrete specimen this bonding was found in between 810 cm^{-1} to 850 cm^{-1}. The geopolymer concrete with granite, gravel and carbonate exhibited strong peaks at 920 cm^{-1} and 925 cm^{-1} which can be related to asymmetric stretching Si-O-Al bond of the newly formed geopolymer gel. Similar bonding was obtained in case of OPC concrete specimen in the range of 880 cm^{-1} to 905 cm^{-1} wavenumber, which contributes to the alkali silica reaction.

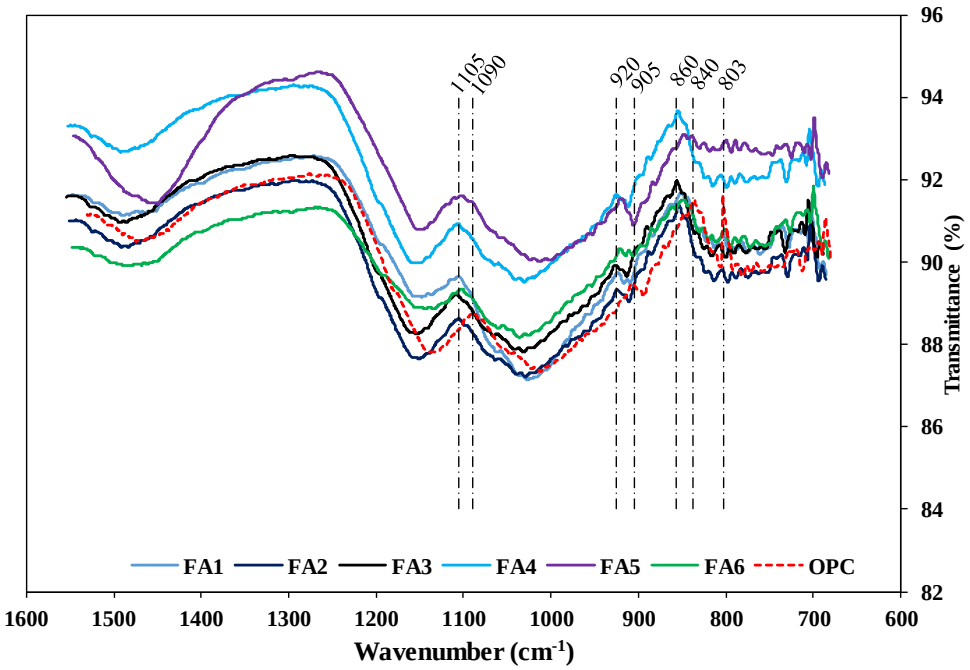

Figure 4.22. FTIR analysis of GPC and OPC concrete specimens with Granite

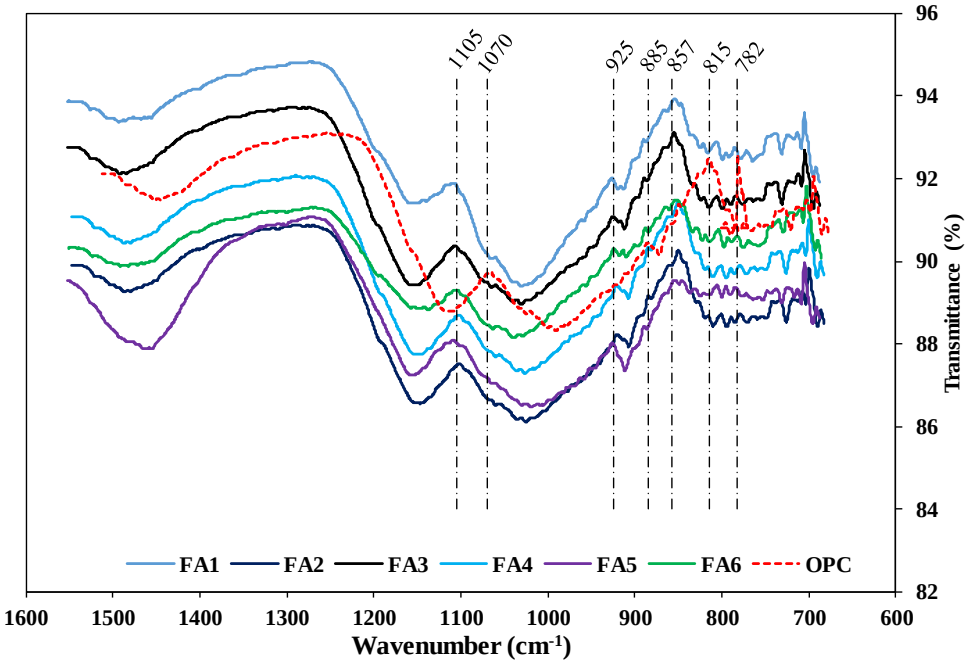

Figure 4.23. FTIR analysis of GPC and OPC concrete specimens with Carbonate

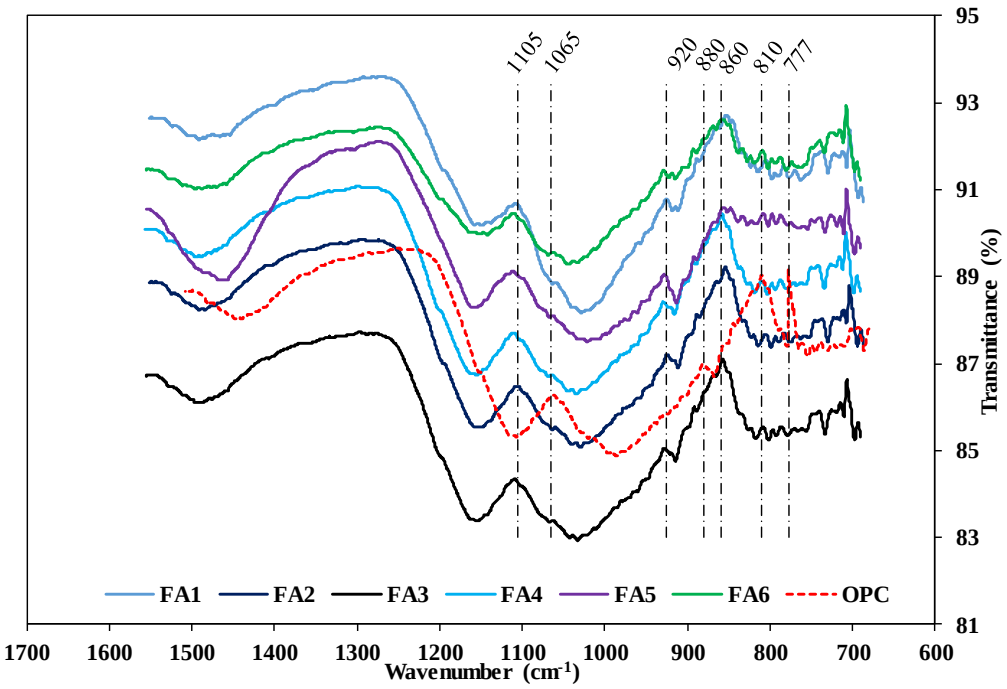

Figure 4.24. FTIR analysis of GPC and OPC concrete specimens with Gravel

Si-O-Al bonding was obtained in geopolymer concrete and OPC concrete in the range of 1000^{-1} to 1110 cm^{-1} because of the presence of mullite or mullite like structure. This spectrum shows the stretching vibration of bulk Si-O-Si bonding. The bulk asymmetric Si-O-Si bonding was also found in less wavelength in OPC compared to that of GPC because of presence of large amount of unreacted Si-O-Si bond. In case of geopolymer concrete with different types of aggregates, the amount of unreacted bulk Si-O-(Si, Al) bonding is present at higher amount in case of gravel as compared to carbonate and granite. However, the presence of higher amount of aluminum in gravel helps to reduce the rate of alkali silica reaction compared to the other aggregates.

The result shows that amount of the alkaline activator solution does not have a very big impact on the reaction mechanism but the presence of higher amount of sodium can contribute towards carbonation in terms of CO_3^{2-} , which may not have been involved in the reaction. The

OPC specimen with granite, gravel and carbonate also exhibited presence of alkali silica reaction gel in the form of Si-O-Si (Al) bond vibration at 803 cm^{-1}, 782cm^{-1}, and 777 cm^{-1} respectively. This peak was not observed in any of the GPC specimen.

4.6. Summary

This chapter focused on the results obtained from expansion test, pore solution extraction test, SEM imaging and FTIR spectroscopy of the hardened concrete samples. The expansion test shows that there is negligible expansion in geopolymer concrete with all three types of aggregates at the end of test. It has been found that the pH of OPC concrete pore solution is less at the beginning and increases with time whereas the pH of pore solution extracted from geopolymer concrete is higher at first and keeps decreasing. From SEM images and FTIR, it can be concluded that the amount of unreacted Si-O-Si, which is a major contributor in alkali silica reaction, is more in OPC concrete than that in geopolymer concrete. Aggregate with higher amount of calcium and silica shows less resistive to ASR compared to aggregate with higher amount of aluminum.

CHAPTER 5. EXPANSION MEASUREMENT AND POROSITY ANALYSIS USING MICRO-COMPUTED TOMOGRAPHY (MICRO-CT)

5.1. Introduction

Micro computed tomography (Micro-CT) scanning was used to scan the specimen and several analysis including 3-dimensional expansion measurement, porosity measurement and pore size distribution were performed. This chapter will contain a thorough interpretation of the results obtained for each analysis, and how to use these results to explain the ASR mechanism in geopolymer concrete.

5.2. Expansion measurement through microCT images

Table 5.1 shows the average expansion of each cube of GPC mix from Table 3.5 and OPC mix from Table 3.6 in X, Y, and Z directions. In case of geopolymer concrete, only mix 6 was used for microstructural analysis. The expansion of OPC concrete with different reactive aggregates were also calculated in all direction in a similar way for the comparison purpose and to validate the data obtained from expansion testing using ASTM C1293 (Chapter 4).

From Table 5.1 we can see that, expansion of the prism depends upon several variables including types of binders, types of aggregates, reactivity of aggregates, chemical composition of the aggregates, mixing procedure of concrete, size of the aggregates, and distribution of the aggregates in the specimen, etc.

Table 5.1. Expansion of geopolymer and OPC concrete specimen with different aggregates

Aggregate Type	OPC concrete			GPC concrete		
	X-axis (%)	**Y-axis (%)**	**Z-axis (%)**	**X-axis (%)**	**Y-axis (%)**	**Z-axis (%)**
Granite	0.0746	0.0737	0.0761	0.0132	0.0129	0.0165
Carbonate	0.1206	0.0909	0.1215	0.0281	0.0269	0.0287
Gravel	0.0698	0.0714	0.0735	0.0228	0.0250	0.0253

The OPC prisms made with Granite, Carbonate, and Gravel exhibit an average expansion of 0.0746%, 0.0737%, and 0.0761% of expansion in X, Y, and Z direction at the end of 90 days after initial curing. However, the expansions in the GPC prisms with the same granite aggregate are less than 0.02% for all directions. It has been also seen that in both GPC and OPC specimen with all three aggregates, the expansion is maximum in Z-axis which is parallel to ground when we placed the sample for curing and storage. Even though the expansions in all three directions are not so much different, the expansion in X - axis remains in the second place where the expansion in Y axis remains the least for all mixes, which may be due to the self-weight effect of the specimen.

In case of both geopolymer concrete and OPC concrete, the expansion was found maximum in case of granite aggregate as compared to those of gravel and granite.

5.3. Porosity measurement

The porosity of both OPC and GPC specimen with all three kinds of aggregate were calculated at initial condition i.e. just after demolding of specimen and at 90 days after alkali silica reaction took place. The same sample was used for both days just to make sure homogeneity. The porosity was calculated by dividing the volume of void present on specific sample on specific day by the total volume of the sample on the same day. While scanning the specimen, there will be problem in detecting the edge and thresholding, which can change the total porosity value of the specimen. To overcome this problem, a 1.75” x 1.75” x 1.75” block in specimen was extracted from the whole block using myVGL. To extract the new block, four reference points on the specimen were used to find out the center so that select the same volume was selected in both times. The threshold was kept constant for each sample and the background properties were also kept same during all the scanning to mitigate the problem that can arises because of thresholding.

Figure 5.1 to 5.6 shows the pore distribution in the extracted OPC and GPC concrete cubes with Granite, Carbonate, and Gravel aggregates.

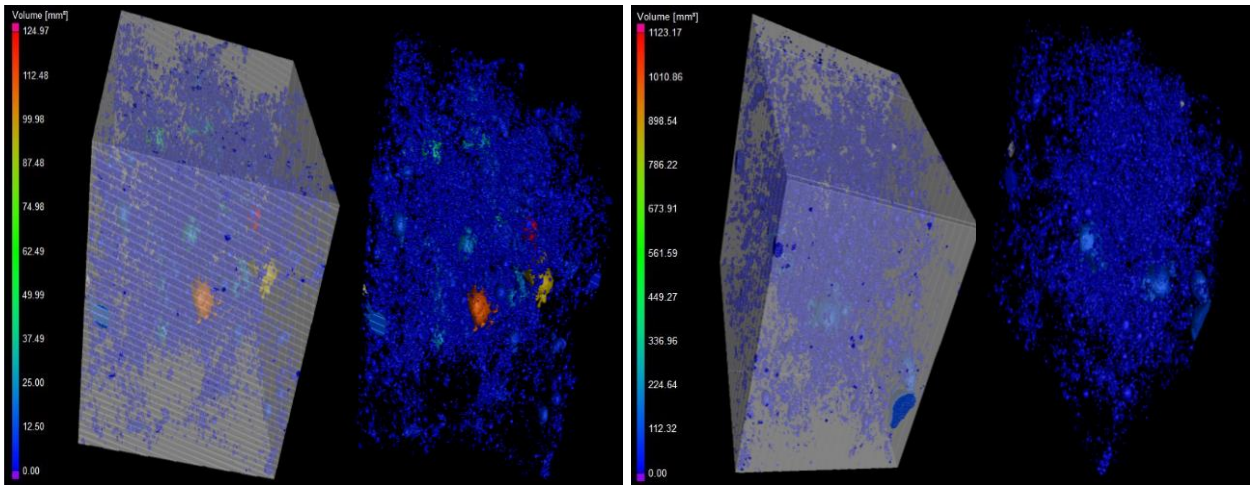

Figure 5.1. Pore distribution of OPC concrete with Granite aggregate (a) 1 day and (b) 90 days

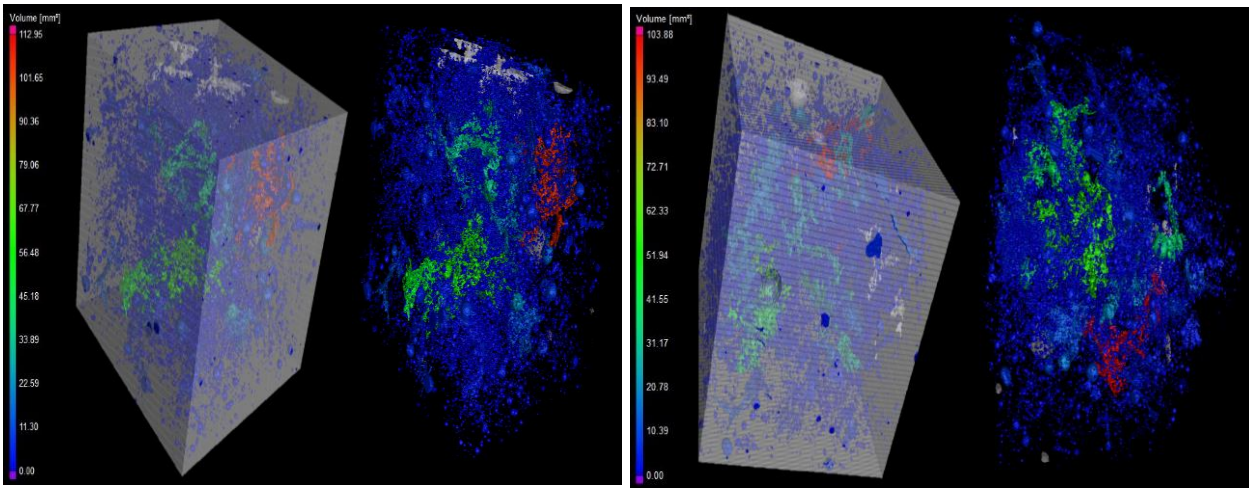

Figure 5.2. Pore distribution of GPC concrete with Granite aggregate (a) 1 day and (b) 90 days

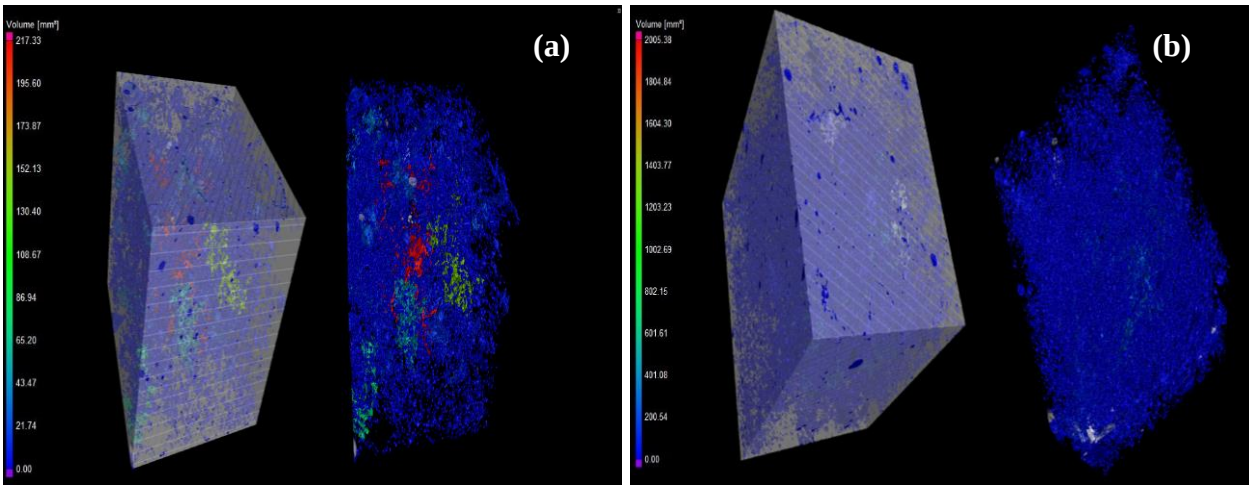

Figure 5.3. Pore distribution of OPC concrete with Carbonate aggregate (a) 1 day and (b) 90 days

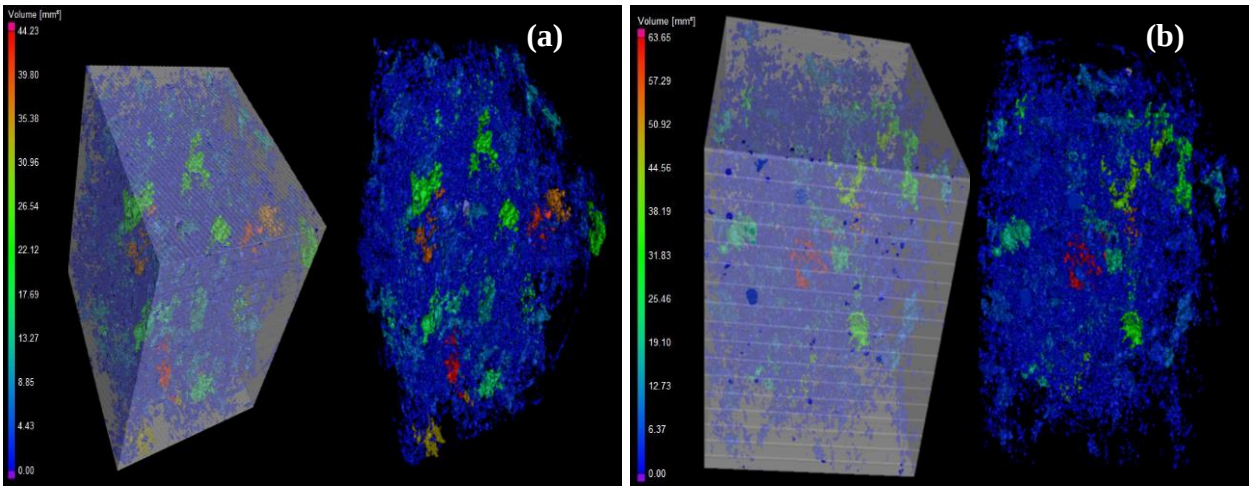

Figure 5.4. Pore distribution of GPC concrete with Carbonate aggregate (a) 1 day and (b) 90 days

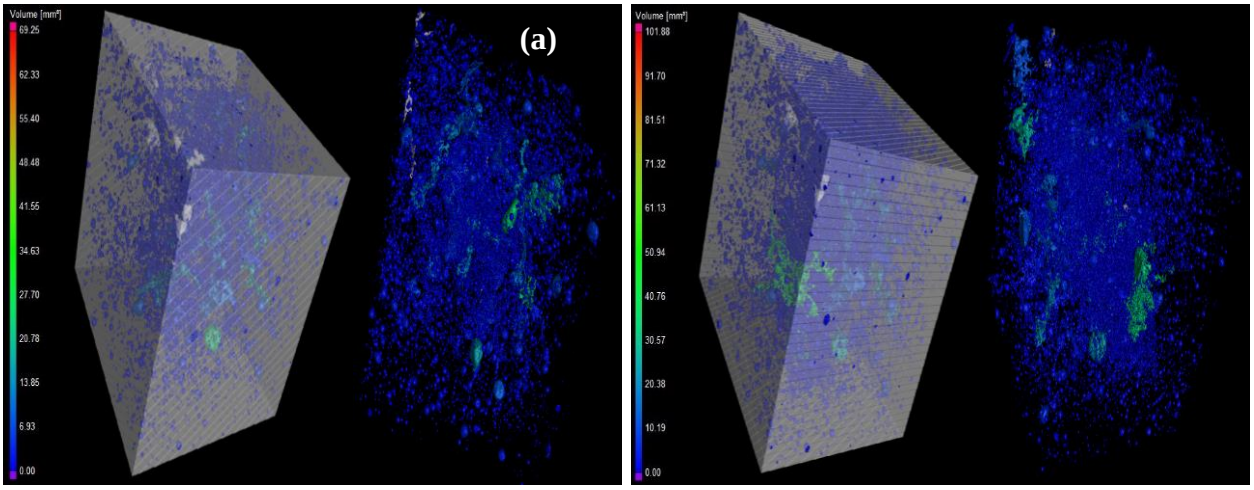

Figure 5.5. Pore distribution of OPC concrete with Gravel aggregate (a) 1 day and (b) 90 days

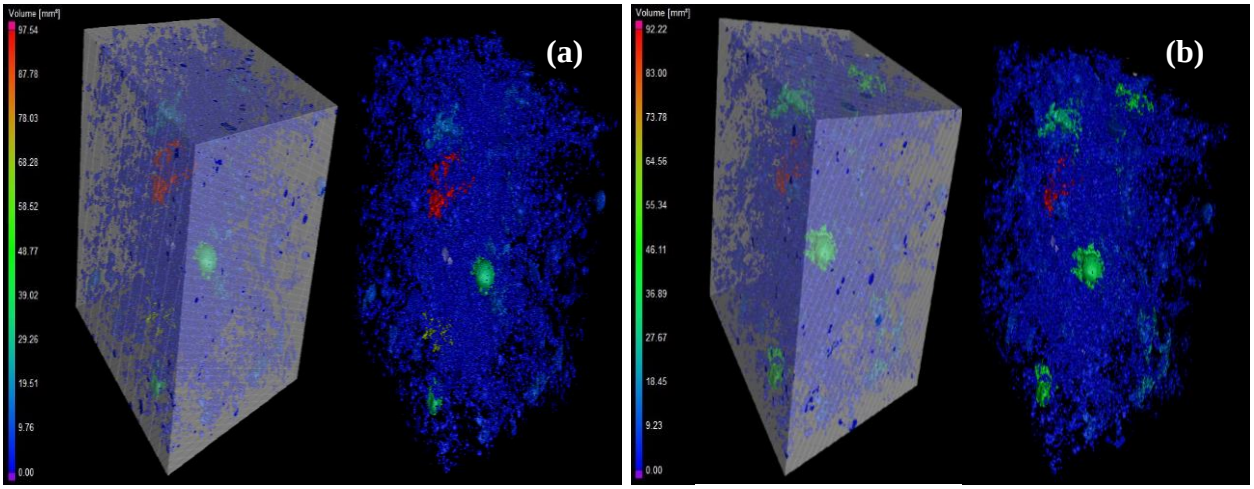

Figure 5.6. Pore distribution of GPC concrete with Gravel aggregate (a) 1 day and (b) 90 days

Figure 5.7, 5.8, and 5.9 shows the change in porosity of the OPC and GPC concrete specimen from the first day test to the 90 days test. It has been found that the porosity of fly ash based geopolymer concrete is very less compared to that of ordinary Portland cement concrete.

This might be because the grain sizes of fly ashes are smaller than those of Portland cement. The fly ash consists of silt-sized particles which are generally spherical, typically ranging in size between 0.5 and 100 micron whereas Portland cement can go up to 500 microns. These small glass spheres in fly ash improve the fluidity and workability of fresh concrete and ultimately reduce the porosity of the concrete.

From Figures 5.7, 5.8 and 5.9, we can see that the percentage of void in fly ash based geopolymer concrete is quite similar for all of mixes with different aggregates. The size and amount of the coarse aggregate used have kept constant in all of the sample preparation. The difference at the first day might be because of the shape of the aggregates and compaction during the sample preparation. It has been found that the porosity of OPC sample with granite increased from 2.97% to 3.17% , whereas, the porosity of fly ash based geopolymer concrete with similar aggregate changes from 2.91% to 2.93%. Similarly, the porosity of OPC concrete with carbonate aggregate and gravel aggregates were increased from 2.04% to 2.87% and from 2.11% to 2.79% respectively. In case of fly ash geopolymer concrete, the porosity was found almost same in both days for all of the aggregates. However, within geopolymer concrete the porosity at initial test ranges from 1.3% for gravel aggregate to 2.93% for granite aggregate, which might be because of the variation in geopolymerization reaction progress and evaporation of water present in alkaline activator solution. However, if we compare within a single sample, the change in porosity of OPC concrete is quite high compared to that of geopolymer concrete.

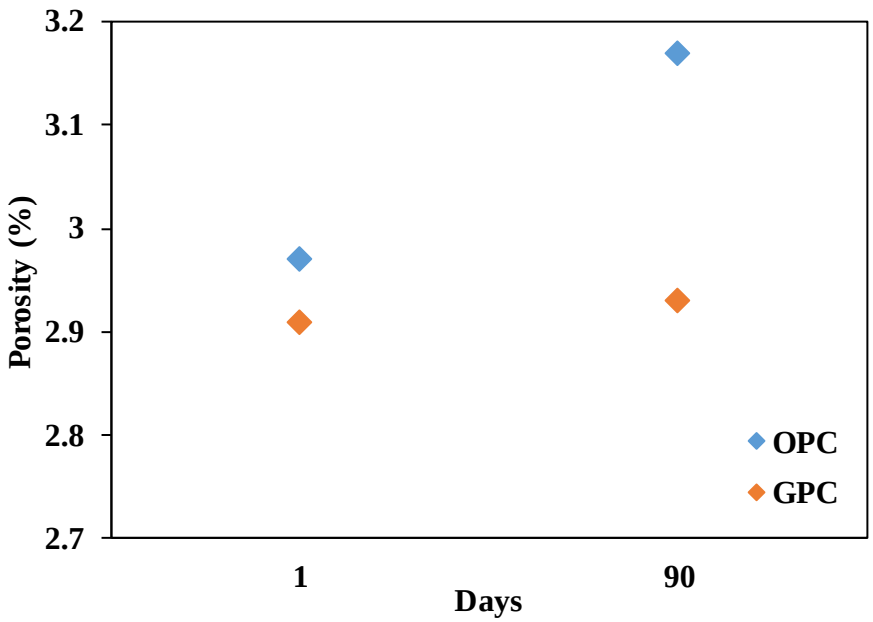

Figure 5.7. Porosity of OPC and GPC concrete cubes made with Granite

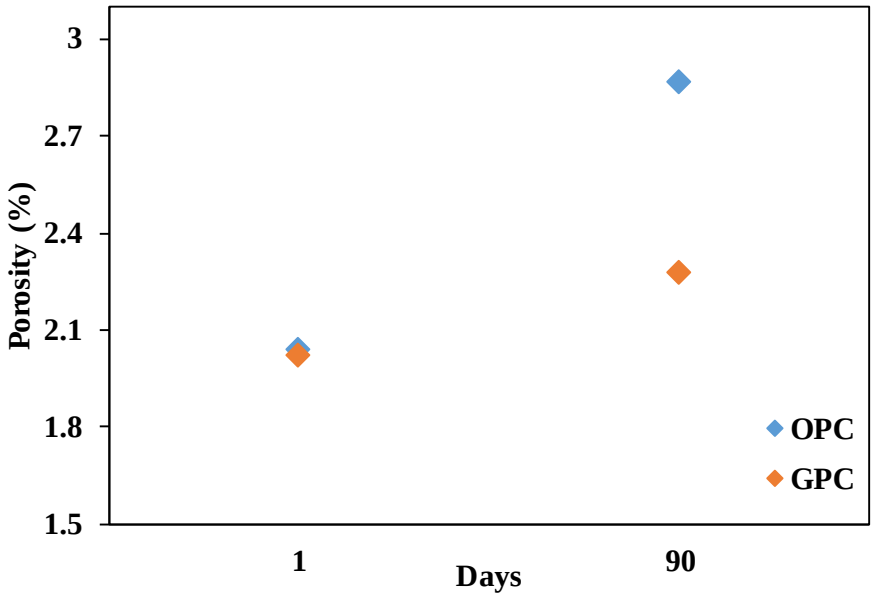

Figure 5.8. Porosity of OPC and GPC concrete cubes made with Carbonate

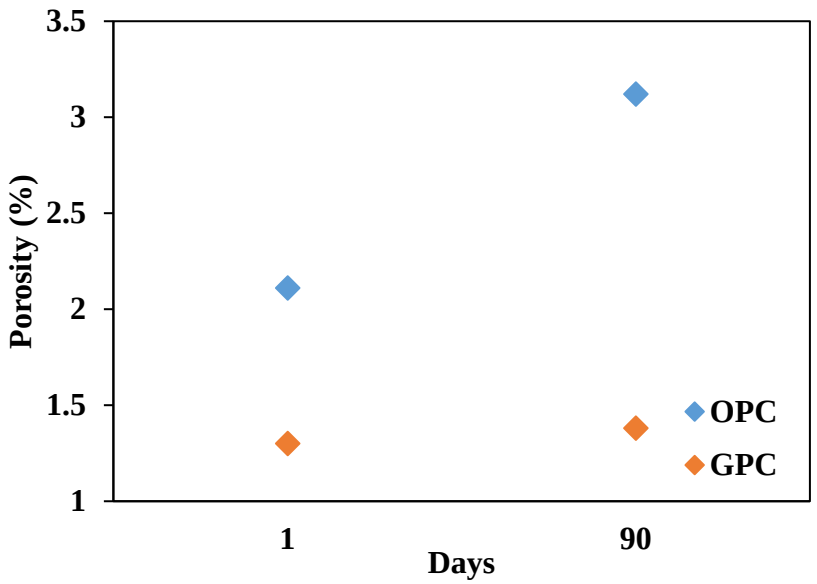

Figure 5.9. Porosity of OPC and GPC concrete cubes made with Gravel

The porosity analysis of these concrete specimen shows the amount of void is increasing in OPC concrete with all types of aggregates compared to that of geopolymer concrete with respective to all types of aggregates. It can be because the formation of the alkali silica gel into the pore pushes the aggregates away. This force helps to increase the volume of voids inside a constant volume and exerts an expansive pressure. If the gel can not find ways to move and keeps increasing in volume, it could lead to cracks and failure.

5.3.1. Pore size distribution

After knowing the change in porosity of OPC and GPC concrete specimen with different types of reactive aggregates, pore size distribution analysis was conducted, which will provide the shape and size of the pores in concrete and help to explain the ASR mechanism in concrete.

5.3.1.1. Sphericity Vs diameter

The void volume was found increased for all specimen in case of the Portland cement concrete after alkali silica reaction. Figure 5.10 to 5.12 shows the relationship between sphericity and diameter of the pores of different concrete sample at initial test and test after alkali silica reaction. The term “sphericity” here means the spherical percentage of the pores. The relationship between shape and diameter of the pores present in concrete confirms that the sizes/amount of the pores present in fly ash based geopolymer concrete are smaller as compared to that of Portland cement based concrete specimen at the same age. The sphericity of the pores was found to be reduced and diameter was found to be increased in case of the Portland cement based concrete in case of all aggregates. In case of geopolymer concrete, the size of the pores and sphericity of pores remains almost constant. Even if there is change in sphericity, it has a negligible amount of change compared to that of Portland cement concrete.

The biggest pore was found on Portland cement concrete with carbonate at 90 days with an average diameter of 0.9 inch. The size of the pores in geopolymer concrete was found smaller than 0.7 inch diameter. The sphericity percentage has been reduced in case of Portland cement concrete which might be because of pressure generated by expansion of gel formed by alkali silica reaction.

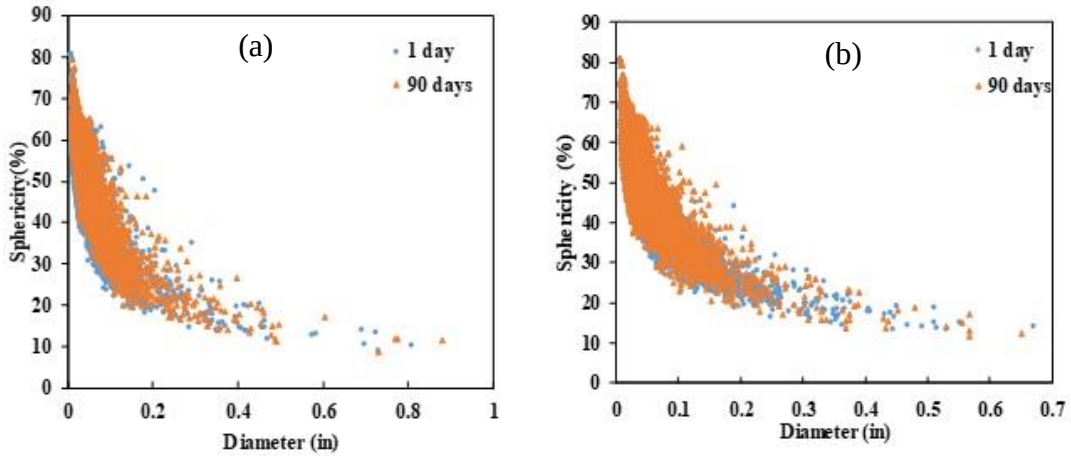

Figure 5.10. Sphericity Vs Diameter relationship of pores for concrete sample with Granite (a) OPC and (b) GPC

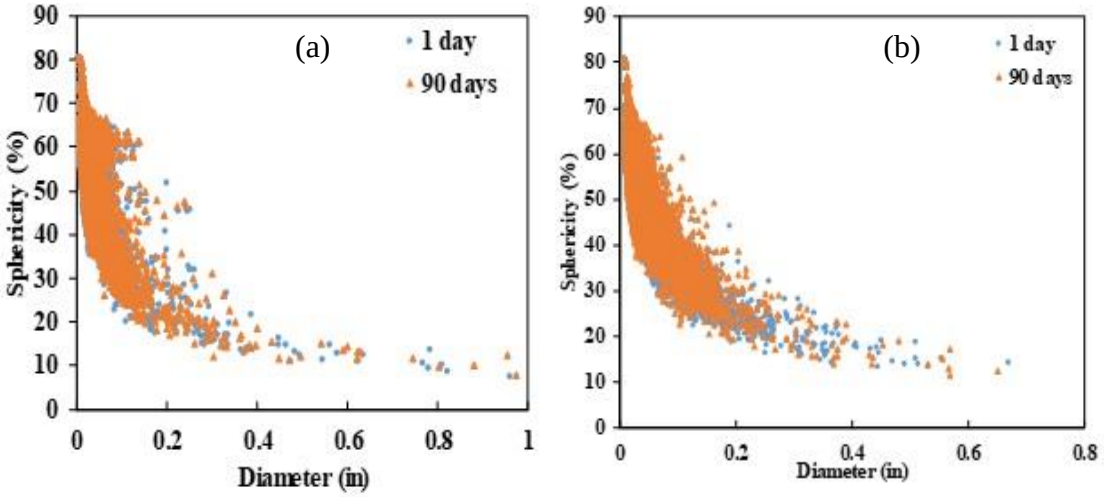

Figure 5.11. Sphericity Vs Diameter relationship of pores for concrete sample with Carbonate (a) OPC and (b) GPC

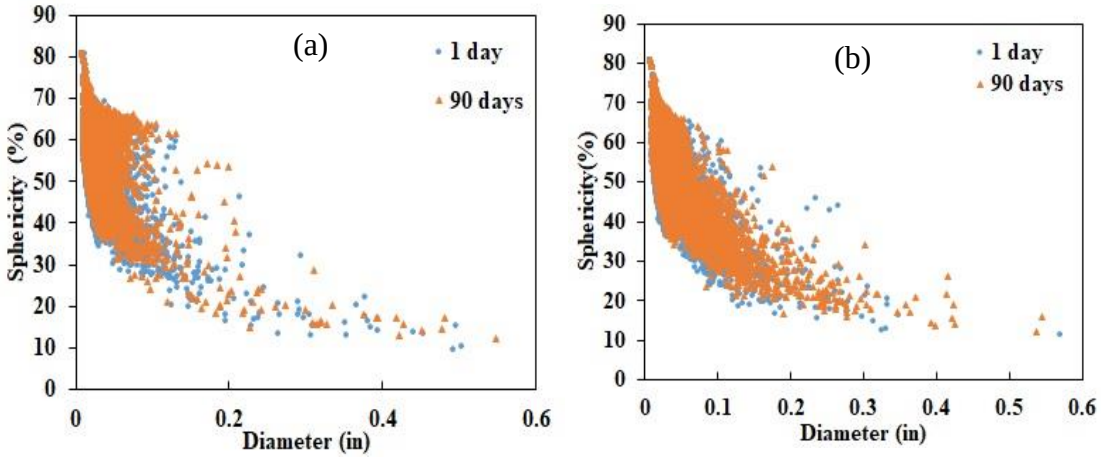

Figure 5.12. Sphericity Vs Diameter relationship of pores for concrete sample with Gravel (a) OPC and (b) GPC

5.3.1.2. Volume Vs diameter

Figure 5.13 to 5.15 shows the change in relationship between volume and diameter of pores inside OPC and GPC concrete prism at 1 day and 90 days after curing. The Figure shows that the volume of pores remains almost constant or changes negligibly in fly ash based geopolymer concrete whereas the volume of pores found to be increased in case of OPC concrete will all kinds of aggregates. The OPC concrete has less number of pores with higher volume and GPC has large number of pores but with very small volume; which might be because of the finer particle size of fly ash. From the Figure we can say that, the slight change in pore diameter and volume in case of fly ash based concrete might be because of late geopolymerization reaction. The OPC concrete with carbonate exerts the largest increment on the volume of pores from 1 day test to 90 day test compared to OPC with other aggregates.

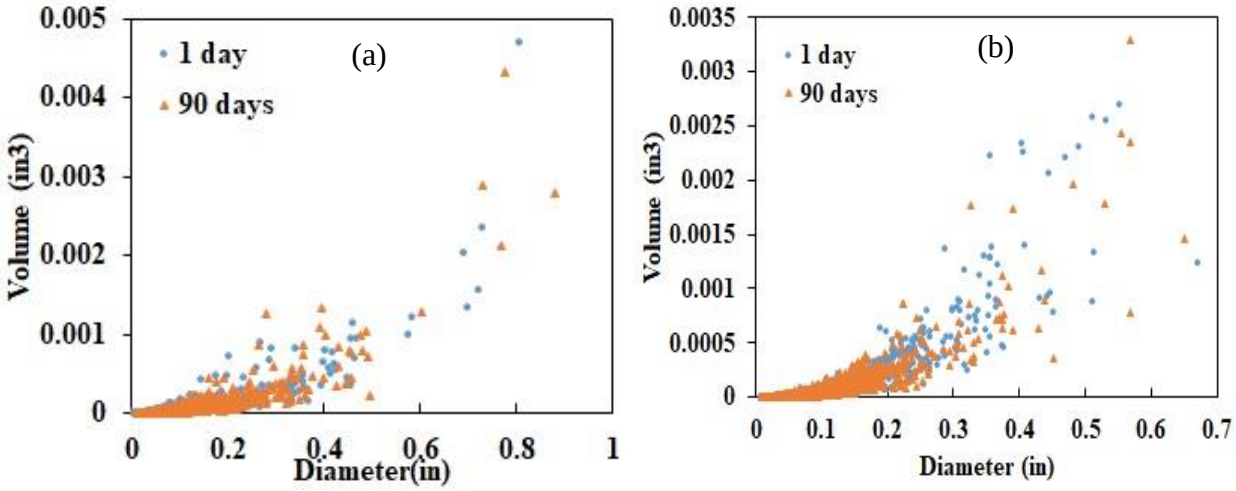

Figure 5.13. Volume Vs Diameter relationship of pores for concrete sample with Granite (a) OPC and (b) GPC

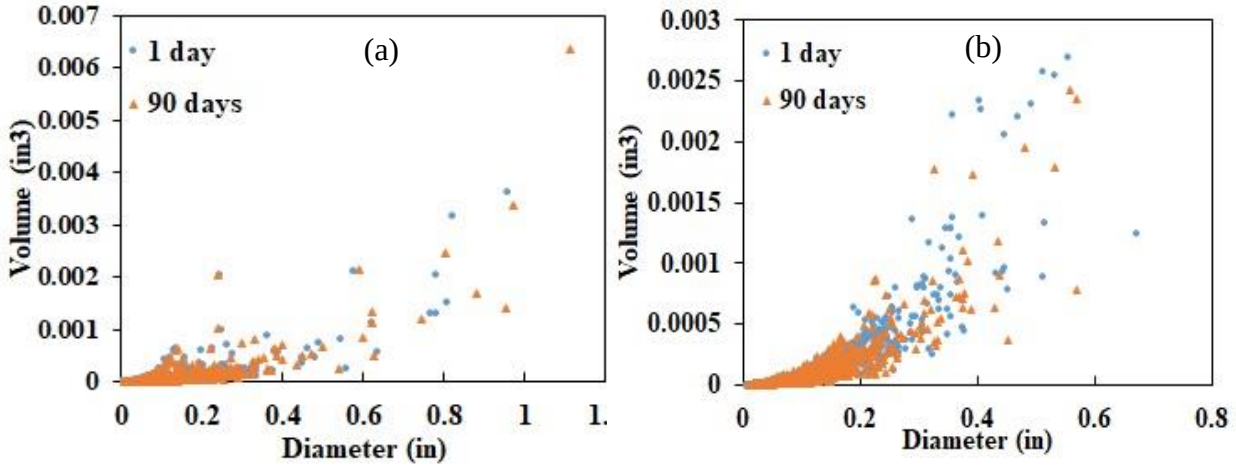

Figure 5.14. Volume Vs Diameter relationship of pores for concrete sample with Carbonate (a) OPC and (b) GPC

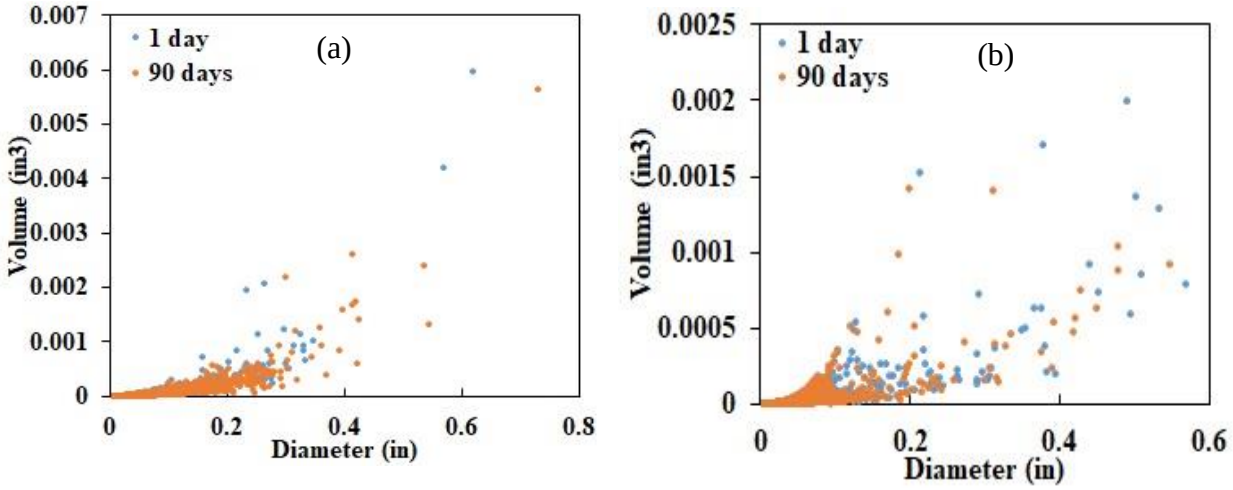

Figure 5.15. Volume Vs Diameter relationship of pores for concrete sample with Gravel (a) OPC and (b) GPC

5.4. Summary

The results obtained from microstructural analysis of OPC and geopolymer concrete was explained in detail in this chapter. The expansion of concrete prism in X, Y, and Z axes is measured using section plane cutting technique. It shows that the expansion in each direction is almost similar, however, axis 'Y' shows the lowest expansion due to the self-weight of the concrete. Porosity and pore size distribution analysis show that OPC has large number of pores as compared to that of geopolymer concrete. It also shows that volume of pores gets increased in OPC concrete after 90 days of time and change in shape of pores is also higher compared to that of geopolymer concrete. This increment in size and decrement in number of pores in OPC concrete might be caused by merging of the pores due to the expansive force exerted through alkali silica gel.

CHAPTER 6. SUMMARY, CONCLUSION AND RECOMMENDATION

6.1. Thesis summary

Alkali silica reaction is the most common form of alkali aggregate reaction (AAR) in concrete while the other much less common form of ASR is alkali carbonate reaction (ACR). Alkali silica reaction is a time dependent degradation that occurs during the life of a concrete structure. Presently, many problems related to ASR usually arises years after construction and causes serious damage in existing structure. There are three essential requirements for deleterious ASR to occur: a sufficient concentration of alkali hydroxides in the pore solution of concrete, a sufficient quantity of reactive minerals in the aggregate, and a sufficient supply of moisture. Many researches have been carried out to investigate the alkali silica reaction in Portland cement concrete but the best solution found till the date is only by avoiding the reactive aggregates in the construction. There are some studies which show that use of suitable supplementary cementing materials to replace the Portland cement can help in reducing the alkali content and ultimately can reduce the effect of alkali silica reaction.

The main purpose of this research was to study the alkali silica reaction in fly ash class C based geopolymer concrete with different reactive aggregates. Three different types of aggregates, namely Granite, Carbonate, and Gravel with different chemical composition and reactivity, were used in whole experiment. Generally, low calcium (ASTM Class F) fly ash has been recommended than high calcium (ASTM Class C) fly ash for the construction purpose. However, the production of class C fly ash is very high compared to the class F in power plants, which is the reason why class C fly ash was chosen in this research. For the comparison purpose, the ordinary Portland cement (OPC) based concrete samples were made for each experiment and analyzed in similar methods. Since the hardening mechanism of OPC concrete and fly ash based

geopolymer concrete are different, the curing method used were also different. The OPC based samples were cured in water while not performing the test whereas, fly ash based concrete samples were cured in air. However, for the specific type of ASTM standard test, the procedure mentioned on standard was followed.

In this research, both lab experiments and microstructural analysis of fly ash based geopolymer concrete and Portland cement concrete with three different types of reactive aggregate were performed and analyzed. The length change experiment of concrete prism were performed for 1 year period as per ASTM C1293 standard. The cumulative expansion of the GPC and OPC concrete prisms were measured on 1, 3, 14, 28, 60, 90, 120, 150, 180, 250, and 365 days of sample preparation. The pore solution of hardened concrete was extracted on same ages as expansion test carried out and pH value of pore solution was measured. For expansion measurement and pore solution extraction, six different mixes were prepared for geopolymer concrete by varying alkaline activator modulus and sodium oxide doses into the alkaline activator solution only one mix design was used for OPC concrete. To keep consistence between OPC and GPC, same mix ratio (1:2:3) was used for both types of concrete mix.

FTIR spectroscopy was performed on 1 year old samples and used to analyze the change in chemical bonding in the concrete. The SEM/EDS analysis was performed on only one mix for both OPC and GPC concrete based on the result achieved on expansion measurement and pore solution alkalinity measurement.

Micro-Computed Tomography (Micro-CT) scanning was used to study the change in microstructural properties of the concrete specimen because of alkali silica reaction. In case of Micro-CT scanning, only mix 6 for all three types of aggregates was chosen for geopolymer concrete based on the vulnerability found on other laboratory experiments. Similar

microstructural analysis was performed for OPC based concrete with all types of aggregates for the comparison purpose.

The concrete prism expansion test indicated that the changes in length of fly ash based geopolymer concrete with all three types of aggregates are very low compared to that of OPC concrete. The pore solution measurement shows that the pH value of pore solution obtained from GPC concrete is very high at early days but keeps decreasing. The exact opposite mechanism was seen in pH value of pore solution obtained from OPC concrete. From FTIR spectroscopy it was noticeably seen that in case of OPC concrete the amount of unreacted silica is in higher amount than that in GPC.

The throughout observation from laboratory experiments showed that the effect of alkali silica reaction is higher in OPC concrete than that in GPC. It was also found that ASR depends upon several factors including chemical composition of aggregates used in sample preparation. MicroCT scan was also performed and analyzed to understand the change in porosity and pore size distribution of the concrete samples. From the results, it was discovered that the pore size gets increased in case of OPC concrete and the number of pores is reduced, which might be because of the expansive force generated from the increasing amount of ASR gel formation.

6.2. Conclusion

This study was carried out to investigate alkali silica reaction potential of different types of aggregates inside fly ash based geopolymer concrete and OPC based concrete. Understanding the mechanism of ASR, factors affecting on ASR, effects of chemical composition of aggregates, and effects of ASR in the concrete are the goals of this research.

From this study several results were observed for all types of concrete mix used, which are:

1. The cumulative expansion of concrete prism was found extensively higher in OPC concrete with all three types of aggregates compared to expansion in fly ash based geopolymer concrete. All the OPC concrete prisms exceeds ASTM threshold (0.04%) before 28 days (Figure 4.1 to 4.3).
2. The slope of expansion was found higher at 1 to 90 days for OPC concrete prism and gets reduced after that (Figure 4.1 to 4.3).
3. The total expansion was found maximum in case of concrete mix with carbonate aggregate for both OPC and GPC. The total expansion of concrete mix with gravel remains at the second place where the total expansion of the mix with granite is the least in all mixes (Figure 4.1 to 4.3).
4. The pH value of pore solution extracted from OPC concrete was found less than that of GPC concrete at early days but after 60 days, the pH value of pore solution extracted from OPC concrete exceeds the value from GPC concrete. It shows, in case of geopolymer concrete, the alkalis available takes part in geopolymerization reaction at early ages and there will not be enough unreacted alkalis to participate in ASR (Figure 4.10 to 4.12).
5. In case of geopolymer concrete with different types of aggregates, the amount of unreacted bulk Si-O-(Si, Al) bonding was obtained at higher amount in case of gravel compared to those with carbonate and granite. However, the presence of higher amount of aluminum in gravel helps to reduce the rate of alkali silica reaction.
6. The alkali silica reaction potential was found to be directly proportional to activator modulus and sodium oxide doses used in geopolymer concrete with all three types of aggregates (Figure 4.4 to 4.9 and Figure 4.11 to 4.18).

7. The amount of silica, calcium, and aluminum in aggregate were found to be very important for reactivity of the aggregate. The addition of silica lowers the Ca/Si ratio of C-S-H in the system, which increases the absorption of alkalis and the formation of ASR gel. The calcium content does not have a huge impact on the alkali silica reaction but it helps to enhance the alkali carbonate reaction which leads to the similar damage on structures. The aluminum content of the aggregate was found to be very good for reducing the ASR. It has been found that the alumina in the pore solution limit the dissolution of the amorphous silica from aggregate by attaching on the silica surface, restricting ASR.
8. The expansion of both OPC and GPC concrete cubes with all three types of aggregates were found different in X, Y, and Z axes. This could be because of the shape, size, orientation, and distribution of the aggregates inside the sample (Table 5.1).
9. The porosity of all OPC concrete specimen with granite, carbonate, and gravel were found increased but the number of pores gets reduced after 90 days whereas the porosity and number of pores of GPC concrete specimen remains almost same. It could be because of expansive pressure generated by the increase in volume of ASR gel in OPC concrete (Figure 5.7 to 5.15).
10. The alkali silica reaction was found more sever in OPC concrete than that of GPC in regardless of types of aggregates used.

6.3. Recommendations

1. Effectiveness of fly ash with moderate level of lime should be conducted. This study has shown that some of these ashes can perform better than high-calcium ashes.
2. More studies are recommended to study the effects of each chemical compound present in aggregate towards the alkali silica reaction of concrete.

3. The change in alkali silica reaction potential of OPC concrete with certain amount of Portland cement replacement by supplementary cementitious materials can be investigated.
4. Effect of alkali silica reaction on the structural behavior of reinforced concrete can be studied.
5. Finite element modeling with the microstructural image obtained from microCT would be very helpful to investigate the effect of ASR in reduction of stiffness and strength of the concrete.

REFERENCES

Abdullah, M., Hussin, K., Bnhussain, M., Ismail, K., and Ibrahim, W. (2011). "Mechanism and chemical reaction of fly ash geopolymer cement-a review." *Int. J. Pure Appl. Sci. Technol*, 6(1), 35-44.

ACAA (2014). "Beneficial Use of Coal Combustion Products: An American Recycling Success Story." ACAA Farmington Hills, MI, USA.

Ahmaruzzaman, M. (2010). "A review on the utilization of fly ash." *Progress in energy and combustion science*, 36(3), 327-363.

Arjunan, P., Silsbee, M., and Roy, D. (2001). "Chemical Activation of Low Calcium Fly Ash Part II: Effect of Mineralogical Composition on Alkali Activation." *Center for Applied Energy Research*, 1-8.

ASTM, A. I. (2008). "ASTM C1293-08b Standard Test Method for Determination of Length Change of Concrete Due to Alkali-Silica Reaction." ASTM International, West Conshohocken, PA.

ASTM, A. I. (2014). "ASTM C1260-14 Standard Test Method for Potential Alkali Reactivity of Aggregates (Mortar-Bar Method)." ASTM International, West Conshohocken, PA.

ASTM, A. I. (2016). "ASTM C109/C109M-16a Standard Test Method for Compressive Strength of Hydraulic Cement Mortars (Using 2-in. or [50-mm] Cube Specimens)." ASTM International, West Conshohocken, PA.

ASTM, A. I. (2016). "ASTM C457/C457M-16 Standard Test Method for Microscopical Determination of Parameters of the Air-Void System in Hardened Concrete." ASTM International, West Conshohocken, PA.

ASTM, A. I. (2018). "ASTM C33/C33M-18 Standard Specification for Concrete Aggregates." ASTM International, West Conshohocken, PA.

ASTM, A. I. (2018). "ASTM C39/C39M-18 Standard Test Method for Compressive Strength of Cylindrical Concrete Specimens." ASTM International, West Conshohocken, PA.

ASTM, A. I. (2018). "ASTM C192/C192M-18 Standard Practice for Making and Curing Concrete Test Specimens in the Laboratory." ASTM International, West Conshohocken, PA.

ASTM, A. I. (2018). "ASTM C618-19 Standard Specification for Coal Fly Ash and Raw or Calcined Natural Pozzolan for Use in Concrete." ASTM International, West Conshohocken, PA.

Attiogbe, E. K., and Darwin, D. (1987). "Submicrocracking in cement paste and mortar." *Materials Journal*, 84(6), 491-500.

Bakharev, T. (2005). "Geopolymeric materials prepared using Class F fly ash and elevated temperature curing." *Cement and concrete research*, 35(6), 1224-1232.

Barneyback Jr, R., and Diamond, S. (1981). "Expression and analysis of pore fluids from hardened cement pastes and mortars." *Cement and Concrete Research*, 11(2), 279-285.

Basu, M., Pande, M., Bhadoria, P., and Mahapatra, S. (2009). "Potential fly-ash utilization in agriculture: a global review." *Progress in Natural Science*, 19(10), 1173-1186.

Bažant, Z. P., and Steffens, A. (2000). "Mathematical model for kinetics of alkali–silica reaction in concrete." *Cement and Concrete Research*, 30(3), 419-428.

Bleszynski, R. F., and Thomas, M. D. (1998). "Microstructural studies of alkali-silica reaction in fly ash concrete immersed in alkaline solutions." *Advanced Cement Based Materials*, 7(2), 66-78.

Brykov, A., Anisimova, A., and Rozenkova, N. (2014). "The Mitigation of Alkali-Silica Reactions by Aluminum-Bearing Substances." *Materials Sciences and Applications,* 5(06), 363.

Buck, A. D., and Mather, K. (1987). "Methods for Controlling Effects of Alkali-Silica Reaction in Concrete." *Army Engineer Waterways Experiment Station Vicksburg Ms Structures Lab.*

Bérubé, M., and Duchesne, J. (1992). "Evaluation of testing methods used for assessing the effectiveness of mineral admixtures in suppressing expansion due to alkali-aggregate reaction." *Special Publication*, 132, 549-576.

Carrasquillo, R. L., and Snow, P. G. (1987). "Effect of fly ash on alkali-aggregate reaction in concrete." *Materials Journal*, 84(4), 299-305.

Chappex, T., and Scrivener, K. L. (2012). "The influence of aluminium on the dissolution of amorphous silica and its relation to alkali silica reaction." *Cement and Concrete Research*, 42(12), 1645-1649.

Cox, H. P., Coleman, R., and White, L. (1950). "Effect of blastfurnace-slag cement on alkali-aggregate reaction in concrete." *Pit and Quarry*, 45(5), 95-96.

Cyr, M., Rivard, P., Labrecque, F., and Daidie, A. (2008). "High-Pressure Device for Fluid Extraction from Porous Materials: Application to Cement-Based Materials." *Journal of the American Ceramic Society,* 91(8), 2653-2658.

Dalgleish, B., Pratt, P., and Toulson, E. (1982). "Fractographic studies of microstructural development in hydrated Portland cement." *Journal of Materials Science,* 17(8), 2199-2207.

Davidovits, J. (1982). "Mineral polymers and methods of making them." Google Patents.

Davidovits, J. (1989). "Geopolymers and geopolymeric materials." *Journal of thermal analysis*, 35(2), 429-441.

Davidovits, J. (1991). "Geopolymers: inorganic polymeric new materials." *Journal of Thermal Analysis and calorimetry*, 37(8), 1633-1656.

Davidovits, J. "Properties of geopolymer cements." *Proc., First international conference on alkaline cements and concretes*, Scientific Research Institute on Binders and Materials Kiev State Technical University, Ukraine, 131-149.

Davidovits, J. "Chemistry of geopolymeric systems, terminology." *Proc., Geopolymer*, 9-39.

Davidovits, J., Davidovics, M., and Davidovits, N. (1994). "Geopolymeric fluoro-alumino-silicate binder and process for obtaining it." Google Patents.

De La O, F. B. "Alkali-aggregate expansion corrected with Portland-slag cement." *Proc., Journal Proceedings*, 545-552.

Diamond, S. (1976). "A review of alkali-silica reaction and expansion mechanisms 2. Reactive aggregates." *Cement and Concrete Research*, 6(4), 549-560.

Diamond, S. "Cement paste microstructure-an overview at several levels." *Proc., Proc. Conference held at University of Sheffield Hydtaulic Cement Paste-Their structure and properties'*, Cement and Concrete Association, 5-31.

Diamond, S. (1983). "Effects of Microsilica (Silica Fume) on Pore-Solution Chemistry of Cement Pastes." *Journal of the American Ceramic Society*, 66(5), C-82-C-84.

Diamond, S., and Lopez-Flores, F. "Comparative studies of the effects of lignitic and bituminous fly ashes in hydrated cement systems." *Proc., Material Research Society. In: Effects of Fly Ash Incorporation in Cement an Concrete: Proc. Sympos. N AnnuaI Meeting.(Diamond, S.(Ed.)). Boston*, 112-123.

Dunstan, E. (1981). "The effect of fly ash on concrete alkali-aggregate reaction." *Cement, Concrete and Aggregates*, 3(2), 101-104.

Farzam, H., Bollin, G., Howe, R., Marin, J., Erlin, B., and Isabelle, H. (2005). *Cement and Concrete Terminology*, ACI Committee.

Ferdous, M., Kayali, O., and Khennane, A. "A detailed procedure of mix design for fly ash based geopolymer concrete." *Proc., Fourth Asia-Pacific Conference on FRP in Structures (APFIS), Melbourne, Australia*, 11-13.

Fernandes, I. (2009). "Composition of alkali–silica reaction products at different locations within concrete structures." *Materials Characterization*, 60(7), 655-668.

Fernandes, I., Broekmans, M. A., Nixon, P., Sims, I., dos Anjos Ribeiro, M., Noronha, F., and Wigum, B. (2013). "Alkali–silica reactivity of some common rock types. A global petrographic atlas." *Quarterly Journal of Engineering Geology and Hydrogeology*, 46(2), 215-220.

Fernández-Jiménez, A., Palomo, A., and Criado, M. (2006). "Alkali activated fly ash binders. A comparative study between sodium and potassium activators." *Materiales de Construcción*, 56(281), 51-65.

Glasser, L. D., and Kataoka, N. (1981). "The chemistry of 'alkali-aggregate'reaction." *Cement and concrete research*, 11(1), 1-9.

Grattan-Bellew, P., Mitchell, L., Margeson, J., and Min, D. (2010). "Is alkali–carbonate reaction just a variant of alkali–silica reaction ACR= ASR?" *Cement and Concrete Research*, 40(4), 556-562.

Groves, G. W., and Zhang, X. (1990). "A dilatation model for the expansion of silica glass/OPC mortars." *Cement and Concrete Research*, 20(3), 453-460.

Habert, G., Billard, C., Rossi, P., Chen, C., and Roussel, N. (2010). "Cement production technology improvement compared to factor 4 objectives." *Cement and Concrete Research*, 40(5), 820-826.

Haha, M. B., Gallucci, E., Guidoum, A., and Scrivener, K. L. (2007). "Relation of expansion due to alkali silica reaction to the degree of reaction measured by SEM image analysis." *Cement and Concrete Research*, 37(8), 1206-1214.

Hanson, W. "Studies Relating To the Mechanism by Which the Alkali-Aggregate Reaction Produces Expansion in Concrete." *Proc., Journal Proceedings*, 213-228.

Hardjito, D., Cheak, C. C., and Ing, C. H. L. (2008). "Strength and setting times of low calcium fly ash-based geopolymer mortar." *Modern applied science*, 2(4), 3.

Hardjito, D., and Rangan, B. V. (2005). "Development and properties of low-calcium fly ash-based geopolymer concrete."

Hardjito, D., Wallah, S., Sumajouw, D., and Rangan, B. "Introducing fly ash-based geopolymer concrete: manufacture and engineering properties." *Proc., 30th Conference on our World in Concrete and Structures*, 23-24.

Hardjito, D., Wallah, S. E., Sumajouw, D. M., and Rangan, B. (2004). "Factors influencing the compressive strength of fly ash-based geopolymer concrete." *civil engineering dimension*, 6(2), pp. 88-93.

Hardjito, D., Wallah, S. E., Sumajouw, D. M., and Rangan, B. V. (2004). "On the development of fly ash-based geopolymer concrete." *Materials Journal*, 101(6), 467-472.

Hassaan, M., and Abdel-Hakeem, N. (1989). "Study of anhydrous and hydrated Portland cement containing alkali ions by infrared spectroscopy." *Journal of materials science letters*, 8(5), 578-580.

Helmuth, R., Stark, D., Diamond, S., and Moranville-Regourd, M. (1993). "Alkali-silica reactivity: an overview of research." *Contract*, 100, 202.

Hobbs, D. (1986). "Deleterious expansion of concrete due to alkali-silica reaction: influence of pfa and slag." *Magazine of Concrete Research*, 38(137), 191-205.

Horgnies, M., Chen, J., and Bouillon, C. (2013). "Overview about the use of Fourier transform infrared spectroscopy to study cementitious materials." *WIT Trans. Eng. Sci*, 77, 251-262.

Hou, X., Kirkpatrick, R. J., Struble, L. J., and Monteiro, P. J. (2005). "Structural investigations of alkali silicate gels." *Journal of the American Ceramic Society*, 88(4), 943-949.

Hou, X., Struble, L. J., and Kirkpatrick, R. J. (2004). "Formation of ASR gel and the roles of CSH and portlandite." *Cement and Concrete Research*, 34(9), 1683-1696.

Hughes, T. L., Methven, C. M., Jones, T. G., Pelham, S. E., Fletcher, P., and Hall, C. (1995). "Determining cement composition by Fourier transform infrared spectroscopy." *Advanced Cement Based Materials*, 2(3), 91-104.

Ichikawa, T., and Miura, M. (2007). "Modified model of alkali-silica reaction." *Cement and Concrete research*, 37(9), 1291-1297.

Joshi, S., and Kadu, M. (2012). "Role of alkaline activator in development of eco-friendly fly ash based geo polymer concrete." *International Journal of Environmental Science and Development*, 3(5), 417.

Jun, S. S., and Jin, C. S. (2010). "ASR products on the content of reactive aggregate." *KSCE Journal of Civil Engineering*, 14(4), 539-545.

Jóźwiak-Niedźwiedzka, D., Dąbrowski, M., Gibas, K., Antolik, A., and Glinicki, M. A. "Alkali-silica reaction and microstructure of concrete subjected to combined chemical and

physical exposure conditions." *Proc., MATEC Web of Conferences*, EDP Sciences, 05009.

Kalyoncu, R. S., and Olson, D. W. (2001). *Coal combustion products*, US Department of the Interior, US Geological Survey.

Kapat, C., Pradhan, B., and Bhattacharjee, B. (2006). "Potentiostatic study of reinforcing steel in chloride contaminated concrete powder solution extracts." *Corrosion Science*, 48(7), 1757-1769.

Khale, D., and Chaudhary, R. (2007). "Mechanism of geopolymerization and factors influencing its development: a review." *Journal of materials science*, 42(3), 729-746.

Kim, K. Y., Yun, T. S., Choo, J., Kang, D. H., and Shin, H. S. (2012). "Determination of air-void parameters of hardened cement-based materials using X-ray computed tomography." *Construction and Building Materials*, 37, 93-101.

Klieger, P., and Gebler, S. (1987). "Fly ash and concrete durability." *Special Publication*, 100, 1043-1069.

Kupwade-Patil, K., and Allouche, E. N. (2012). "Impact of alkali silica reaction on fly ash-based geopolymer concrete." *Journal of materials in Civil Engineering*, 25(1), 131-139.

Leemann, A., Katayama, T., Fernandes, I., and Broekmans, M. A. (2016). "Types of alkali–aggregate reactions and the products formed." *Proceedings of the Institution of Civil Engineers-Construction Materials*, 169(3), 128-135.

Li, L., Nam, J., and Hartt, W. H. (2005). "Ex situ leaching measurement of concrete alkalinity." *Cement and concrete research*, 35(2), 277-283.

Lippiatt, B. C., and Ahmad, S. "Measuring the life-cycle environmental and economic performance of concrete: the BEES approach." *Proc., Proceedings of the International Workshop on Sustainable Development and Concrete Technology*, 213-230.

Lopez-Flores, F. (1982). "Flyash and Effects of Partial Cement Replacement by Flyash: Informational Report."

McGowan, J. (1952). "Studies in Cement-Aggregate Reaction XX, The CorrelationBetween Crack Development and Expansion of Mortar." *Aust. J. Appl. Sci.*, 3, 228-232.

Meyer, C., and Xi, Y. (1999). "Use of recycled glass and fly ash for precast concrete." *Journal of materials in civil engineering*, 11(2).

Motorwala, A., Shah, V., Kammula, R., Nannapaneni, P., and Raijiwala, D. (2013). "ALKALI activated FLY-ASH based geopolymer concrete." *International journal of emerging technology and advanced engineering*, 3(1), 159-166.

Mukhopadhyay, A., Ghanem, H., Shon, C., Zollinger, D., Gress, D., and Hooton, D. (2009). "Mitigation of ASR in Concrete-Combined Materials Test Procedure." IPRF Report DOT/FAA-01-G-003-2, Innovative Pavement Research Foundation ….

Nixon, P., and Page, C. (1987). "Pore solution chemistry and alkali aggregate reaction." *Special Publication*, 100, 1833-1862.

Owsiak, Z. (2003). "Microstructure of alkali-silica reaction products in conventional standard and accelerated testing." *Ceramics-Silikáty*, 47(3), 108-115.

Palomo, A., Grutzeck, M. W., and Blanco, M. T. (1999). "Alkali-activated fly ashes: A cement for the future." *Cement and Concrete Research*, 29(8), 1323-1329.

Pan, J., Feng, Y., Wang, J., Sun, Q., Zhang, C., and Owen, D. (2012). "Modeling of alkali-silica reaction in concrete: a review." *Frontiers of Structural and Civil Engineering*, 6(1), 1-18.

Petermann, J. C., Saeed, A., and Hammons, M. I. (2010). "Alkali-activated geopolymers: a literature review." Applied Research Associates Inc Panama City Fl.

Pietruszczak, S. (1996). "On the mechanical behaviour of concrete subjected to alkali-aggregate reaction." *Computers & structures*, 58(6), 1093-1097.

Pike, R. G., and Hubbard, D. (1958). "Miscellaneous Observations on the Alkali-Aggregate Reaction and the Ionic Charge on Hydrated Cement." *Highway Research Board Bulletin*(171).

Poole, A. B. (2002). "Introduction to alkali-aggregate reaction in concrete." *The alkali-silica reaction in concrete*, CRC Press, 17-45.

Pouhet, R., and Cyr, M. (2015). "Alkali–silica reaction in metakaolin-based geopolymer mortar." *Materials and Structures*, 48(3), 571-583.

Powers, T. C., and Willis, T. "The air requirement of frost resistant concrete." *Proc., Highway Research Board Proceedings*.

Pradhan, B., and Bhattacharjee, B. (2007). "Corrosion zones of rebar in chloride contaminated concrete through potentiostatic study in concrete powder solution extracts." *Corrosion Science*, 49(10), 3935-3952.

Promentilla, M., Sugiyama, T., and Shimura, K. "Three dimensional characterization of air void system in cement-based materials." *Proc., 3rd ACF International Conference ACF/VCA*, 940-947.

Provis, J. L., Duxson, P., Kavalerova, E., Krivenko, P. V., Pan, Z., Puertas, F., and van Deventer, J. S. (2014). "Historical aspects and overview." *Alkali activated materials*, Springer, 11-57.

Provis, J. L., Myers, R. J., White, C. E., Rose, V., and van Deventer, J. S. (2012). "X-ray microtomography shows pore structure and tortuosity in alkali-activated binders." *Cement and Concrete Research*, 42(6), 855-864.

Puertas, F., and Fernández-Jiménez, A. (2003). "Mineralogical and microstructural characterisation of alkali-activated fly ash/slag pastes." *Cement and Concrete composites*, 25(3), 287-292.

Puertas, F., Fernández-Jiménez, A., and Blanco-Varela, M. (2004). "Pore solution in alkali-activated slag cement pastes. Relation to the composition and structure of calcium silicate hydrate." *Cement and Concrete Research*, 34(1), 139-148.

Rangan, B. V. (2008). "Fly ash-based geopolymer concrete." Curtin University of Technology.

Rattanasak, U., and Kendall, K. (2005). "Pore structure of cement/pozzolan composites by X-ray microtomography." *Cement and concrete research*, 35(4), 637-640.

Razak, R. A., Abdullah, M. M. A. B., Hussin, K., Ismail, K. N., Sandu, I. G., Hardjito, D., Yahya, Z., and Sandu, A. V. (2014). "Assessment on the potential of volcano ash as artificial lightweight aggregates using geopolymerisation method." *Rev. Chim.(Buchar.)*, 65, 828-834.

Regourd, M., Hornain, H., and Poitevin, P. (1981). "The alkali-aggregate reaction-concrete microstructure evolution." *Proceedings:5 International Conference on Alkali-Aggregae Reaction in Concrete*, (p.444). South Africa: National Building Research Institute, Council for Scientific and Industrial Research.

Roskos, C., Cross, D., Berry, M., and Stephens, J. "Identification and verification of self–cementing fly ash binders for 'Green'concrete." *Proc., proceedings of the 2011 world of coal ash (WOCA) conference—May*, 9-12.

Roy, D., Arjunan, P., and Silsbee, M. (2001). "Effect of silica fume, metakaolin, and low-calcium fly ash on chemical resistance of concrete." *Cement and Concrete Research*, 31(12), 1809-1813.

Rubenstein, M. (2012). "Emissions from the cement industry." *State of the Planet*.

Saha, A. K., Khan, M., Sarker, P. K., Shaikh, F. A., and Pramanik, A. (2018). "The ASR mechanism of reactive aggregates in concrete and its mitigation by fly ash: A critical review." *Construction and Building Materials*, 171, 743-758.

Sansui, O., Tempest, B., Ogunro, V., Gergely, J., and Daniels, J. (2009). "Effect of hydroxy ion on immobilization of oxyanions forming trace elements from fly ash-based geopolymer concrete." *World of Coal Ash*.

Saouma, V., and Perotti, L. (2006). "Constitutive model for alkali-aggregate reactions." *ACI materials journal*, 103(3), 194.

Scrivener, K. L., and Pratt, P. "Backscattered electron images of polished cement sections in the scanning electron microscope." *Proc., Proceedings of the International Conference on Cement Microscopy*, 145-155.

Shehata, M. H., Thomas, M. D., and Bleszynski, R. F. (1999). "The effects of fly ash composition on the chemistry of pore solution in hydrated cement pastes." *Cement and Concrete Research*, 29(12), 1915-1920.

Shi, Z., Shi, C., Zhang, J., Wan, S., Zhang, Z., and Ou, Z. (2018). "Alkali-silica reaction in waterglass-activated slag mortars incorporating fly ash and metakaolin." *Cement and Concrete Research*, 108, 10-19.

Shin, J.-H. (2009). *Modeling alkali-silica reaction using image analysis and finite element method*, University of Illinois at Urbana-Champaign.

Shin, J. H., Jee, N. Y., Struble, L. J., and Kirkpatrick, R. J. "Modeling Alkali-Silica Reaction Using Image Analysis and Finite Element Analysis." *Proc., Advanced Materials Research*, Trans Tech Publ, 1050-1053.

Sims, I., and Poole, A. B. (2017). *Alkali-Aggregate Reaction in Concrete: A World Review*, CRC Press.

Singh, N. B. (2018). "Fly ash-based geopolymer binder: A future construction material." *Minerals*, 8(7), 299.

Smith, R. L. (1987). "Is the Available Alkalitest a Good Durability Predictor for Fly Ash Concrete Incorporating Reactive Aggregate?" *MRS Online Proceedings Library Archive*, 114.

Stanton, T. "Studies of use of pozzolans for counteracting excessive concrete expansion resulting from reaction between aggregates and the alkalies in cement." *Proc., Symposium on Use of Pozzolanic Materials in Mortars and Concretes*, ASTM International.

Stanton, T. E., Porter, O., Meder, L., and Nicol, A. "California experience with the expansion of concrete through reaction between cement and aggregate." *Proc., Journal Proceedings*, 209-236.

Stokes, J. (2011). "An Analysis of the Design and Assembly of the AAR Tri-axial Machine."

Struble, L., and Diamond, S. (1986). "Influence of cement alkali distribution on expansion due to alkali-silica reaction." *Alkalies in concrete*, ASTM International.

Swaddle, T. W., Salerno, J., and Tregloan, P. A. (1994). "Aqueous aluminates, silicates, and aluminosilicates." *Chemical Society Reviews*, 23(5), 319-325.

Swamy, R. N. (2002). *The alkali-silica reaction in concrete*, CRC Press.

Swenson, E. G. (1957). "A reactive aggregate undetected by ASTM tests." *ASTM Bulletin*(226), 48-51.

Swenson, E. G., and Gillott, J. E. (1964). "Alkali-carbonate rock reaction." *Highway Research Record*(45).

Thaulow, N., Jakobsen, U. H., and Clark, B. (1996). "Composition of alkali silica gel and ettringite in concrete railroad ties: SEM-EDX and X-ray diffraction analyses." *Cement and Concrete Research*, 26(2), 309-318.

Thomas, M. (1996). *Review of the effect of fly ash and slag on alkali-aggregate reaction in concrete*, Building Research Establishment.

Thomas, M., Fournier, B., Folliard, K., and Resendez, Y. (2011). "Alkali-Silica Reactivity Field Identification Handbook."

Thomas, M., Hooton, R. D., and Rogers, C. (1997). "Prevention of damage due to alkali-aggregate reaction (AAR) in concrete construction—Canadian approach." *Cement, Concrete and Aggregates*, 19(1), 26-30.

Turner, L. K., and Collins, F. G. (2013). "Carbon dioxide equivalent (CO2-e) emissions: A comparison between geopolymer and OPC cement concrete." *Construction and Building Materials*, 43, 125-130.

Tänzer, R., Jin, Y., and Stephan, D. (2017). "Effect of the inherent alkalis of alkali activated slag on the risk of alkali silica reaction." *Cement and Concrete Research*, 98, 82-90.

Van Jaarsveld, J., Van Deventer, J., and Lorenzen, L. (1997). "The potential use of geopolymeric materials to immobilise toxic metals: Part I. Theory and applications." *Minerals engineering*, 10(7), 659-669.

Williamson, R. B. (1969). "Portland Cement: Pseudomorphs of Original Cement Grains Observed in Hardened Pastes." *Science*, 164(3879), 549-551.

Williamson, R. B. (1970). "Solidification of Portland cement." California Univ Berkeley Div Of Structural Engineering and Structural Mechanics.

Williamson, T., and Juenger, M. C. (2016). "The role of activating solution concentration on alkali–silica reaction in alkali-activated fly ash concrete." *Cement and Concrete Research*, 83, 124-130.

Wong, R., and Chau, K. (2005). "Estimation of air void and aggregate spatial distributions in concrete under uniaxial compression using computer tomography scanning." *Cement and Concrete Research*, 35(8), 1566-1576.

Xu, H., and Van Deventer, J. S. J. (2000). "The geopolymerisation of alumino-silicate minerals." *International Journal of Mineral Processing*, 59(3), 247-266.

Xu, H., and Van Deventer, J. S. J. (2002). "Geopolymerisation of multiple minerals." *Minerals Engineering*, 15(12), 1131-1139.

Yun, T. S., Kim, K. Y., Choo, J., and Kang, D. H. (2012). "Quantifying the distribution of paste-void spacing of hardened cement paste using X-ray computed tomography." *Materials Characterization*, 73, 137-143.

Zhao, H., and Darwin, D. (1990). "Quantitative Backscattered Electron Analysis Techniques for Cement-Based Materials." University of Kansas Center for Research, Inc.

Štukovnik, P., Prinčič, T., Pejovnik, R. S., and Bosiljkov, V. B. (2014). "Alkali-carbonate reaction in concrete and its implications for a high rate of long-term compressive strength increase." *Construction and building materials*, 50, 699-709.